

Aus dem Bereich Physiologie
Theoretische Medizin und Biowissenschaften
der Medizinischen Fakultät
der Universität des Saarlandes, Homburg/Saar

GABA_B receptor signalling of OPCs attenuates a burst of OPC proliferation and oligodendrocyte formation at the onset of chronic TLE

**Dissertation zur Erlangung des Grades eines Doktors der Medizin der Medizinischen
Fakultät**

der UNIVERSITÄT DES SAARLANDES

2023

vorgelegt von: Annika Marie Liebmann
geb. am: 01.01.1997 in Lübeck

Content

List of abbreviations.....	I
List of figures	III
List of supplementary figures.....	IV
Abstract	V
.....	
1. Abstract.....	1
1.1 Abstract.....	1
1.2 Zusammenfassung.....	2
2. Introduction.....	3
2.1 Epilepsy and Temporal Lobe Epilepsy.....	3
2.2 The GABAergic system.....	3
2.2.1 GABA and interneurons in health and epilepsy.....	3
2.3 Glial cells in epilepsy.....	5
2.3.1 Oligodendrocyte precursors.....	5
2.3.2 OPC-interneuron communication.....	6
2.3.3 Gliosis in epilepsy.....	7
2.4 Animals models of MTLE.....	8
2.5 Aim of the study.....	9
3. Material und Methods.....	10
3.1 <i>Materials</i>	10
3.1.1 Chemicals.....	10
3.1.2 Consumables.....	11
3.1.3 Devices.....	11
3.1.4 Buffers and aqueous solutions.....	12
3.1.5 Drugs.....	13
3.1.6 Antibodies.....	13
3.1.7 Dyes.....	14
3.1.8 Primers.....	14
3.1.9 Genetically modified mouse lines.....	15
3.1.10 Software.....	16
3.2 <i>Methods</i>	16
3.2.1 Mouse administration and ethics statement.....	16
3.2.2 Experimental design.....	16
3.2.3 Genotyping.....	17
3.2.4 Tamoxifen administration.....	17
3.2.5 Unilateral intracortical kainate injection.....	17
3.2.6 Whole body perfusion fixation.....	18
3.2.7 Slice preparation.....	18
3.2.8 Immunohistochemistry.....	18
3.2.9 Automated epifluorescence microscopy.....	19
3.2.10 Data analysis.....	19
3.2.11 Statistics.....	20
4. Results.....	21
4.1 Conditional knock-out of GABA _B R in OPCs and oligodendrocytes.....	21
4.2 OPC and oligodendrocyte density is increased in the cKO cortex at one week after kainate injection.....	23
4.3 OPC proliferation is increased in epileptic GABA _B R cKO mice in the ipsilateral cortex and CA1 region.....	28
4.4 Loss of PV ⁺ interneurons in the epileptic brain.....	30
4.5 Astrogliosis and microglia activation is not altered in the epileptic cKO brain.....	36

5. Discussion	39
5.1 OPC-GABA _B receptor transiently promotes cortical OPC proliferation and density.....	39
5.2 OPC-GABA _B receptor for oligodendrocyte generation in the epileptic cortex.....	41
5.3 Interneurons demonstrate increased resistance to excitotoxicity in OPC-GABA _B cKO mice.....	42
5.4 Soma-somatic communication between OPCs and PV ⁺ interneurons doesn't mediate increased OPC proliferation and resistance to excitotoxicity.....	43
5.5 GABA _B receptor mediated signalling on OPCs does not affect the activation of astrocytes and microglia in the epileptic cortex.....	44
5.6 Outlook.....	45
6. Supplementary Figures	48
7. References	58
8. Acknowledgements	65
9. Curriculum vitae	66

List of abbreviations

1dpl	1 day post injection
1wpl	1 week post injection
2wpl	2 weeks post injection
AED	anti-epileptic drug
AMPA	aminomethylphosphonic acid receptor
BDNF	brain-derived neurotrophic factor
CA	cornu ammonis
cAMP	cyclic adenosine monophosphate
cKO	conditional knock-out
CNS	central nervous system
Cre	cre-DNA recombinase
CREB	cAMP response element binding protein
ctl	control
ctx	cortex
DAPI	4',6-diamidino-2-phenylindole
DG	dentate gyrus
DNA	deoxyribonucleic acid
E/I balance	excitatory/inhibitory balance
EDTA	ethylenediaminetetraacetate
EEG	electroencephalography
ER	estrogen receptor
FI	fluorescence intensity
fl	floxed
GABA	γ -aminobutyric acid
GABA _A R	γ -aminobutyric acid receptor type A
GABA _B R	γ -aminobutyric acid receptor type B
gabbr1	γ -aminobutyric acid type B receptor subunit 1
GAD	glutamic acid decarboxylase
GAT	GABA transporter
GFAP	glial fibrillary acid protein
GS	glutamine synthetase
HSP	heat shock protein
ht	hippocampus
Iba1	ionized calcium binding adapter molecule 1
Iba1	ionized calcium binding adapter molecule 1
IBE	International Bureau for Epilepsy
ILAE	International League Against Epilepsy
KA	kainate
KI	knock-in
loxP	locus of crossover of the bacteriophage P1
Isl	fl/stop/fl
MBP	myelin basic protein
mPFC	medial prefrontal cortex
mRNA	messenger ribonucleic acid
MTLE	mesial temporal lobe epilepsy
NG2	nerve/glia antigen-2
NTLE	neocortical temporal lobe epilepsy
OL	oligodendrocyte
OPC	oligodendrocyte progenitor cell
p	postnatal day
PBS	<i>phosphate buffered saline</i>

PCR	polymerase chain reaction
PDGFR α	platelet-derived growth factor receptor α
PFA	paraformaldehyde
PV	parvalbumin
rpm	revolutions per minute
SA	saline
SE	status epilepticus
sIPSC	spontaneous inhibitory post-synaptic currents
SRS	spontaneous recurrent seizures
TAE	<i>tris-acetate-EDTA-buffer</i>
TAM	tamoxifen
TgH	transgenic mouse generated via homologous recombination
TLE	temporal lobe epilepsy
TWEAK	tumor necrosis factor-like weak inducer of apoptosis
vGAT	vesicular GABA transporter
WT	wild type

The dimensions of this thesis are consistent with the International System of Units (SI).

List of figures

Figure 1.	Interplay of interneurons, astrocytes and OPCs in GABA metabolism and neurotransmission.....	4
Figure 2.	Tamoxifen administration induces Cre recombination of exon 7 and 8 in the <i>gabbr1</i> gene.....	15
Figure 3.	Construct of the NG2-Cre ^{ERT2} x GABA _B 1R ^{fl/fl} x GCamp3 Mouse.....	17
Figure 4.	Experimental schedule.....	17
Figure 5.	Fluorescence intensity measurement.....	20
Figure 6.	Transgenic mouse model for conditional deletion of GABA _B Rs in OPCs.....	22
Figure 7.	Kainate injection induces an intensive OPC reaction at the injection site.....	23
Figure 8.	Kainate injection induces OPC and OL density increase at the ipsilateral cortex of GABA _B R knock-out mice at 1wpl.....	25
Figure 9.	Cortical OPC and OL density at the epileptic lesion peaks 1 week after kainate injection.....	27
Figure 10.	Kainate injection induces an increase of OPC proliferation in GABA _B R conditional knock out mice at 1 week post kainite injection.....	29
Figure 11.	OPC proliferating rate at the epileptic lesion peaks at 1 week after kainate injection in the mice.....	30
Figure 12.	Kainate injection induces the loss of PV ⁺ neurons at the injection site.....	31
Figure 13.	Kainate injection induces the loss of PV ⁺ neurons in ipsilateral cortex and CA1 region.....	32
Figure 14.	Kainate injection induces the loss of PV ⁺ neurons in ipsilateral cortex and CA1 region.....	33
Figure 15.	Reduction of PV ⁺ interneurons and interneuron-OPC pairs in kainate treated ipsilateral cortex.....	35
Figure 16.	Kainate injection induces an increase of GFAP and Iba1 immunofluorescence intensity near the lesion site 1wpl.....	36
Figure 17.	Oligodendroglial GABA _B R signalling does not affect astrocyte and microglia activation at the site of epileptic lesion.....	37

List of supplementary figures

Supplementary Figure 1.	OPC and OL density 1dpl.....	48
Supplementary Figure 2.	OPC and OL density 1wpl.....	49
Supplementary Figure 3.	OPC and OL density 2wpl.....	50
Supplementary Figure 4.	Density of recombined OPCs and OLs 1 day, 1 week and 2 weeks post injection.....	51
Supplementary Figure 5.	Density of non-recombined OPCs and OLs 1 day, 1 week and 2 weeks post injection.....	53
Supplementary Figure 6.	Density of proliferating OPCs 1dpl.....	53
Supplementary Figure 7.	Density of proliferating OPCs 1wpl.....	54
Supplementary Figure 8.	Density of proliferating OPCs 2wpl.....	54
Supplementary Figure 9.	Density of proliferating recombined and non-recombined OPCs 1 day, 1 week and 2 weeks post injection.....	55
Supplementary Figure 10.	Density of interneurons and interneuron-OPC pairs 1dpl.....	56
Supplementary Figure 11.	Density of interneurons and interneuron-OPC pairs 2wpl.....	57

List of tables

Table 1. List of chemicals.....	10
Table 2. List of Consumables.....	11
Table 3. List of Devices.....	11
Table 4. List of primary antibodies.....	13
Table 5. List of secondary antibodies.....	14
Table 6. List of dyes.....	14
Table 7. List of primers for genotyping.....	14
Table 8. List of transgenic mouse lines.....	15

1. Abstract

1.1 Abstract

Epilepsy is a neurological disorder characterized by hyperexcitability of neuronal circuits, manifesting in recurrent seizures. Despite the abundance of anti-epileptic drugs available, targeting neurons, as many as 30% of patients cannot achieve a seizure free state. Several studies suggest that the balance between excitatory and inhibitory neurotransmission (E/I balance) is disturbed in the epileptic brain, favouring excitation. Uniquely among glia cells, oligodendrocyte progenitor cells (OPCs) form synaptic connections with inhibitory as well as excitatory neurons making them promising candidates as potential novel targets of research. Through pairing, they even form close anatomical and functional relationships with interneurons and mirror their electrical activity. A recent study from our group demonstrates, that GABA_B receptor (GABA_BR) mediated OPC-interneuron communication is crucial for determining interneuronal density and function during early development, thereby regulating E/I balance under healthy conditions. Moreover, in several epileptic paradigms OPCs have been shown to react to the induction of recurrent seizures. Therefore, the central aim of this study is to investigate the role of OPC-GABA_BR signaling in regulating the response of OPCs and interneurons following hyperexcitable network dysfunction in epilepsy.

We induced epileptic condition in transgenic mice carrying OPC-specific GABA_BR cKO by employing the mouse model of temporal lobe epilepsy by intracortical kainate injections. Immunohistochemistry was performed in the acute phase directly following status epilepticus, as well as one week later at the onset of the chronic phase and two weeks later during the early chronic phase.

Our results demonstrated that GABA_BR signaling on OPCs impedes a transient burst of OPC proliferation and oligodendrocyte formation at the cortical epileptic lesion at the onset of the chronic phase. While OPC proliferation and density only peaks transiently in OPC-GABA_BR cKO mice, the density of oligodendrocytes at the cortical lesion remains elevated during the early chronic phase. Therefore, we hypothesize that reduction of GABA_BR signaling might be beneficial in attenuating myelin damage observed during the chronic phase of epileptogenesis. Furthermore, we show that interneuronal susceptibility to excitotoxicity in GABA_BR cKO mice is reduced. While the contralateral cortex of control mice was slowly depleted of interneurons as epileptogenesis progressed, interneuronal density at the contralateral cortex was preserved in GABA_BR cKO mice. Therefore, reduction of GABA_BR activation of OPCs could potentially attenuate severity of epilepsy by preventing myelin damage and curtailing loss of inhibitory neurotransmission during the chronic phase.

1.2 Zusammenfassung

Epilepsie ist eine Erkrankung, welche durch Übererregbarkeit neuronaler Netzwerke gekennzeichnet ist und sich in wiederkehrenden Krampfanfällen manifestiert. Trotz der Vielzahl zu Verfügung stehender auf Neuronen wirkenden Antiepileptika, erreichen 30% der Patienten keine Anfallsfreiheit. Etliche Studien schlagen vor, dass das Gleichgewicht zwischen inhibitorischer und exzitatorischer Neurotransmission im epileptischen Gehirn zugunsten der Exzitation verschoben ist. Oligodendrozyten Vorläuferzellen (OPCs) besitzen die Eigenschaft, synaptische Verbindungen mit exzitatorischen sowie inhibitorischen Neuronen einzugehen. Sie gehen enge anatomische und funktionelle Verbindungen mit Interneuronen ein und spiegeln deren elektrische Aktivität wider. Eine kürzlich publizierte Studie unserer Arbeitsgruppe zeigt, dass GABA_B Rezeptor (GABA_BR) vermittelte OPC-Interneuron-Kommunikation die Dichte und Funktion von Interneuronen und dadurch das Gleichgewicht von Exzitation und Inhibition entscheidend beeinflusst. In zahlreichen Epilepsiemodellen zeigte sich ein Einfluss von wiederkehrenden Krampfanfällen auf OPCs. Das zentrale Ziel dieser Arbeit ist daher, den Einfluss von OPC-GABA_BR vermittelter Signalübertragung auf die Dynamik von OPCs und Interneuronen im übererregbaren epileptischen Gehirn zu erforschen.

Durch intrakortikale Kainate-Injektionen induzierten wir epileptische Bedingungen im Gehirn von transgenen Mäusen, welche Träger eines OPC-spezifischen cKOs des GABA_BRs sind. Immunohistochemie wurde unmittelbar nach Status epilepticus (akute Phase), sowie eine Woche später (Beginn der chronischen Phase) und zwei Wochen später (chronische Phase) durchgeführt.

Unsere Ergebnisse zeigen, dass OPC-GABA_BR abhängige Signalübertragung zu Beginn der chronischen Phase einen vorübergehenden Schub von OPC-Proliferation und Oligodendrozytenbildung an der kortikalen epileptischen Läsion verhindert. Während die Dichte und Proliferation von OPCs in OPC-GABA_BR cKO-Mäusen nur kurzzeitig erhöht ist, bleibt die Dichte von Oligodendrozyten auch noch in der frühen chronischen Phase erhöht. Daher liegt die Vermutung nahe, dass eine Reduktion von OPC-GABA_BR abhängiger Signalübertragung die Ausprägung von Myelinschäden wie sie in der chronischen Phase beobachtet wurden, günstig beeinflussen könnte. Des Weiteren demonstrieren wir eine reduzierte Anfälligkeit von Interneuronen für Exzitotoxizität in OPC-GABA_BR cKO Mäusen. Während die interneuronale Dichte im kontralateralen Kortex von Mäusen der Kontrollgruppe mit Fortschreiten der Erkrankung langsam abnahm, blieb die Dichte von Interneuronen im kontralateralen Kortex der cKO-Mäuse unbeeinträchtigt. Deswegen könnte eine Reduktion der OPC-GABA_BR abhängigen Signalübertragung den Verlauf von epileptischen Erkrankungen durch Verringerung von Myelinschäden und Erhalt der inhibitorischen Neurotransmission mildern.

2. Introduction

2.1 Epilepsy and Temporal Lobe Epilepsy

With around 50 million people affected globally and a lifetime prevalence of 7.60 per 1000 persons, epilepsy is among the most common neurological disorders (Fiest et al., 2017). The International League Against Epilepsy (ILAE) and the International Bureau for Epilepsy (IBE) define epileptic seizures as “transient occurrences of signs and/or symptoms due to abnormal excessive or synchronous neuronal activity in the brain” (Fisher et al., 2005). According to the region of the onset, seizures are defined as focal onset, generalized onset and unknown onset. Each epilepsy type (focal, generalized, combined generalized and focal) can include a spectrum of different seizure types and the diagnosis might be supported by characteristic interictal electroencephalography (EEG) findings. Although the complete pathophysiological pathways leading to the development of epilepsy are far from resolved, several studies indicate that the balance of excitatory and inhibitory neurotransmission (E/I balance) is disturbed in the epileptic brain, favouring excitation. Ultimately, this imbalance is hypothesized to result in hyperexcitability and hypersynchronous overshooting excitation, capable of disrupting physiological network activity (Fisher et al., 2005; Kumar and Buckmaster, 2006; Avoli et al., 2016; Patel et al., 2019). Temporal lobe epilepsy (TLE) has a prevalence of 0,1% in the general population, making it the most frequently seen type of human epilepsy (Keränen and Riekkinen, 1988). TLE can be divided into mesial temporal lobe epilepsy (MTLE) and neocortical temporal lobe epilepsy (NTLE). As the name suggest, MTLE originates from medial temporal structures such as hippocampus, entorhinal cortex and amygdala (Pascual, 2007). In as many as 60% of patients TLE is classified as idiopathic, meaning the etiology remains unresolved (Blümcke et al., 2007). In other cases, an initial insult (such as brain infections, trauma, stroke) or underlying pathology (malformation of cortical development, benign tumor, vascular malformation) postulates the onset of epileptogenesis and the development of spontaneous recurrent seizures (SRS) down the line (Zentner et al., 1995; Quarato et al., 2005; Jefferys et al., 2016). Despite the abundance of available anti-epileptic drugs (AEDs), as many as 30% of the patients treated can't achieve a seizure-free state, thereby exhibiting pharmacoresistance (Sillanpää et al., 1998; Kwan and Brodie, 2000; Sharma et al., 2015). This underscores the importance of revealing new potential targets for pharmacotherapy.

2.2 The GABAergic system

2.2.1 GABA and interneurons in health and epilepsy

Around one third of central neurons synthesize gamma-aminobutyric acid (GABA) (Bloom and Iversen, 1971), the main inhibitory neurotransmitter of the central nervous system (CNS). GABA is synthesized mainly from glutamate by the enzyme glutamic acid decarboxylase

(GAD) (Fig. 1) (Roberts and Frankel, 1950, 1951), GAD65 and GAD67 (Petroff, 2002; Lee et al., 2019).

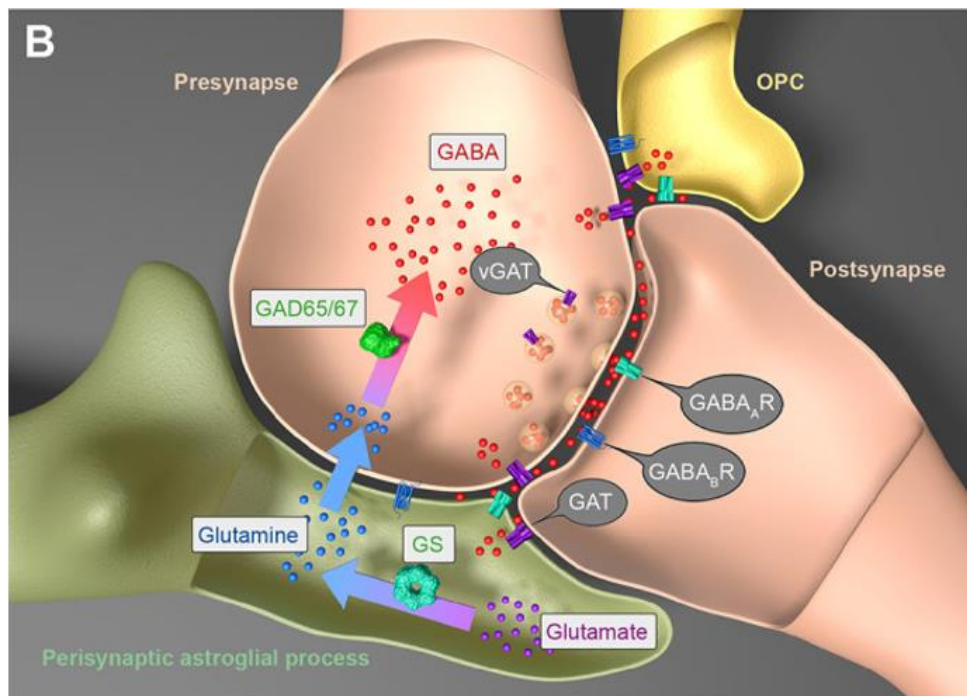


Figure 1. Interplay of interneurons, astrocytes and OPCs in GABA metabolism and neurotransmission. Astrocytes take up glutamate from the extracellular space, transform it via their enzyme glutamine synthetase (GS) to glutamine and release glutamine into the extracellular space. Interneurons take up glutamine and use it to synthesize GABA via glutamate decarboxylases GAD 65 and/or GAD67. Next, GABA is packed in GABA transporter expressing vesicles (vGATs) and ready to be released in the synaptic cleft. Once released from the presynaptic terminal, GABA acts on postsynaptic neuronal GABA_A and GABA_B receptors as well as GABA_A and GABA_B receptors on OPCs. GABAergic transmission is temporally limited by GABA uptake through neuronal GABA transporter GAT1 and astroglial GAT3 transporters. OPCs express GATs as well, but their function needs to be addressed in further studies. (Bai et al., 2021).

Interneurons are the main inhibitory neurons of the CNS, exerting their inhibitory function via release of GABA. They constitute a highly diverse group of cells made up by numerous subclasses (Klausberger and Somogyi, 2008; DeFelipe et al., 2013). Interneurons are classified by 3 main criteria: i) expression of molecular markers such as neuropeptides (somatostatin, cholecystinin, vasoactive intestinal peptide, neuropeptide-Y) or Ca²⁺ binding proteins (parvalbumin, calretinin, calbindin), (ii) morphological aspects, including subcellular target in the postsynaptic neuron (somatic, perisomatic, dendritic), and (iii) action potential firing pattern (fast-spiking, regular-spiking) (Hu et al., 2014). Parvalbumin positive (PV⁺) cells form the main subclass of interneurons, making up 40-50% of all neocortical GABAergic neurons (Rudy et al., 2011) and 30% of all hippocampal GABAergic neurons (Katsumaru et al., 1988; Bezaire and Soltesz, 2013). Their main representatives are basket cells and to a

smaller extend chandelier cells, which both are extensively integrated in local circuits (Pelkey et al., 2017). PV⁺ neurons exhibit highly arborized axons and target the perisomatic domain of mostly excitatory neurons (Freund and Buzsáki, 1996). Many electrophysiological properties of PV⁺ interneurons are optimized for extremely high propagation velocity and reliability (Zaitsev et al., 2007; Bucurenciu et al., 2010; Hu and Jonas, 2014), allowing them to generate stable and precisely timed inhibitory output at high firing frequencies (Liu et al., 2014b). The highly synchronized nature of firing as well as their target domain close to action potential initiation zone prompts the assumption of great inhibitory power of PV⁺ interneurons (Hu et al., 2014), making them an important subject of epilepsy research.

A growing body of evidence links interneuronal cell death and loss of function to epilepsy (Dinocourt et al., 2003; Epsztein et al., 2006; Kumar and Buckmaster, 2006; Sieu et al., 2017). Altering interneuron density has been shown to directly affect E/I balance, underscoring their importance as regulators of cortical excitability (Orduz et al., 2019; Wang et al., 2021; Fang et al., 2022). As previously stated, epileptogenesis is commonly conceptualized as a disturbance of E/I balance with a loss of inhibition, resulting inhibitory restraint being insufficient to contain overshooting excitation (Trevelyan et al., 2006; Trevelyan et al., 2007). Therefore, drugs promoting inhibition or decreasing excitation show clinical effects in seizure suppression (Rogawski and Löscher, 2004; Mula, 2011). Up to this date, the pathophysiological understanding of epileptogenesis is incomplete and research focusses mainly on neuronal cell death and dysfunction. Conversely, AEDs generally target neurons, aiming to reduce neuronal hyperexcitability and promote inhibition (Rogawski and Löscher, 2004). However, therapeutic failure in as much as 30% of patients treated with AEDs (Asadi-Pooya et al., 2017) underscores the importance of considering a broader spectrum of therapeutic targets.

2.3 Glial cells in epilepsy

2.3.1 Oligodendrocyte precursors

Oligodendrocyte progenitor cells (OPCs) are abundantly present throughout the entire CNS (Guo et al., 2021). Due to their expression of nerve/glia antigen-2 (NG2) they are also frequently referred to as NG2 glia (Horner et al., 2002). Besides NG2, they also express platelet-derived growth factor receptor α (PDGFR α) which therefore is well established as a marker for OPCs (Nishiyama et al., 1996). OPCs represent the largest population of proliferating glia cells in the CNS (Dawson et al., 2003), being capable of asymmetrical division (Hill et al., 2014) as well as self-renewal in health and even in response to injury (Hughes et al., 2013). As the name suggests, OPCs also keep differentiating into oligodendrocytes (OLs) even in the adult brain (Psachoulia et al., 2009; Kang et al., 2010; Huang et al., 2014; Huang et al., 2019). Nevertheless, several studies reported on the existence of a stable population of OPCs throughout neurodevelopment and in the adult brain, not serving as a source for

oligodendrogenesis under healthy conditions (Psachoulia et al., 2009; Hughes et al., 2013; Huang et al., 2014; Guo et al., 2021). The existence of this stable group of cells challenges the view of OPCs solely as progenitors for OLs and raises the question, whether they could be involved in physiological and pathophysiological processes beyond myelination (Eugenín-von Bernhardt and Dimou, 2016).

OPCs receive glutamatergic input from excitatory pyramidal neurons (Mangin et al., 2008; Mount et al., 2019) as well as GABAergic input from inhibitory interneurons (Orduz et al., 2015; Orduz et al., 2019) and thus are well integrated in local networks makes them promising candidates for further consideration. Even more so, if considering that OPC proliferation and differentiation into myelinating oligodendrocytes is influenced by neuronal activity (Li et al., 2010; Gibson et al., 2014; Mitew et al., 2018). In several epileptic paradigms (viral encephalitis model, intraperitoneal pilocarpine model and lithium-pilocarpine model), OPC density in the hippocampus is increased (Luo et al., 2015; Wu et al., 2019; Bell et al., 2020). However, Luo (2015) reported that OPC density was lower than in the control group in the late chronic phase, defined as 2 months after the first occurrence of SRSs, and oligodendrocyte densities as well as myelination were compromised already within 24 hours of inducing status epilepticus (SE). In a model of focal cortical dysplasia, a common pathology in medically intractable TLE, OPC densities in the dysplastic cortex grey matter as well as the proliferation of cultured OPCs isolated from the dysplastic cortex were decreased (Donkels et al., 2020). Similarly, mature oligodendrocytes were diminished and myelin sheath thickness was reduced. Therefore, how OPCs react towards induction of SE and their role in epileptogenesis are still controversial and elusive.

2.3.2 OPC-interneuron communication

OPCs display interesting physiological properties normally only ascribed to neurons. For instance, they form synapses with excitatory and inhibitory neurons, making them unique among glia cells (Bergles et al., 2000; Ge et al., 2006; Kukley et al., 2008; Vélez-Fort et al., 2010; Orduz et al., 2015). While OPCs across all regions of the adult brain receive direct synaptic input predominantly from excitatory neurons (Mount et al., 2019), it has been shown that in the developing mouse neocortex OPCs receive massive synaptic input from fast spiking PV⁺ interneurons via a γ 2-subunit containing GABA_A receptor (Orduz et al., 2015; Orduz et al., 2019). A peak of synaptic transmission between interneurons and OPCs is reached in the second postnatal week, directly preceding a major burst of differentiation into OLs (Orduz et al., 2015). This indicates a close relationship between GABA_AR mediated OPC-interneuron signaling and OPC differentiation as well as interneuron myelination (Bai et al., 2021). Moreover, disruption of γ 2-dependent GABAergic signalling between OPCs and PV⁺ interneurons leads to abnormal myelination later during development, characterized by longer

internodes and nodes and aberrant myelin distribution. Those changes result in insufficient feedforward inhibition, ultimately perturbing E/I balance (Benamer et al., 2020). Recent evidence shows that OPC-Interneuron crosstalk via a GABA_BR-TWEAK (tumor necrosis factor-like weak inducer of apoptosis) pathway is pivotal in regulating interneuron density and function in the medial prefrontal cortex (mPFC) during early developmental stages (Fang et al., 2022). In OPC-GABA_BR ablated mice, the density of cortical interneurons was found to be increased, however the frequency of spontaneous inhibitory post synaptic currents (sIPSCs) and GABAergic release onto OPCs was decreased. Moreover, myelin formation was deficient, and the mice exhibited severe cognitive impairments. Thus, GABA_BR mediated OPC-Interneuron crosstalk appears to be crucial for fine-tuning E/I balance. These studies suggest that GABAergic communication between OPC and interneurons is a pivotal determinant of the E/I balance in healthy conditions. However, whether and how OPC-interneuron communication affects epileptogenesis remains largely unknown.

2.3.3 Gliosis in epilepsy

Microglia are the innate immune cells of the CNS, which respond to injury by releasing pro-inflammatory cytokines and performing phagocytosis (Takahashi et al., 2005). Among brain cells, they can be identified by their expression of ionized calcium binding adapter molecule 1 (Iba1) (Imai et al., 1996). Through their motile processes, they monitor an area up to ten times their size and form extensive contacts with neurons and astrocytes. This allows them to influence synaptic transmission and respond to injury (Davalos et al., 2005; Nimmerjahn et al., 2005; Dibaj et al., 2010; Kettenmann et al., 2013). The observation, that some anti-inflammatory drugs also exert anticonvulsive effects has given rise to the hypothesis that brain inflammation takes part in epileptogenesis (Vezzani et al., 2011; Colonna and Butovsky, 2017). However, the precise role of microglia in epileptogenesis is still subject to controversial debate. It is well established in human tissue and several animal models, that microglia acquire reactive morphology following SE (Liu et al., 2014a; van Vliet et al., 2016). In fact, preventing microglial activation and proliferation showed neuroprotective effects and mitigated the course of disease (Heo et al., 2006; Wang et al., 2015).

Astrocytes are abundantly and ubiquitously distributed throughout the CNS, displaying great functional and morphological heterogeneity (Köhler et al., 2021). Astrocytic role in maintaining CNS homeostasis include assisting neuronal metabolism (Rouach et al., 2008), regulating blood-brain barrier permeability and activity-dependent blood-flow (Attwell et al., 2010; MacVicar and Newman, 2015), K⁺ buffering (Seifert et al., 2009) and neurotransmitter homeostasis (Walls et al., 2015; Boddum et al., 2016; Mahmoud et al., 2019). Astrocytes acquire a reactive phenotype in several pathologic conditions of the CNS, including TLE (Sofroniew, 2014; Patel et al., 2019). This process, termed astrogliosis, is characterized by

cellular hypertrophy, increased proliferation and intensely up-regulated expression of proteins such as glial fibrillary acid protein (GFAP) and vimentin (Silver and Miller, 2004).

2.4 Animals models of MTLE

Depending on the focus of research, various models are available to study epileptic disorders. To study epileptogenesis, in vivo application of chemoconvulsants such as kainate (KA) (glutamate agonist) or pilocarpine (cholinomimetic) is used most commonly (Leite et al., 2002). Upon injection animals enter SE triggering progressive network changes, which after a latent period result in spontaneous recurrent seizures (SRS). Moreover, key histopathological hallmarks found in resected tissue from patients undergoing anti-epileptic surgery are reproduced (Lévesque and Avoli, 2013). Systemic application of chemoconvulsants (intraperitoneal, intravenous or subcutaneous) requires the least resources or technical expertise, but falls short compared to local application forms in regards to several aspects. For instance, excitotoxic damage is created mainly in the hippocampus but also extends beyond limbic structures (Becker, 2018). Moreover, the mortality rate is higher and SRS are produced less reliably (Jefferys et al., 2016). Local application (intrahippocampal, intracortical) allows for controlled creation of an epileptic focus in limbic structures, resembling the human condition more closely. Intrahippocampal kainate administration is a well-established model to study epileptogenesis, recapitulating key features of human MTLE epilepsy (Suzuki et al., 1995; Bouilleret et al., 1999). While being generally considered to be well-tolerable and reliable, data on mortality rates (0% to 20%) and development of SRS (88% to 100%) still varies (Riban et al., 2002; Gröticke et al., 2008).

In this study, we decided to utilize the model of intracortical kainate application. The main advantage of this model lies in reduced traumatic damage, especially to the first subfield of the cornu ammonis (CA1) (Bedner et al., 2015). Mortality rates in this model are very low (3,4% within the first week), despite evoking extensive histopathological changes and high seizure frequency. Upon injection mice enter status epilepticus lasting up to several hours. This acute phase characterized by convulsive behaviour (rearing, forelimb clonus, falling) is followed by a latent, seizure free period of approximately 4-6 days duration. In the subsequent chronic phase SRS occur in 93% of the mice, recruiting the hippocampus bilaterally (Bedner et al., 2015; Jefferys et al., 2016). Already 2 days after initial kainate injection, pronounced neuronal loss in the CA1, CA3 and hilus region of the hippocampus can be observed, progressing even further with time and being accompanied by reactive gliosis and granule cell dispersion (Jefferys et al., 2016). Intracortical injection of kainate is a well-tolerable model which reliably reproduces functional as well as histopathological features of human MTLE. However, this procedure bears some resemblance to cortical stab wound injury, a model commonly used to investigate traumatic brain injury which has previously been linked to OPC reactivity (Levine

et al., 2001; Scheller et al., 2017). In this study, an adapted version of intracortical kainate injections was used aiming to reduce traumatic tissue damage even further, while still reproducing histopathological and functional features of human MTLE.

2.5 Aim of the study

After centuries of neuro-centric research, glial cells are now increasingly receiving attention for their involvement in the process of epileptogenesis. OPCs are extensively integrated in local networks and engage in somatic and synaptic communication with neurons. Moreover, OPCs have been shown to react in the epileptic brain, but the precise quality of this reaction requires further investigation. A recent study from our group has demonstrated that OPCs regulate interneuronal apoptosis in a GABA_BR dependent manner and influence E/I balance.

Therefore, the central aim of this study is to investigate the role of OPC-GABA_BR signaling in regulating the response of OPCs and PV⁺ interneurons to hyperexcitable network dysfunction in TLE.

To this end, we will address the following topics:

We will evaluate the influence of OPC-GABA_BR on the cells of the oligodendroglial lineage in cortex and hippocampus during the acute and chronic phase of epilepsy. GABA_BR function will be investigated by utilizing OPC-specific GABA_BR deletion and reporter expression (GCaMP3) induced at postnatal day 7 and 8 in transgenic mice. Epileptogenic network changes will be elicited by induction of SE at postnatal week 9 via intracortical injection of kainate. Cell population will be assessed with immunohistochemistry of cell specific markers.

We will furthermore explore the effect of GABA_BR of OPCs on interneuron susceptibility towards excitotoxicity during the early stages of epileptogenesis. For that, we will quantify interneuron density in the cortex and hippocampus with immunohistochemistry and compare cell density in ctl and cKO cortex and hippocampus at 1 day and 1week post kainite injection.

We will also assess the effect of OPC-GABA_BR signaling on gliosis by quantifying the fluorescent intensity of astrocytic GFAP and microglial Iba1 immunoreactivity at the site of the epileptic lesion.

With these studies, we will reveal the impact of OPC-GABA_BRs on OPC and interneuron changes during the progress of epilepsy in the mouse model of temporal lobe epilepsy.

3. Materials and Methods

3.1 Materials

3.1.1 Chemicals

Table 1. List of chemicals

Substance	Manufacturer
Acetic acid (100%)	VWR International, Darmstadt, Germany
Agarose low melt	Greiner Bio One, Frickenhausen, Germany
Agarose powder	Serva Electrophoresis, Heidelberg, Germany
Bepathen balm	Bayer, Leverkusen, Germany
Bovine Serum albumin	Sigma Aldrich
Buprenorphine (Temgesic®)	Indivior Europe Limited, Dublin, Ireland
DreamTaq™ Hot Start Green DNA Polymerase	Thermo Fischer Scientific, Dreieich, Germany
Ethanol (99 %)	VWR International, Darmstadt, Germany
Ethylenediaminetetraacetate (EDTA)	Grüssing GmbH, Filsum, Germany
HCl	Bernd Kraft, Duisburg, Germany
Horse Serum	Thermo Fisher Scientific, Dreieich, Germany
Immuno-Mount medium	Shandon, Pittsburgh, Pennsylvania
Isoflurane	Piramal, Bethlehem, Pennsylvania
Kainate	Tocris, Wiesbaden-Nordenstadt, Germany
Ketamine (100 mg/ml)	Ketavet, Pfizer, Karlsruhe, Germany
MgCl ₂	Carl Roth, Karlsruhe, Germany
Miglyol ®812	Ceasar & Loretz GmbH, Hilden, Germany
NaCl	VWR International, Darmstadt, Germany
NaCl solution (0,9 %)	B. Braun AG, Melsungen, Germany
NaOH	Grüssing GmbH, Filsum, Germany
Nitrous Oxide	provided by Universität des Saarlandes
Oxygen	provided by Universität des Saarlandes
Paraformaldehyde	Sigma Aldrich, Taufkirchen, Germany
ROTI®Seal	Carl Roth, Karlsruhe, Germany
Sodium phosphate buffer (PBS)	neuFroxx GmbH, Einhausen, Germany
Tamoxifen	Carbolution, Neunkirchen, Germany
Tris(hydroxymethyl)aminomethane	Sigma Aldrich, Taufkirchen, Germany
Triton-X-100	AppliChem GmbH, Darmstadt, Germany

Xylazine (20 mg/ml)	Bayer, Leverkusen, Germany
---------------------	----------------------------

3.1.2 Consumables

Table 2. List of consumables

Consumble	Manufacturer
Coverslips	Menzelgläser, Braunschweig, Germany
Eppendorf® reaction tubes 0.5 ml, 1.5 ml, 2 ml, and 5 ml	Sarstedt, Nümbrecht, Germany
Falcon tubes	Greiner Bio-One, Frickenhausen, Germany
Glass pipettes	VWR International, Darmstadt, Germany
Non absorbable braided silk suture	F.S.T. Pharmacia, Heidelberg, Germany
Object slides	Karl Hecht, Sondheim, Germany
Optical clear cover foil	Sarstedt, Nümbrecht, Germany
Pipette tips	Sarstedt, Nümbrecht, Germany
Single-use pipette 5 ml and 20 ml	Greiner Bio One, Frickenhausen, Germany
Syringe 0.5 ml	B.Braun AG, Melsungen, Germany
48-well cell culture plates	Sarstedt, Nümbrecht, Germany
96-well PCR plates	Brand, Wertheim, Germany

3.1.3 Devices

Table 3. List of devices

Device	Manufacturer
AxioScan.Z1	Zeiss, Oberkochen, Germany
Centrifuges	Eppendorf, Hamburg, Germany
Head holder	Custom-made (G. Stopper, Molecular Physiology)
peqSTAR Thermo Cycler	Peqlab Biotechnology GmbH, Erlangen, Germany
Pipettes	Brand, Wertheim, Germany
Preparations- and perfusion instruments	F.S.T. Pharmacia, Heidelberg, Germany
Quantum gel documentation system	Peqlab Biotechnology GmbH, Erlangen, Germany
Scales (CPA 8201/CPA 2245)	Sartorius, Göttingen, Germany
Shaker DRS-12	NeoLab, Heidelberg, Germany
Stereotaxic frame	Robot stereotaxic, Neurostar, Tübingen, Germany

Vibratom VT1000S	Leica, Wetzlar, Germany
10 µl Nanofil syringe with 34 GA blunt needle	World Precision Instruments, Sarasota, USA

3.1.4 Buffers and aqueous solutions

Phosphate buffered saline (PBS, 1x)
pH= 7.2-7.4

PBS (10x)	10%	(v/v)
ddH ₂ O	90%	(v/v)

Phosphate-buffered saline (PBS, 10x)

NaCl	1370	mM
Na ₂ HPO ₄	100	mM
KCl	27	mM
KH ₂ PO ₄	18	mM

4% PFA in PBS

Paraformaldehyde (PFA)	4.0 %	(v/v)
Na ₂ HPO ₄	10.000	mM
NaH ₂ PO ₄	6000	mM

Tris-Acetate-EDTA-buffer (TAE, 50x)

Tris(hydroxymethyl)aminomethane	2000	mM
Acetic acid (100 %)	1	mM
Ethylenediaminetetraacetate (EDTA), 0,5 M, pH 8	1	mM

Agarose gel (1.5% or 2%)

Agarose powder	7.5 or 10	g
TAE buffer	500	ml
Ethidium bromide (1 %)	0.00025 %	(v/v)

Blocking and antibody solution

1x PBS	94.5 %	(v/v)
Horse serum	5.0 %	(v/v)
Triton-X-10	0.5 %	(v/v)

Tissue preparation solution (Sigma Aldrich)

KCl	250	mM
Tris(hydroxymethyl)aminomethane	100	mM
EDTA	10	mM

Neutralisation solution

ddH ₂ O	97%	(v/v)
Bovine serum albumin	3%	(v/v)

Syringe cleaning solution in ddH₂O

Hamilton cleaning solution	25%	(v/v)
----------------------------	-----	-------

3.1.5 Drugs

Ketamine/Xylazine in 0.9% NaCl

NaCl solution (0.9 %)	81%	(v/v)
Ketamine (100 mg/ml)	14%	(v/v)
Xylazine (200 mg/ml)	5%	(v/v)

Respiration gas mixture

Oxygen	0.6	L/min
Nitrous oxide	0.4	L/min
Isoflurane	1.5 % - 5 %	(v/v)

Tamoxifen in Miglyol

Tamoxifen	10	mg
Miglyol	1	ml

Kainate in 0.9 % NaCl

Kainate	20	mM
---------	----	----

3.1.6 Antibodies

Primary antibodies

Table 4. List of primary antibodies

Antigen	Clonality	Host	Dilution	Manufacturer
GFP	pc	chicken	1:1000	Invitrogen
PDGFR α	pc	goat	1:1000	R & D Systems
Ki67	pc	rabbit	1:500	Thermo
Ki67	mc	rat	1:500	Invitrogen
CD31	mc	rat	1:100	BD Pharmingen
CC1	mc	mouse	1:300	Calbiochem
Olig2	pc	rabbit	1:1000	Millipore
Iba1	pc	goat	1:1000	abcam
GFAP	pc	rabbit	1:1000	Dako
NeuN	mc	mouse	1:500	Millipore
NeuN	pc	rabbit	1:1000	abcam
PV	pc	rabbit	1:1000	Swant
PV	mc	mouse	1:500	Sigma
Zo1	pc	rabbit	1:200	Thermo Fisher

Secondary antibodies

Table 5. List of secondary antibodies

Host anti-target	Conjugated fluorophore	Dilution	Manufacturer
Donkey anti-chicken	Alexa Fluor® 488	1:1000	Jackson Immuno
Donkey anti-goat	Alexa Fluor® 546	1:1000	Life Technologies Cooperation
Donkey anti-rabbit	Alexa Fluor® 647	1:1000	Invitrogen
Donkey anti-mouse			Life Technologies Cooperation
Donkey anti-rat	Alexa Fluor® 750	1:1000	Invitrogen
Donkey anti-rabbit			Abcam
Donkey anti-mouse			Invitrogen

3.1.7 Dyes

Table 6. List of dyes

Component	Working solution	Manufacturer
4',6-Diamidin-2-phenylindol (DAPI)	0.025 µg/ml	Sigma, Taufkirchen
Ethidium bromide	0.015%	Carl Roth, Karlsruhe
Easy ladder	-	Bioline, Neunkirchen

3.1.8 Primers

Table 7. List of primers for genotyping

Mouse line	Primer number	Sequence	Product size [bp]
GABA _B	24392 fwd	5'-GCTCTTCACCTTTCAACCCAGCCT-CAGGCAGGG-3'	KI 742 WT 526
	24393 rev	5'-CCTCCTGCCTTCCTCCACATGTTT-CTCCT-3'	
GCaMP3 KI	27632 fwd	5'-CACGTGATGACAAACCTTGG-3'	KI 245 WT 327
	27490 rev	5'-ACATTAAGCAGCGTATCC-3'	
GCaMP3 WT	14025 fwd	5'-CTCTGCTGCCTCCTGGCTTCT-3'	
	14026 rev	5'-CGAGGCGGATCACAAGCAATA-3'	
NG2-CreERT2	19398 fwd	5'-GGCAAACCCAGAGCCCTGCC-3'	KI 829 WT 557
	19399 rev	5'-GCCGGCAAACCCAGAGCCCTGCC-3'	
	19400 CreERT2 rev	5'-GCCCGGACCGACGATGAAGC-3'	

3.1.9 Genetically modified mouse lines

The goal of this study is to investigate the function of GABA_B receptors specifically in cells of the oligodendroglial lineage. Therefore, we took advantage of the *Cre-loxP* system, which is a reliable tool for the generation of spatiotemporally controlled mutant mice (Fig. 2).

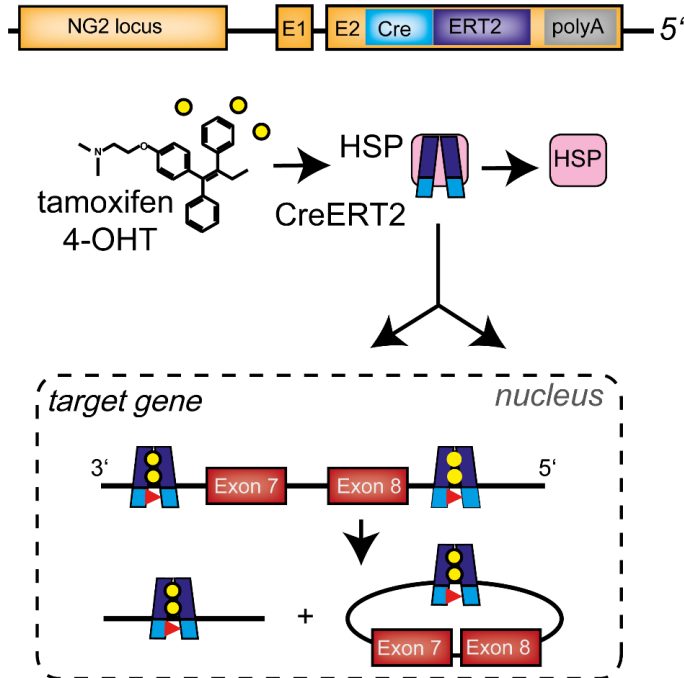


Figure 2. Tamoxifen administration induces Cre recombination of exon 7 and 8 in the *gabbr1* gene. The open reading frame for the estrogen receptor bound Cre DNA recombinase CreERT2 is knocked into the NG2 locus. In the inactivated state, CreERT2 is bound to heat shock protein HSP90 and located in the cytosol. Upon administration of 4-hydroxy-tamoxifen, a ligand to the estrogen receptor ERT2, HSP90 dissociates. CreERT2 translocates into the nucleus and catalyses site specific recombination by targeting *loxP* sites framing exon 7 and 8 of the *gabbr1* gene, excising the DNA strands located in between.

To target both OPCs and oligodendrocytes, induction of recombination at the OPC stage is necessary. To this purpose we used TgH (NG2-Cre^{ERT2}) mice (Huang et al., 2014), which express CreERT2 in an OPC specific manner. Crossbreeding with TgH (GABA_{B1}R^{fl/fl}) mice introduced the GABA binding region (exon 7 and 8) of the *gabbr1* gene as target for Cre recombination (Haller et al., 2004). Consequently, OPCs in double transgenic mice are incapacitated of functional GABA_B receptor expression. In addition, the TgH (Rosa-26-CAG-IsI-GCaMP3) mouse line was introduced (Paukert et al., 2014). This mouse line contains a loxP flanked stop codon in front of the gene for the Ca²⁺ indicator GCaMP3, thus GCaMP3 is expressed upon activation of CreERT2, indicating recombination success.

Table 8: List of transgenic mouse lines

Transgenic mouse line	Brief	MGI ID	Reference
TgH (GABA _{B1} R ^{fl/fl})	GABA _B receptor subunit 1 deletion	3512743	(Haller et. al., 2004)
TgH (NG2-Cre ^{ERT2})	OPC-specific Cre ^{ERT2} -driver line		(Huang et al., 2014)
TgH (Rosa-26-CAG-IsI-GCaMP3)	GCaMP3 reporter expression	5659933	(Paukert et al., 2014)



Figure 3. Construct of the NG2-Cre^{ERT2} x GABA_{B1}R^{fl/fl} x GCaMP3

Mice with the genotype NG2^{ct2/wt} x GABA_{B1}R^{fl/fl} x Stop^{fl/fl}-GCaMP3 were used as conditional knock-out (cKO) and mice with the genotypes NG2^{ct2/wt} x GABA_{B1}R^{wt/wt} x Rosa26-Stop^{fl/fl}-GCaMP3 and NG2^{wt/wt} x GABA_{B1}R^{fl/fl} x Rosa26-Stop^{fl/fl} GCaMP3 were used as controls.

3.1.10 Software

FIJI was used for analysis of fluorescence intensity and ZEN 3.1 (blue edition) was used for image analysis. For statistical analysis and generation of graphs GraphPad prism 8 was used. Texts were created in Microsoft Office. EndNote (Clarivate) was used to generate citations.

3.2 Methods

3.2.1 Mouse administration and ethics statement

All experiments were carried out in strict accordance with the European and German guidelines for welfare of experimental animals and approved by the Saarland state's "Landesamt für Gesundheit und Verbraucherschutz" in Saarbrücken, Germany (licence number 34/2016, 36/2016). Animals were kept and bred in the animal facility of the Center for Integrative Physiology and Molecular Medicine (CIPMM, Homburg) and administration was conducted with PyRat (Python based Relational Animal Tracking, Scionics Computer Innovation GmbH).

3.2.2 Experimental design

This study reports of data from three different time points, one day, one week and two weeks after induction of status epilepticus by intracortical kainate injection or control injection with saline. Mice were kept at the animal facility of the CIPMM and fed a breeding diet (V1125) *ad libitum*. They were exposed to a 12-hour light/dark cycle at temperatures of 20° C and a humidity of 55-70%. All groups received intraperitoneal tamoxifen injection at postnatal day 7 or 8 to induce transgene recombination and received intracortical injection of kainate or saline at postnatal week 9. Depending on the group, the mice were sacrificed by perfusion at one day, one week or 2 weeks post injection. Cell counting and fluorescence intensity measurement were performed on immunostained coronal brain slices, focussing on cortex, CA1 region and dentate gyrus (DG). Mice of both genders were included in the experiments.

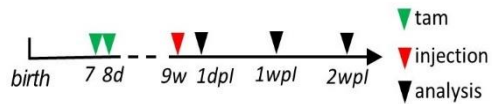


Figure 4. Experimental schedule

3.2.3 Genotyping

DNA extraction

DNA was extracted from tail biopsies, which were stored at -20° C until further processing. The tissue was incubated with 62.5 µl of extraction solution (tissue preparation solution, Sigma Aldrich) with gentle vibration at 600 rpm for 10 minutes at room temperature, then was incubated for 20 minutes at 95° C. Next, 50 µl of neutralizing solution was added. If not used immediately for PCR, the DNA samples were stored at 4° C.

Polymerase chain reaction (PCR)

For genotyping PCRs, the DNA samples were incubated with prepared sample buffer (DreamTaq™ Hot Start Green DNA Polymerase) and oligonucleotide primers in a 96-well PCR plate. The plate was covered with adhesive foil and centrifuged shortly. The reaction was run in PEQ ThermoCyclers with a program appropriate for annealing temperature of the primers and number of cycles needed.

Agarose gel electrophoresis

To separate DNA fragments, 1.5-2 % agarose gels with ethidium bromide were used. Gels were run at 180 V for 30-45 minutes and results were documented with the Quantum Gel documentation system.

3.2.4 Tamoxifen administration

Tamoxifen was diluted with Miglyol to a concentration of 10 mg/ml. The solution was injected intraperitoneally with the dose of tamoxifen adjusted to the body weight (100 mg/kg) at postnatal day 7 and 8 (Fang et al., 2022).

3.2.5 Unilateral intracortical kainate injection

The unilateral intracortical injection of kainate was performed according to the protocol developed by Bedner and colleagues (Bedner et al., 2015) with a few adjustments. Animals were anesthetized with a 5 % isoflurane, 47.5 % O₂ and 47.5 N₂O mix and weighted. Next, the mice were placed in a stereotaxic frame and anaesthesia with isoflurane was continued at 2 %.

The head was fixed with ear bars, and eyes were protected by application of balm. Prior to the operation, buprenorphine was administered subcutaneously (100 μ l/10 g body weight), after the reaction to a metatarsal pain stimulus lapsed. The scalp was disinfected with 70% ethanol and a midline incision was made. The injection site above the right dorsal hippocampus was identified (1.9 mm posterior to bregma, 1.5 mm from the sagittal suture at a depth of 1.3mm from the skull surface), followed by a manual drilling of the skull and dura puncture with a needle. A volume of 70 nl Kainate (20mM in 0.9% NaCl) was injected with the 10 μ l Nanofil syringe (34 GA blunt needle) at the depth of 1 mm. Over the lapse of 1 minute, 70 nl of kainate were injected and the needle was left to remain in the cortex for another minute to prevent reflux. Control injections were performed with 0.9 % saline. The scalp was sewn with simple interrupted sutures (non-absorbable) and animals were moved to a single inhabited cage and placed on heating pad. For three consecutive days after surgery, buprenorphine was administered to mice according to body weight (100 μ l/10 g body weight). Mice were perfused either 1 day, 1 week or 2 weeks after intracortical injection. Due to Sars-Cov2 pandemic, it was not possible for me to obtain the license for animal welfare in scientific settings. Therefore all the surgeries and mouse handling were performed by Dr. Xianshu Bai.

3.2.6 Whole body perfusion fixation

Mice were anesthetized using ketamine/-xylazine (250 mg/kg and 50 mg/kg bodyweight, respectively) diluted in 0.9% NaCl. When no reaction to pain stimuli applied at the metatarsus could be triggered, bilateral axillary thoracotomy was performed. The exposed heart was punctured in the left ventricle with a butterfly needle and the mice were perfused with 1 x PBS. By incision of the right atrium, blood and PBS could be drained from the cardiovascular system. When PBS ran clear and no more blood was drained from the body, perfusion was changed to 4% formaldehyde in PB and continued until 20-25 ml were perfused. Next, the brain was diligently removed from the skull and kept at 4° C in 4 % formaldehyde overnight, which was exchanged with 1 x PBS the following day.

3.2.7 Slice preparation

Fixed brains were cut into free floating coronal slices of 30 μ m thickness in 1x PBS using a Leica VT1000S vibratome. Slices were collected from the injection site, which was visible macroscopically at the brain surface and on the slices, and kept separately in a 48-well plates in PBS.

3.2.8 Immunohistochemistry

Coronal slices were incubated for 1 hour in blocking buffer (5% horse serum, 0.5% Triton X in 1x PBS) at room temperature to make the cell membrane permeable. Next, primary antibodies diluted in blocking buffer were applied to the slices (100 μ l per well) and kept at 4° C overnight.

The following day, 3 washing steps with 1 x PBS were conducted to remove access primary antibodies. Secondary antibodies and DAPI for nucleic acid staining (1:1000 dilution) were diluted in blocking buffer and the brain slices were incubated with the secondary antibody solution for 2 hours in the dark, in order to preserve fluorophores. Again, 3 washing steps with 1 x PBS were performed and the slices were mounted on slides and covered with cover glasses. After the mounting medium had dried, the slices were sealed with fast drying sealing varnish.

3.2.9 Automated epifluorescence microscopy

Immunostained slices were scanned with the automated slide scanner AxioScan.Z1, an epifluorescence microscope equipped with a LED light source (Colibri 7; Zeiss Jena, Germany) as well as Plan-Apochromat 10x / 0.45 and 20x / 0.8 objectives. Appropriate excitation and emission filter settings were chosen and images were recorded in stacks of 7.5 µm thickness.

3.2.10 Data analysis

Cell counting

Manual cell counting was performed for the immunostaining combinations PDGFRα/CC1/Olig2/GFP, PDGFRα/Ki67/GFP/CD31, PDGFRα/Ki67/GFP/Zo1 and PDGFRα/PV/NeuN/GFP. The images were scanned by the automated slide scanner AxioScan.Z1 and analysed with the Zen blue 3.1 software at the region of interest (cortex, CA1 and DG). Within this area, cells positive for the antigens in question were counted under consideration of their morphology (for more details see below in the sections 3.1, 3.3 and 3.4 of the results part). Taking into account that the final analysed images were maximum intensity projection of 7.5 µm thick images, the cell density was determined with the formula:

$$\text{cell density [per } 1 \times 10^{-3} \text{ mm}^3] = \frac{\text{number of counted cells}}{\text{area [in } \mu\text{m}^2] \times 7.5} \times 10^{-6}$$

Fluorescence intensity measurement

Fluorescence intensity measurement was conducted for the immunostaining combination GFP/Iba1/Ki67/GFAP. An area of the ipsilateral cortex of 4000 µm length measured from the longitudinal cerebral fissure and containing the injection site was exported as TIF file. The TIF files for the channels representing Iba1 and GFAP were opened with ImageJ, converted to a stack and the scale was manually set to a length of 4000 µm. Next, the custom-developed LROI plugin was used to determine the fluorescence intensity at different distances to the injection site. For this purpose, a line perpendicular to the injection site extending equal distances to each side was drawn. With the LROI plugin, 21 squares of 100 µm side length were set to appear along the line. Thus, the central square (number 11) covered the area right

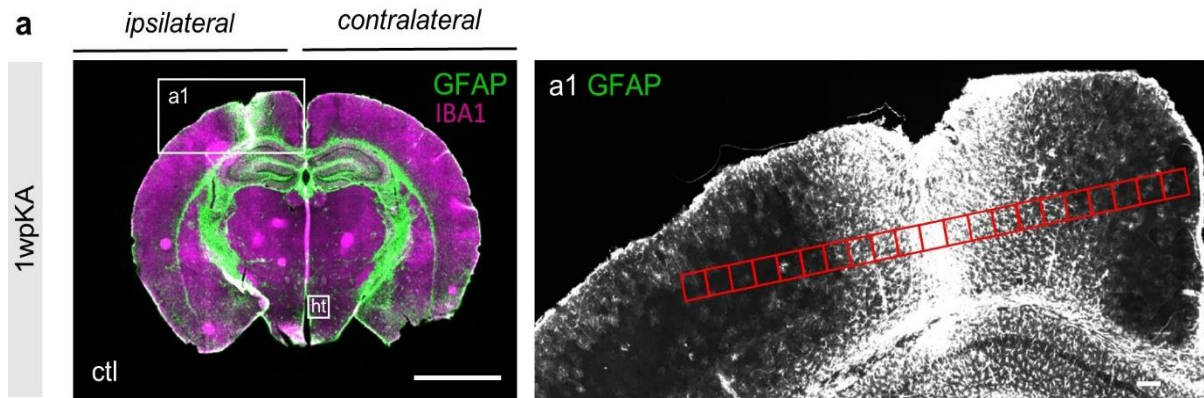


Figure 5. Fluorescence intensity measurement a, Overview (**left column**) of coronal slices of kainate injected mice 1wpI, immunostained with GFAP (astrocytes) and Iba1 (microglia). Magnified image (**right column**) shows analysed region here shown for GFAP (indicated by boxes in the left column). Fluorescence intensity (FI) was measured 1000 μ m to each side of the injection in 100 x 100 μ m segments (red squares). The results were normalized to hypothalamic (ht) FI (indicated by box in the left column). Scalebars = 2000 μ m for the **left column** and 100 μ m for the **right column**.

on the injection site and squares number 1 and 21 were most distant from the injection site. Fluorescence intensity was measured for all the boxes and normalized to fluorescence intensity at the hypothalamus for the respective slice.

3.2.11 Statistics

For statistical analysis, the GraphPad Prism software (GraphPad software Inc., San Diego, CA, USA) was used. For data from cell counting, data points representing mean of cell densities obtained from 2 slices gathered from the same animal were analysed with the 2way ANOVA test. Recombination efficiencies were compared using the unpaired-test. Statistical analysis was performed after checking for outliers using the ROUT method ($Q=1$), however no outliers were identified. For data gained by analysing fluorescence intensity, 2 slices per mouse were analysed and the total mean of all results for one group was used for statistical analysis, performed with multiple t-test. P-values were assumed as: * $p<0.05$, ** $p<0.01$, *** $p<0.001$, **** $p<0.0001$. In the bar graphs, big dots represent mean value of one animal obtained from 2 biological samples. Small dots represent the individual biological sample, samples from the same mouse can be identified by colour.

4. Results

4.1 Conditional knock-out of GABA_BR in OPCs and oligodendrocytes

To study the function of GABA_B receptor (GABA_BR) of OPCs in the development of epilepsy, TgH(NG2-Cre^{ERT2}):GABA_{B1}R^{fl/fl} mice (Fig. 6a) were used to achieve conditional knock-out (cKO) of GABA_BRs in OPCs. To visualize recombined cells, the reporter mouse line GCaMP3 was introduced (Fig. 6a) to create TgH(NG2-Cre^{ERT2}):GABA_{B1}R^{fl/fl}:GCaMP3^{fl/fl} mice. Previous study from our working group has shown that tamoxifen (TAM) injection at the postnatal day 7 and 8 (Fig. 6b) led to recombination of 76% of OPCs at the age of 9 weeks based on the expression of the reporter gene tdTomato. Western blot analysis of magnetic-activated cell sorted OPCs confirmed that the expression of GABA_{B1} subunit is indeed reduced by 75% in GABA_BR cKO mice (Fig. 6c) (Fang et al., 2022). Therefore, in the current study, we employed the same induction protocol, i.e. TAM injection after completion of the first postnatal week, shortly before the onset of oligodendrogenesis at p10 (Orduz et al., 2015), and performed experiments at the age of 9 weeks (Fig. 6b).

First of all, we evaluated the GCaMP3 recombination efficiency in OPCs and OLs in cortex and hippocampus. OPCs were identified by their co-expression of the platelet-derived growth factor receptor α (PDGFR α , P α) and oligodendroglia lineage marker Olig2, as well as their branched morphology with many processes extending into their surroundings (Fig. 6d-f). Oligodendrocytes could be recognized by their expression of CC1 and Olig2 (Fig. 6d-f). In both cortex and hippocampus, the reporter recombination efficiency of OPCs and OLs in ctl and cKO were identical. In the cortex, about 75 % of OPCs (ctl=75.3 \pm 7.5, cKO= 75.4 \pm 5.1) were GCaMP3 positive (Fig. 6d), which is similar to the efficiency of tdTomato labeling as previously reported (Fang et al., 2022). As OPCs keep generating oligodendrocytes, we also observed about 70 % of oligodendrocytes (ctl=73.8 \pm 5.8, cKO= 68.5 \pm 2.0) were recombined for GCaMP3 at 9 weeks (Fig. 6d). In the CA1 region and DG, we found similar recombination efficiency as in the cortex with about 76 % of OPCs ((CA1: ctl=80.0 \pm 5.3, cKO= 85.1 \pm 4.2); (DG: ctl=66.5 \pm 6.1, cKO= 72.2 \pm 7.9)) and 67 % of OLs ((CA1: ctl=71.4 \pm 5.1, cKO= 64.2 \pm 5.3); (DG: ctl=65.0 \pm 5.5, cKO= 66.3 \pm 4.3)) showing GCaMP3 expression (Fig. 6e-f). These results show again that, like tdTomato, GCaMP3 reliably labels recombined OPCs in our mouse model. Moreover, GCaMP3 expression in oligodendrocytes shows that induction of recombination in OPCs

before the onset of oligodendrogenesis is sufficient to target the majority of their oligodendrocyte progeny at postnatal week 9.

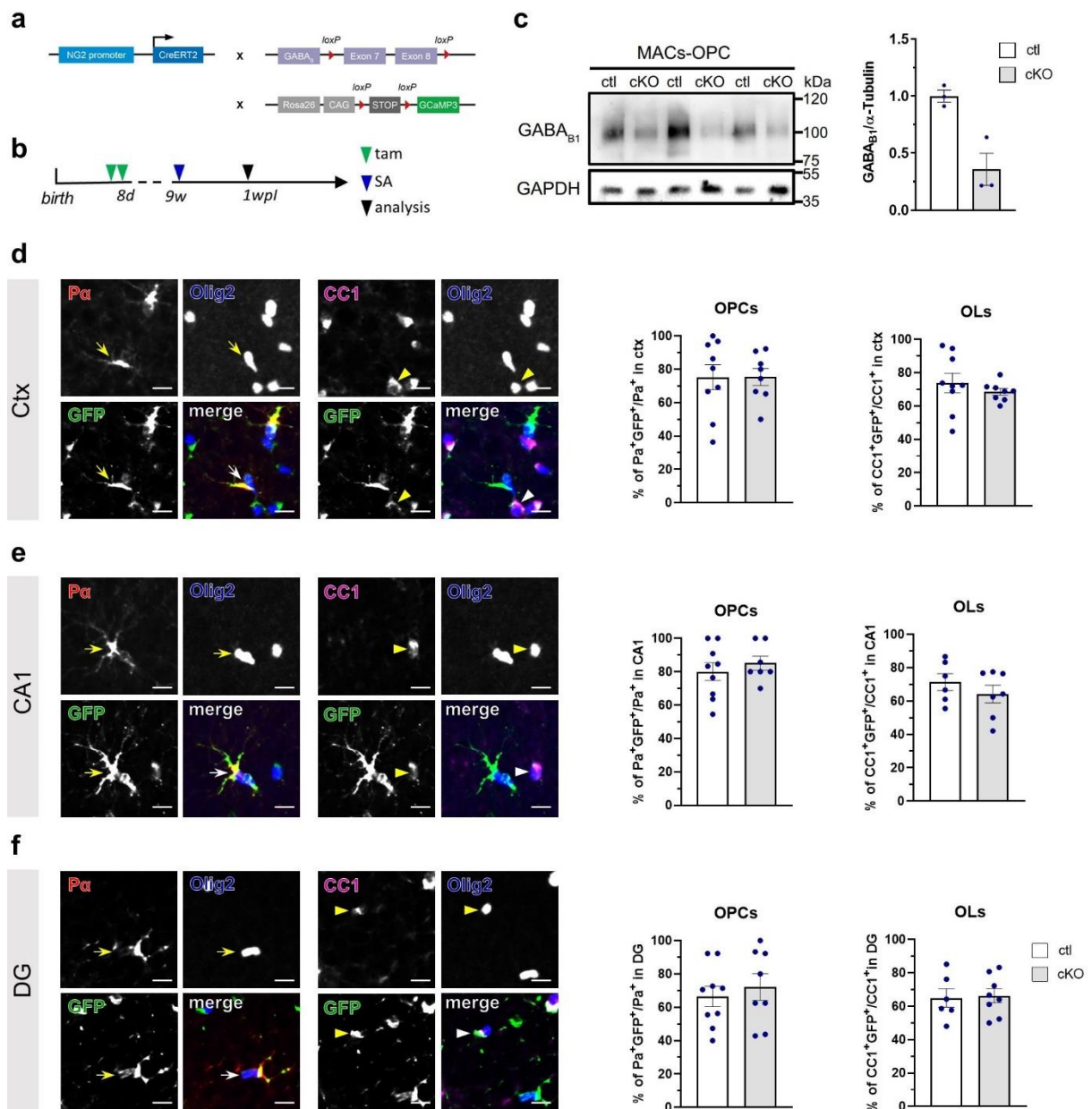


Figure 6. Transgenic mouse model for conditional deletion of GABA_BRs in OPCs. **a**, Scheme of transgene construct. **b**, Experimental schedule. **c**, Western blot analysis of GABA_{B1}R of magnetic activated cell-sorted cortical OPCs (Fang et al., 2022, Fig.1d). **d-f**, Immunostaining (**left column**) and recombination efficiency (**right column**) of OPCs and OLs from the cortex (ctx) (**d**), first subfield of cornu ammonis (CA1) (**e**) and dentate gyrus (DG) (**f**) in the contralateral side at 1wpsA. OPCs are Pa⁺Olig2⁺ (arrow), OLs are CC1⁺Olig2⁺ (triangle), GFP indicates the recombined cells. Statistical analysis: unpaired t-test. Scale bar = 20 μ m. Single dot refers to independent biological sample.

4.2 OPC and oligodendrocyte density is increased in the cKO cortex at one week after kainate injection

OPCs become reactive and increase their proliferating rate under pathological conditions, including epilepsy (Wu et al., 2019). Under epileptic conditions, neuronal network inhibition is mitigated and E/I ratio increases. As OPCs receive direct synaptic input from PV⁺ interneurons (Orduz et al., 2015; Balia et al., 2017) and excitatory neurons (Mount et al., 2019), we asked whether OPCs and oligodendrocytes alter their reaction towards epileptic network changes based on their GABA_BR expression.

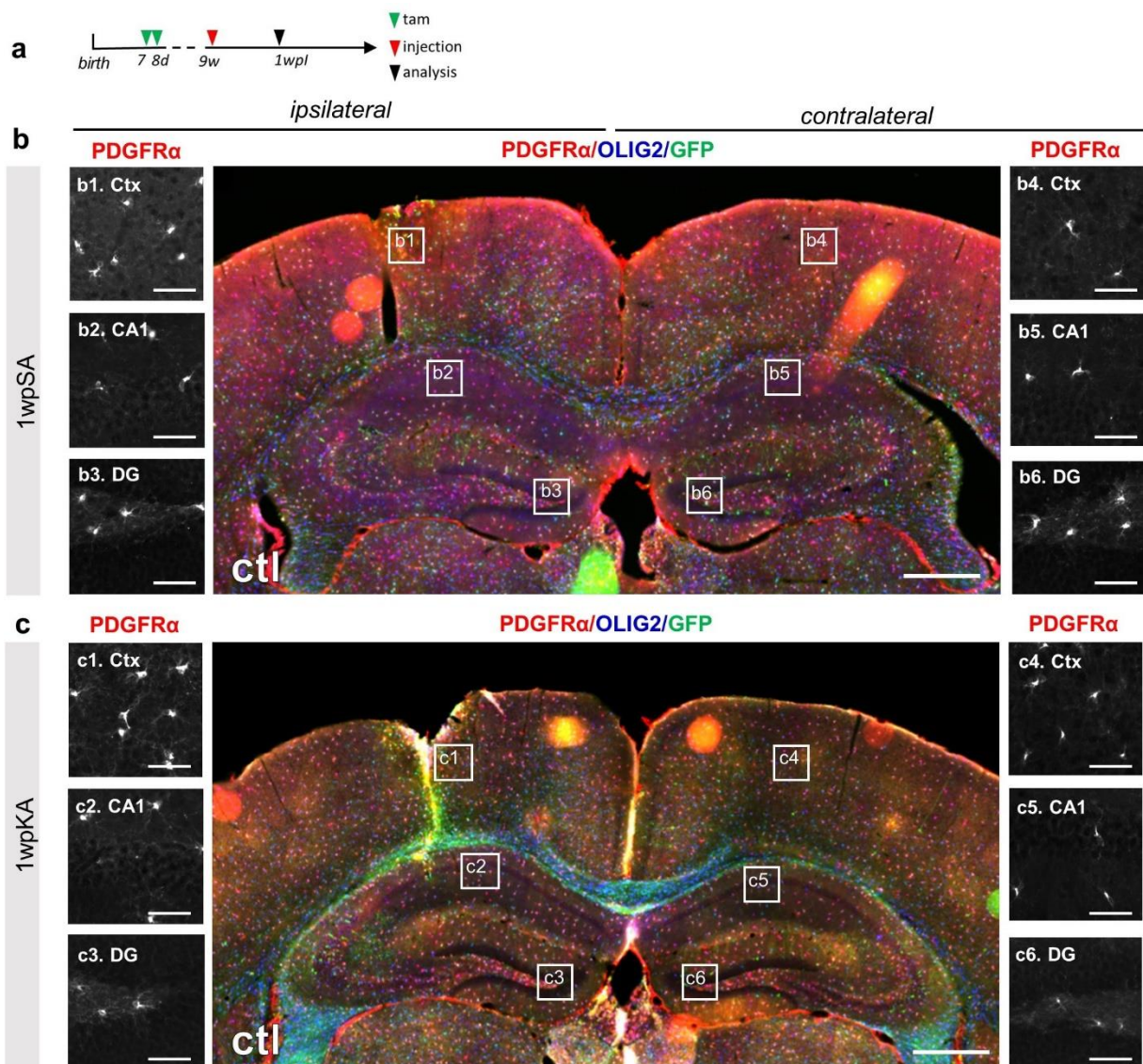


Figure 7. Kainate injection induces an intensive OPC reaction at the injection site. a, Experimental schedule. **b and c**, Overview (middle column) of cortex and hippocampus of saline (**b**) or kainate (**c**) injected ctl mouse brain at 1wpl. Coronal slices were immunostained with P α , Olig2 and GFP. Magnified images of OPCs (P α ⁺) of the ipsilateral (left column) and contralateral side (right column) of ctx, CA1 and DG (indicated boxes in the middle column), respectively. Scale bars = 50 μ m for left and right column and 500 μ m for middle column.

To this end, we investigated the OPC and oligodendrocyte population in the contra- and ipsilateral cortex and hippocampus one week after kainate injection (1wpKA) (Fig. 7a). Saline injection (Fig. 7b) was performed as the sham control of the kainate model (Fig. 7c). Kainate injection induced a notable increase of PDGFR α and GFP fluorescence intensity at the injection site, which was absent in the saline group (Fig. 7b-c). This observation suggests that kainate induces an intensive OPC reaction. After saline injection, in both control and cKO mice, the cell densities of OPCs and OLs at the ipsilateral and contralateral cortex and hippocampus did not differ from healthy control (Fig. 8c-e). These results indicate that injection induced mild stab wound injury does not change OPC and OL density at one week after injection.

We then assessed the effect of OPC-GABA_BR on OPC density at 1wpKA. At the ipsilateral cortex, OPC density did not differ between kainate and saline injected ctl mice (Fig. 8c). However, in cKO animals, kainate injection increased OPC density by 250% compared to saline (KA: 63.5 \pm 3.1 vs SA: 18.0 \pm 1.0) (Fig. 8c). Furthermore, in kainate injected mice OPC density was more than doubled in cKO compared to ctl (cKO: 63.5 \pm 3.1 vs ctl: 29.5 \pm 4.9) (Fig. 8c). Interestingly, mostly recombined cells seemed to participate in the increase of OPC density in the cKO mice. When analysing recombined and non-recombined cells individually, only the recombined OPCs were increased in the cKO mice compared to ctl (Suppl. Fig. 2b).

Contralaterally, OPC density was unaltered between kainate and saline injected mice both in ctl and cKO, as well as between kainate treated ctl and cKO mice (Fig. 8c). Thus, GABA_BR signalling of OPCs tunes down OPC density increase at the onset of the chronic phase 1 week post SE. In the ipsi- and contralateral hippocampal CA1 region and DG, OPC density did not change during the first week of epileptogenesis in both ctl and cKO mice compared to saline injected mice (Fig. 8d-e). Hence, our data show that kainate does not induce OPC density change in the hippocampus at the onset of chronic phase.

Oligodendrocyte density in the ipsilateral cortex was also increased in the cKO mice at 1wpKA. While kainate did not induce oligodendrocyte density change in the ctl mice, the injection of

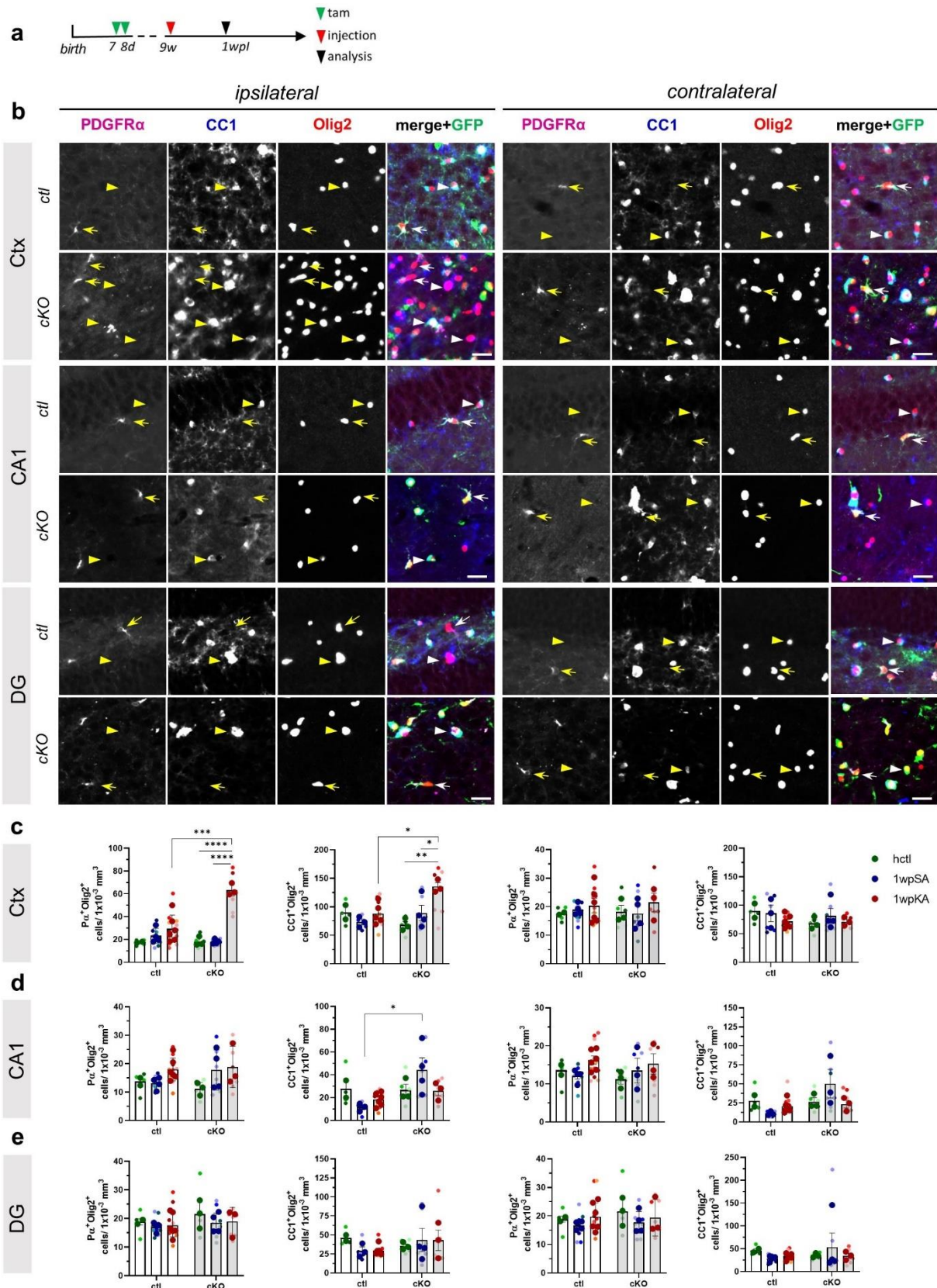


Figure 8. Kainate injection induces OPC and OL density increase only at the ipsilateral cortex of GABA_BR knock-out mice at 1wpi. **a**, Experimental schedule. **b**, Immunostaining of OPCs (P α ⁺Olig2⁺) and OLs (CC1⁺Olig2⁺) in the ipsilateral and contralateral ctx, CA1 and DG of ctl and cKO animals after 1week of KA injection. OPCs: arrow, OLs: triangle. **c-e**, Quantification of OPC and OL density in the ctx, CA1 and DG of healthy control, saline and kainate injected mice (2way ANOVA). Scale bars = 20 μ m

kainate in the cKO mice resulted in an 52% increase of oligodendrocyte density (135.6 ± 6.5) compared to saline injected mice (89.0 ± 13.6) and a 54% increase compared to epileptic ctl mice (88.8 ± 8.1) (Fig. 8c). Contralaterally, oligodendrocyte density did not change between kainate and saline injected mice in both ctl and cKO, as well as between kainate treated ctl and cKO mice (Fig. 8c).

In the hippocampus (CA1 and DG), oligodendrocyte density displayed no reaction towards induction of epilepsy neither in ctl nor cKO mice (Fig. 8d-e). On that account, our data indicate that OPC-GABA_BR signalling prevents an increase of oligodendrocyte density in the ipsilateral cortex but not in the hippocampus during early stages of epileptogenesis.

To investigate the change of OPC and oligodendrocyte density in the development of epilepsy, we analysed cell densities at 1d, 1w and 2wpKA (Fig. 9a), marking the acute stage of epilepsy directly following SE (1dpKA), the onset of the chronic phase (1wpKA) and the early chronic phase (2wpKA). In the cortex of cKO mice, OPC density at the epileptic lesion peaked 1wpKA, significantly exceeding OPC density at 1d and 2wpKA (Fig. 9b). In the ipsilateral CA1 and DG region, OPC density remained unchanged between epileptic and non-epileptic ctl as well as cKO mice at all time points (Fig. 9c, d). Hence, our data suggest that OPC-GABA_BR signalling transiently regulates cortical OPC density at the onset of the chronic phase of epilepsy, but does not regulate OPC density in the hippocampus. Oligodendrocyte density at the cortical lesion site of cKO mice increased at 1wpKA compared to 1dpKA (Fig. 9b) and stayed in a high level at 2wpKA (Fig. 9b). In CA1 and DG, reduction of GABA_BR signalling of OPCs did not alter oligodendrocyte density at 1d, 1w and 2wpKA (Fig. 9c-d). Therefore, our data indicate that OPC-GABA_BR impedes oligodendrocyte density increase in the cortex, but not in the hippocampus.

Taken together, our results suggest that GABA_B receptor signalling of OPCs inhibits a transient increase of OPC density and a sustained increase of oligodendrocyte density occurring in the early phase of epilepsy in the cortex but not in the hippocampus.

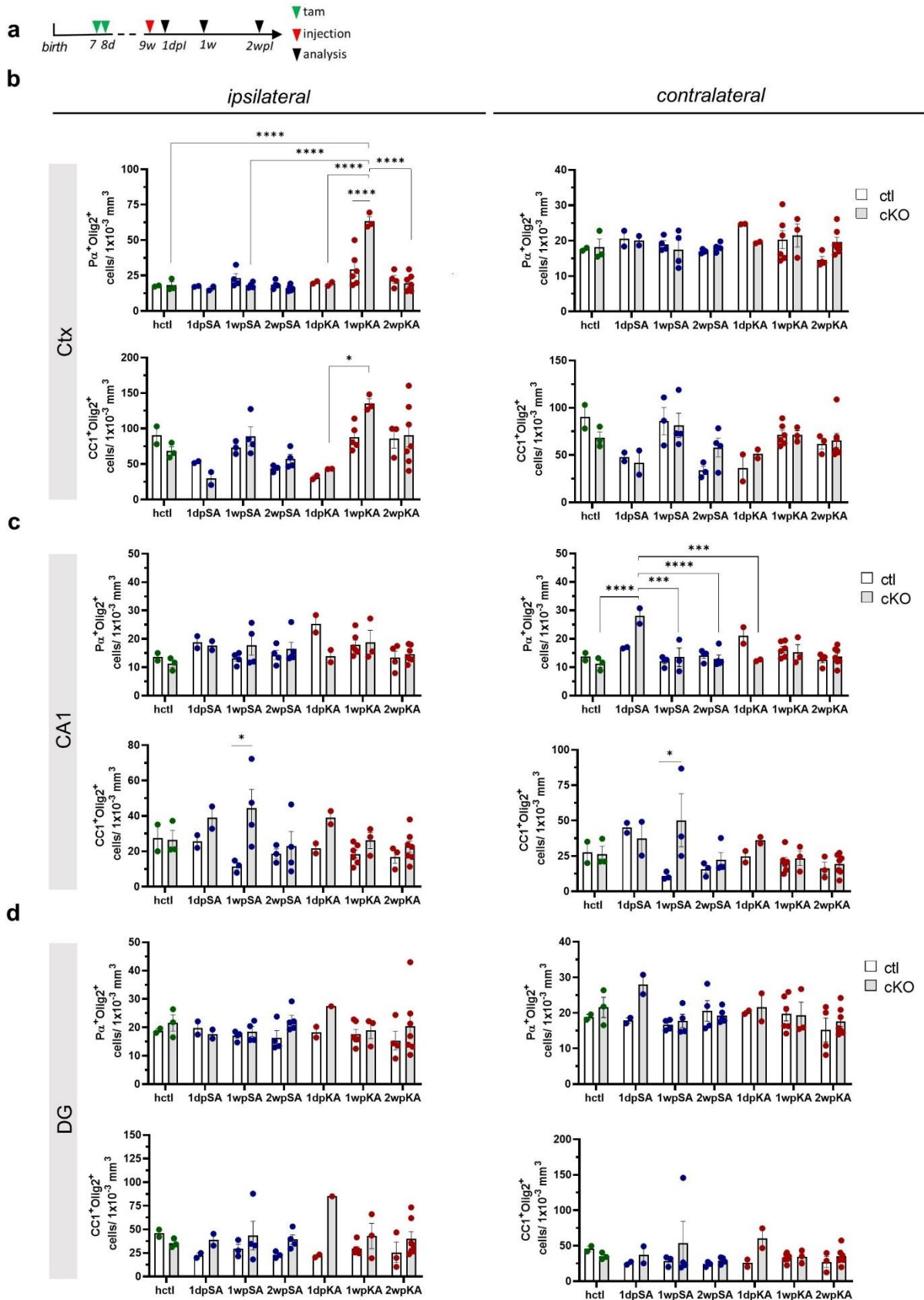


Figure 9. Cortical OPC and OL density at the epileptic lesion peaks 1 week after kainate injection. **a**, Experimental schedule for the groups of 1dpi, 1wpi and 2wpi. **b-d**, Quantification of OPC and OL density in ctl and cKO mice at different time points: 1 day, 1 week and 2 weeks post injection of SA or KA, as well as of healthy control mice (2way ANOVA). Each dot indicates independent biological sample.

4.3 OPC proliferation is increased in epileptic GABA_BR cKO mice in the ipsilateral cortex and CA1 region

To understand whether the increase in OPC and oligodendrocyte density at the epileptic lesion of GABA_B cKO mice was attributable to increased proliferation rate of OPCs, we analysed OPC proliferation by performing Ki67, P α and GFP triple immunostaining at 1wpKA (Fig. 10a-c). While the density of proliferating OPCs in the ipsilateral cortex of the ctl group was unaltered between kainate and saline treated mice, that of kainate treated cKO mice was increased by 285 % compared with saline group (KA: 32.7 ± 6.3 vs SA: 8.5 ± 1.8) (Fig. 10d). Comparing kainate treated cKO and ctl mice, the OPC density in the cKO group was increased by 115 % (14.5 ± 1.5) (Fig. 10d). This was attributed to both recombined and non-recombined OPCs in the cKO cortex (Suppl. Fig. 7b). In the ipsilateral CA1 region, the density of proliferating OPCs was increased by 388 % in the kainate treated cKO group compared to the ctl (cKO: 3.2 ± 1.8 vs ctl: 0.7 ± 0.20) (Fig. 10e). However, OPCs were proliferating more in the contralateral side of cKO DG (4.5 ± 1.7) compared to the ctl (1.6 ± 0.4) (Fig. 10f). Therefore, these results indicate that OPC proliferation in the cortex and CA1, but not in DG, is inhibited by GABA_BR at the onset of chronic phase.

To investigate if GABA_BR generally regulates the OPC proliferation at all phases of epileptogenesis, we analysed OPC proliferation by performing Ki67, P α and GFP triple immunostaining at 1d, 1w and 2wpKA (Fig. 11a). As expected from the increase seen in the total OPC population (Fig. 9), the proliferation at the ipsilateral cortex peaked at the first week after kainate injection in the cKO mice, markedly surpassing the proliferation rate at 1d and 2w (Fig. 11b). Moreover, only at 1 week post kainate, the density of proliferating OPCs differed between epileptic cKO and ctl mice (Fig. 11b). In the ipsi- and contralateral hippocampus (CA1 and DG), the density of proliferating OPCs were comparable during epileptogenesis in both ctl and cKO group (Fig. 11c-d). As well, OPC proliferation were identical between epileptic ctl and cKO mice at all time points (Fig. 11c-d). Therefore, these results suggest that GABA_BR activation impedes OPC proliferation in the cortex at the early chronic phase of epilepsy and this regulation is rather heterogeneous in different brain regions during epilepsy development.

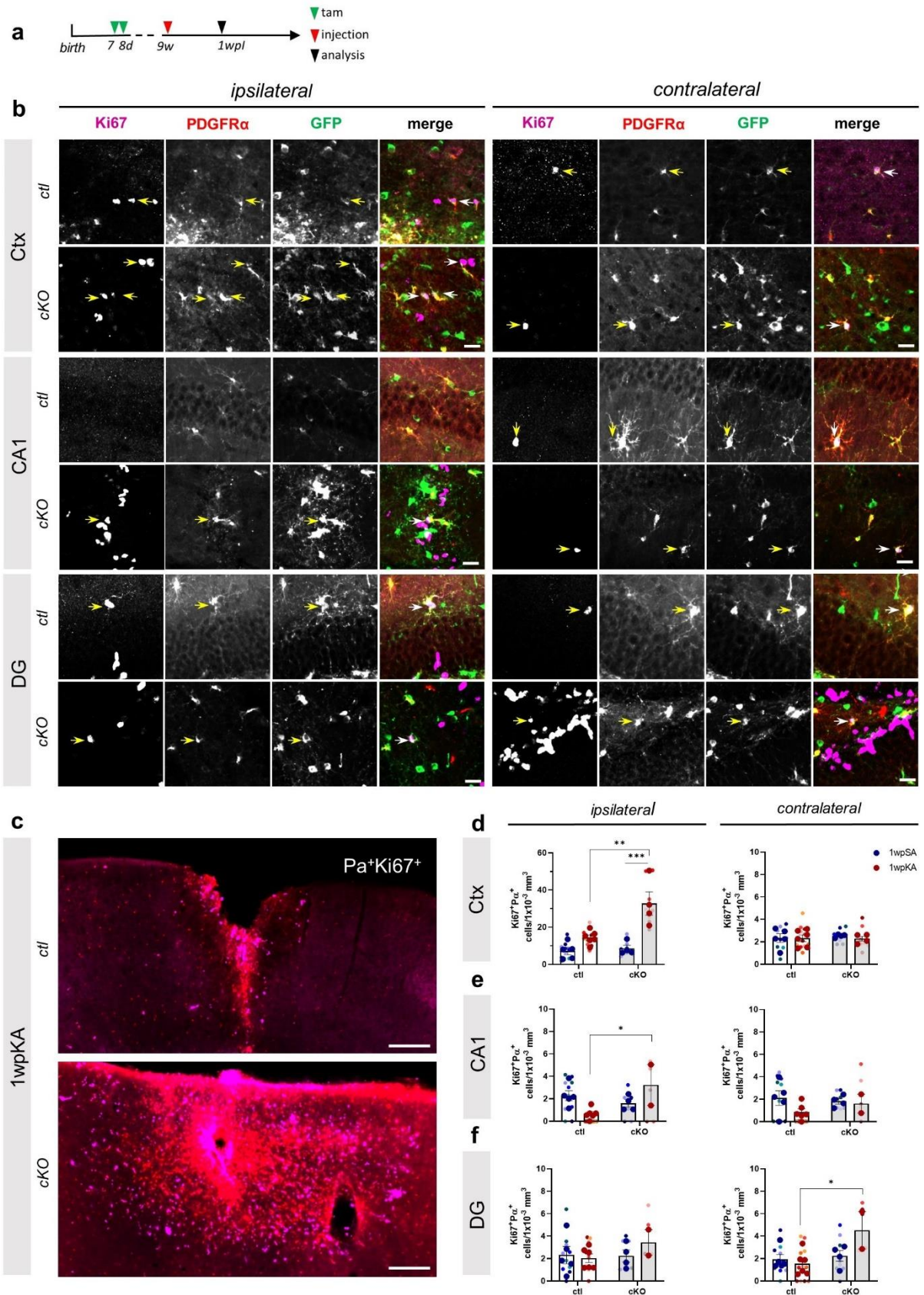


Figure 10. Kainate injection induces an increase of OPC proliferation in GABA_BR conditional knock out mice at 1 week post kainate injection. **a**, Experimental schedule. **b**, Immunostaining of proliferating OPCs (Ki67⁺Pa⁺) in the ipsilateral and contralateral ctx, CA1 and DG of ctl and cKO animals after 1week of KA injection. Proliferating OPCs: arrows. **c**, Magnified image of kainate injected site in ctl and cKO mice, stained with Ki67 and Pa. **d-f**, Quantification of proliferating OPC density in the Ctx, CA1 and DG of saline and kainate injected ctl and cKO mice (2way ANOVA). Scale bars = 20 μ m for **b** and 200 μ m for **c**.

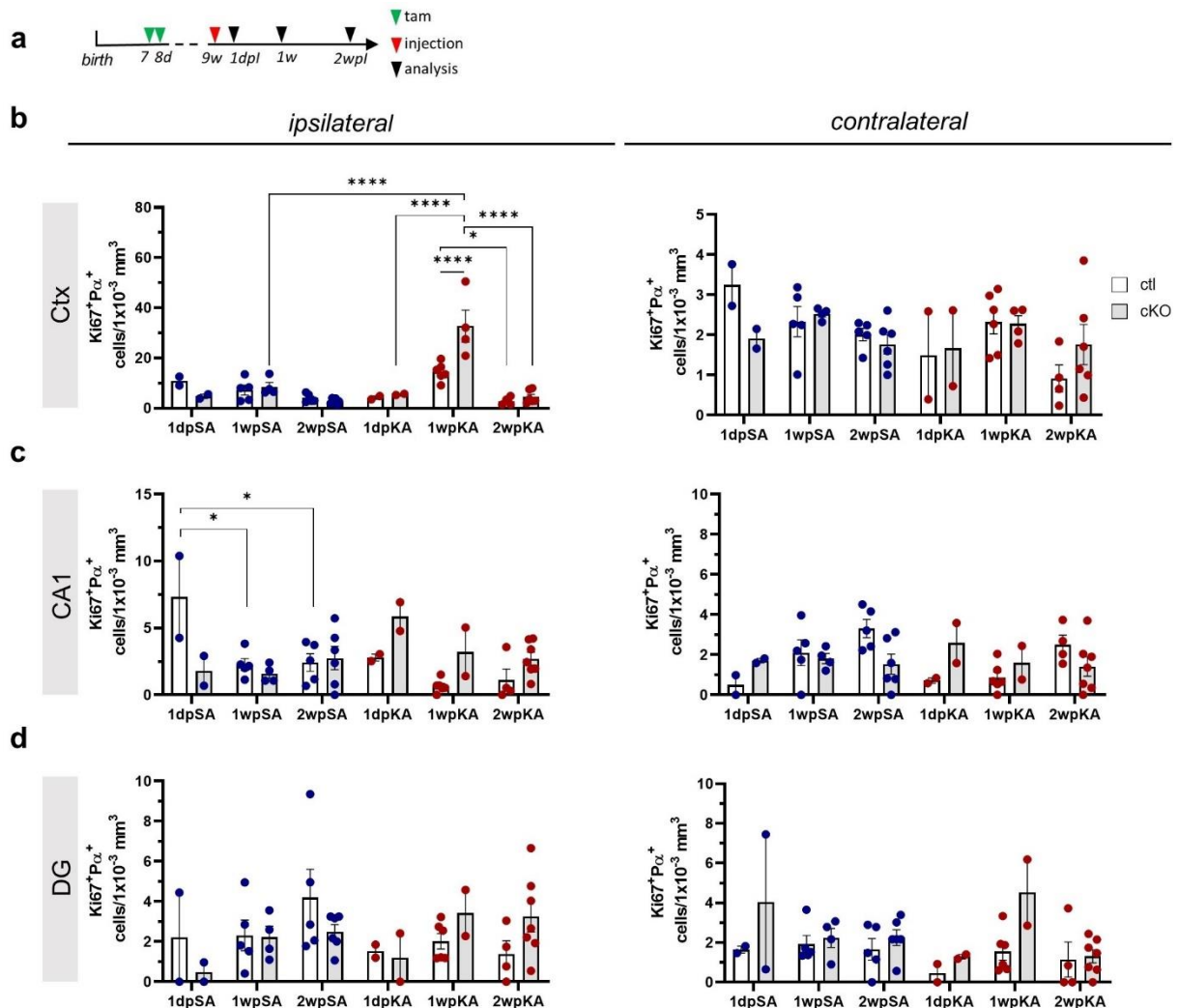


Figure 11. OPC proliferating rate at the epileptic lesion peaks at 1 week after kainate injection in the mice. **a**, Experimental schedule for the groups of 1dpl, 1wpl and 2wpl. **b-d**, Quantification of proliferating OPC density in ctl and cKO mice at different time points: 1 day, 1 week and 2 weeks post injection of SA or KA (2way ANOVA). Each dot indicates independent biological sample.

4.4 Loss of PV⁺ interneurons in the epileptic brain

GABAergic interneurons, including PV⁺ interneurons, are lost in the epileptic brain and surviving interneurons display altered inhibitory connections (de Lanerolle et al., 1989; Cossart et al., 2001; Alhourani et al., 2020; Müller et al., 2020). These changes result in a shift of E/I balance towards overshooting excitation contributing to epileptogenesis (Sloviter, 1994; Fritschy, 2008). Our preliminary work showed that in the OPC-GABA_BR cKO mouse medial prefrontal cortex, PV⁺ interneuron density is increased while their activity is suppressed.

To understand whether these neurons are more vulnerable or resistant to excitotoxicity in the epileptic brain, we evaluated the density of PV⁺ interneurons in cortex and hippocampus. In

saline injected mice, PV⁺ interneurons can be found even in close proximity to the injection site (Fig. 12b; ctl: 22.4±3.3; cKO: 20.9±1.0, Fig. 14b), while in epileptic mice the injection site and surrounding tissue were completely devoid of PV⁺ interneurons (Fig. 12c; Fig. 13b; ctl: 0.4±0.2; cKO: 0.2±0.1, Fig. 14b).

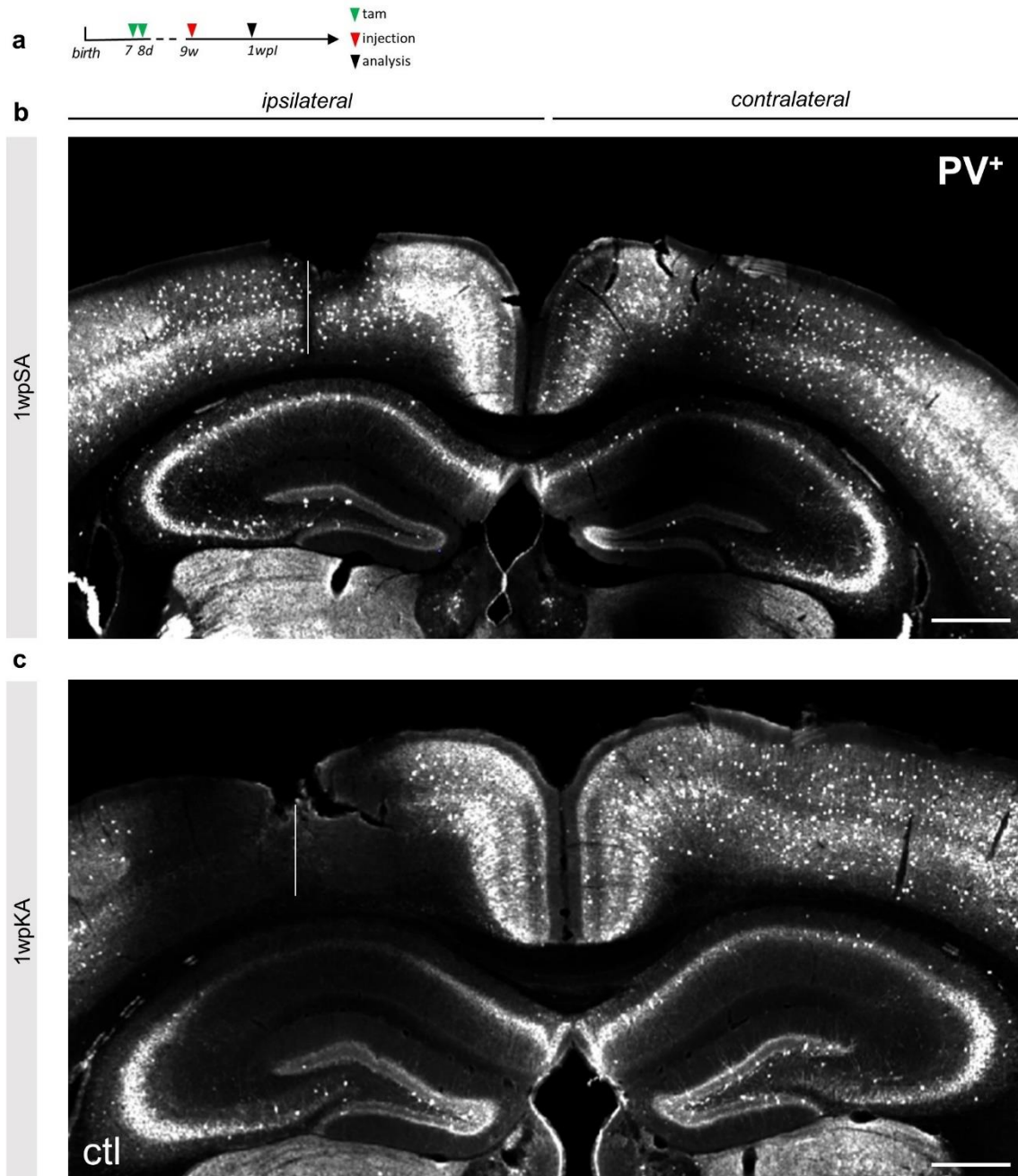


Figure 12. Kainate injection induces the loss of PV⁺ neurons at the injection site. a, Experimental schedule. b and c, Overview of cortex and hippocampus in saline (b) and kainate (c) injected ctl mouse brain at 1wpl, grey line indicates injection site. Coronal slices were immunostained with PV. Scalebars = 500 μm for b and c.

The loss of PV⁺ interneurons was also observed in the ipsilateral side of CA1 region (Fig. 12c, Fig. 13b) in both ctl and cKO mice (ctl: 0.1±0.1; cKO: 1.1±1.1) (Fig. 14b-c). However, in the DG, density of PV⁺ interneurons in neither ctl nor cKO mice was reduced at 1 week post SE

(Fig. 13b, Fig. 14d) compared to saline treated mice ipsilaterally ((KA: ctl: 6.5 ± 0.6 , cKO: 7.0 ± 0.0), (SA: ctl: 5.0 ± 0.9 , cKO: 5.6 ± 0.5)) as well as contralaterally ((KA: ctl: 6.1 ± 1.1 , cKO: 7.1 ± 1.1), (SA: ctl: 5.5 ± 1.1 , cKO: 5.2 ± 0.4)) (Fig. 13b, 14d). Our data suggest that kainate induced epilepsy causes PV⁺ interneuron loss at the injection site and the anatomically close region CA1 and GABA_BR signalling of OPCs does not affect the susceptibility of PV⁺ interneurons towards excitotoxicity either in these areas.

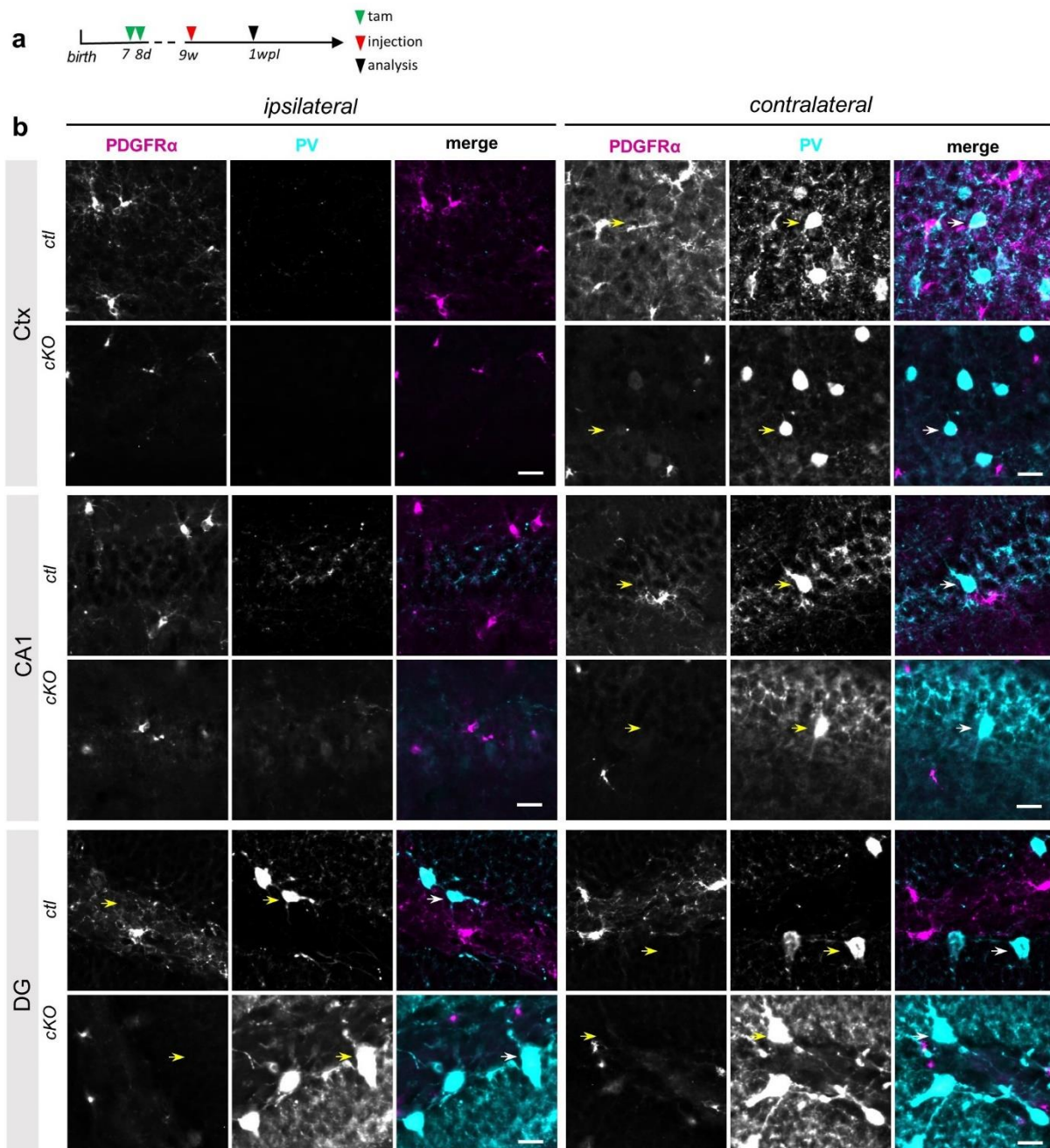


Figure 13. Kainate injection induces the loss of PV neurons in ipsilateral cortex and CA1 region. **a**, Experimental schedule. **b**, Immunostaining of PV⁺ interneurons and OPCs (P α ⁺) in the ipsilateral and contralateral side of Ctx, CA1 and DG of ctl and cKO animals after 1 week of KA injection. PV⁺ interneurons: arrows. Scale bar = 20 μ m

To understand the progress of PV⁺ interneuron loss in the epilepsy model, we analysed PV⁺ interneuron density at 1d, 1w and 2wpKA (Fig. 15a). At the cortical epileptic lesion, PV⁺ interneurons were already not detectable at 1dpKA in both ctl and cKO (ctl: 0.2±0.2, cKO: 0.2±0.2) and remained lost at 1w (ctl: 0.4±0.2, cKO: 0.2±0.1) and 2wpKA (ctl: 0.3±0.2, cKO: 0.8±0.7) (Fig. 15b). In the contralateral cortex, however, PV⁺ interneuron density was affected differentially during the progression of epileptogenesis in ctl and cKO mice. While the amount of PV⁺ interneurons gradually decreased from the acute phase 1dpKA to the early chronic phase 2wpKA in the ctl cortex (1dpKA: 30.2±3.2, 2wpKA: 17.5±1.6) (Fig. 15b), that of cKO mice remained constant over the first two weeks (1dpKA: 25.3±0.2, 2wpKA: 23.0±1.9) (Fig. 15b). In the ipsilateral CA1 region of both ctl and cKO mice, PV⁺ interneurons were also lost from 1dpKA onwards (Fig. 15c). Unlike in the cortex, however, PV⁺ interneurons in the contralateral CA1 region were preserved in ctl and cKO equally at all time points (Fig. 15c). In the ipsilateral and contralateral DG of epileptic mice, PV⁺ interneuron density remained unchanged compared to saline injected mice in both ctl and cKO groups at 1d, 1w and 2wpKA (Fig. 15d). Thus, these data suggest that reduction of GABA_BR signalling of OPCs renders interneurons in the contralateral cortex less susceptible to excitotoxic cell death.

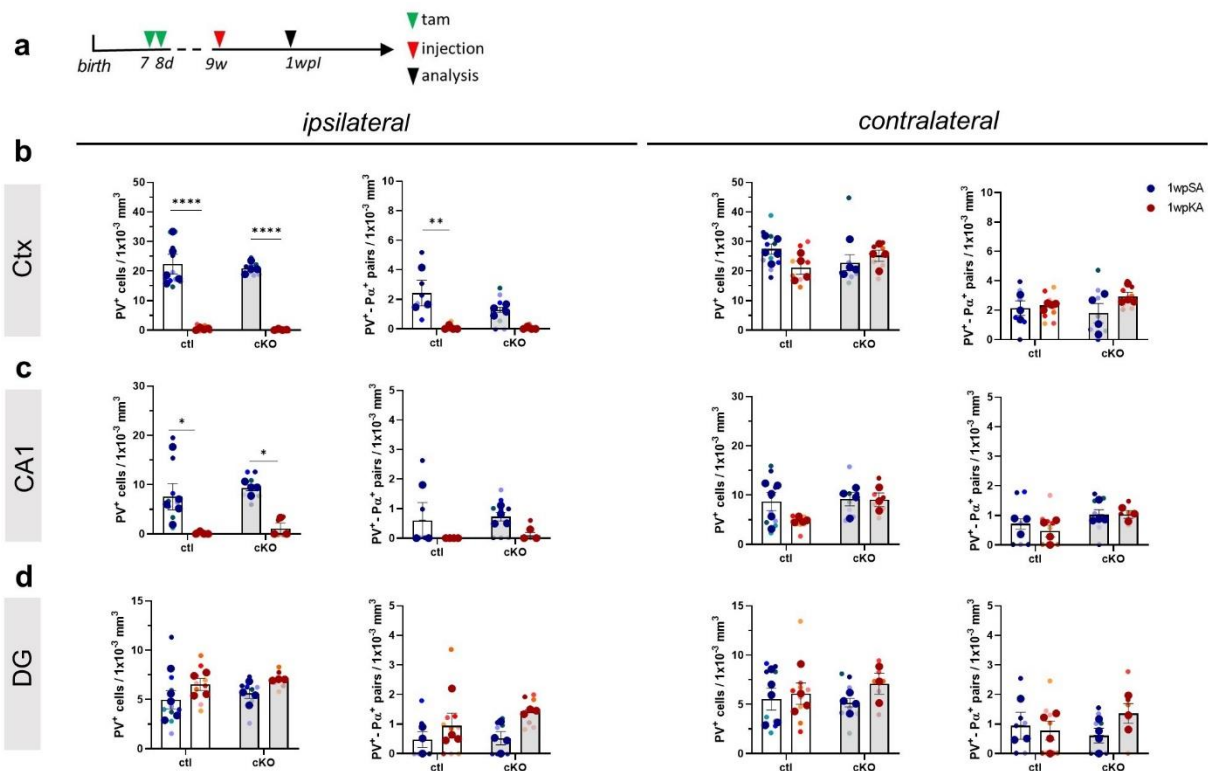


Figure 14. Kainate injection induces the loss of PV neurons in ipsilateral cortex and CA1 region. **a**, Experimental schedule. **b**, Quantification of PV⁺ interneurons and PV⁺Pα⁺ pairs in the Ctx, CA1 and DG of saline and kainate injected ctl and cKO mice (2way ANOVA).

OPCs form somato-somatic pairing with interneurons. Such OPC-interneuron pairs are positively influenced by application of GABA_BR agonist baclofen (Boulangier and Messier, 2017) and such communication is capable of monitoring network excitation in the hippocampus (Mangin et al., 2008). To understand whether such soma-somatic OPC-interneuron communication takes part in the epileptogenesis, we analysed OPC-interneuron pairing with immunostaining. PV⁺ cells displaying oval morphology with central nucleus (DAPI⁺) were identified as PV⁺ interneurons. Pa⁺ and PV⁺ cells with tangent somata were considered as OPCs-interneuron pairs. Areas of extensive interneuronal loss (ipsilateral cortex and CA1) were completely devoid of OPC-interneuron pairs from 1 day post SE onwards in ctl and cKO as well (Fig. 15b-c). In the contralateral cortex, increased survival of PV⁺ interneurons in cKO mice did not coincide with alterations in OPC-interneuron pair density as pairing remained unchanged from saline injected mice during the first 2 weeks of epileptogenesis in both ctl and cKO (Fig. 15b). More so, the density of OPC-interneuron pairs was unchanged between ctl and cKO mice in both epileptic and non-epileptic mice (Fig. 15b). Therefore, our data indicate that OPC-interneuron pairing does not take part in the epileptogenesis, at least not at the early phases.

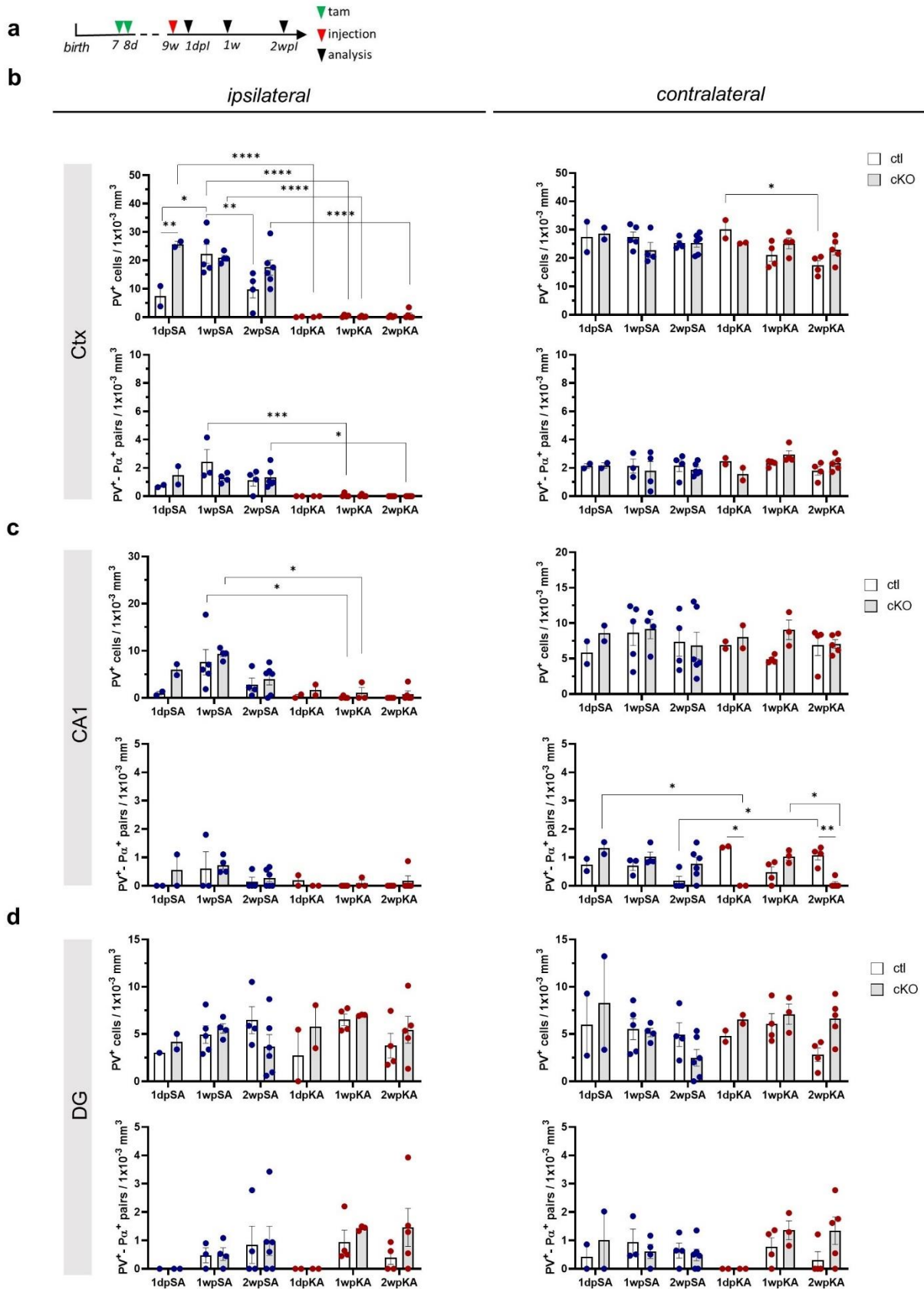


Figure 15. Reduction of PV⁺ interneurons and interneuron-OPC pairs in kainate treated ipsilateral cortex. **a**, Experimental schedule for the groups of 1dpl, 1wpl and 2wpl. **b-d**, Quantification of PV⁺ interneuron and PV⁺Pα⁺ pair density in ctl and cKO mice at different time points: 1 day, 1 week and 2 weeks post injection of SA or KA (2way ANOVA). Each dot indicates independent biological sample.

4.5 Astrogliosis and microglia activation is not altered in the epileptic cKO brain

Astrocytes and microglia sense microenvironmental changes under healthy conditions and become reactive upon pathological stimuli (Benson et al., 2015; Hiragi et al., 2018). Activated astrocytes (or reactive astrocytes) display abnormal functional properties in epileptic network conditions, even preceding neuronal loss and spontaneous seizures (Bedner et al., 2015).

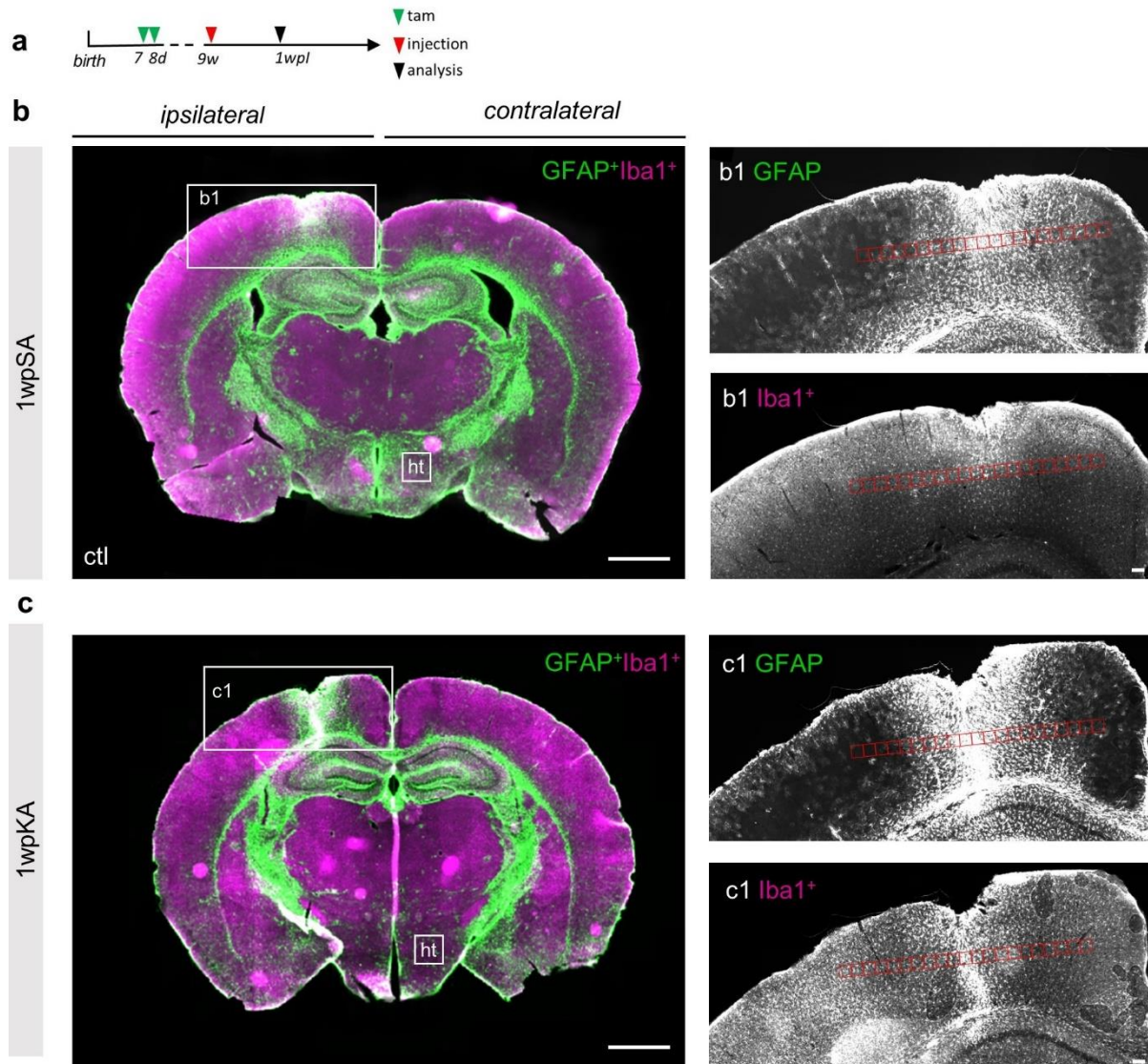


Figure 16. Kainate injection induces an increase of GFAP and Iba1 immunofluorescence intensity near the lesion site 1wpl. a, Experimental schedule. **b and c**, Overview (**left column**) of coronal slices of saline (**b**) and kainate (**c**) injected mice 1wpl, immunostained with GFAP (astrocytes) and Iba1 (microglia). Magnified images (**right column**) show the analysed region (indicated by boxes in the left column). Fluorescence intensity (FI) was measured for 1000 μm to each side of the injection in 100 x 100 μm segments (red squares). The results were normalized to hypothalamic (ht) FI (indicated by box in the left column). Scalebars = 1000 μm for the **left column** and 100 μm for the **right column**.

Since the density of OPCs and PV⁺ neurons were changed in the cortex by the deletion of OPC-GABA_BR, we asked whether such alteration will be accompanied by astro- and microgliosis in the epileptic cortex. To this end, we analysed the astrocyte and microglia activation by measuring the relative change of fluorescence intensity (FI) of the astroglial marker GFAP and the microglial marker Iba1 at the site of injection (Fig. 16b-c), indicative of astrocyte and microglia reactivity.

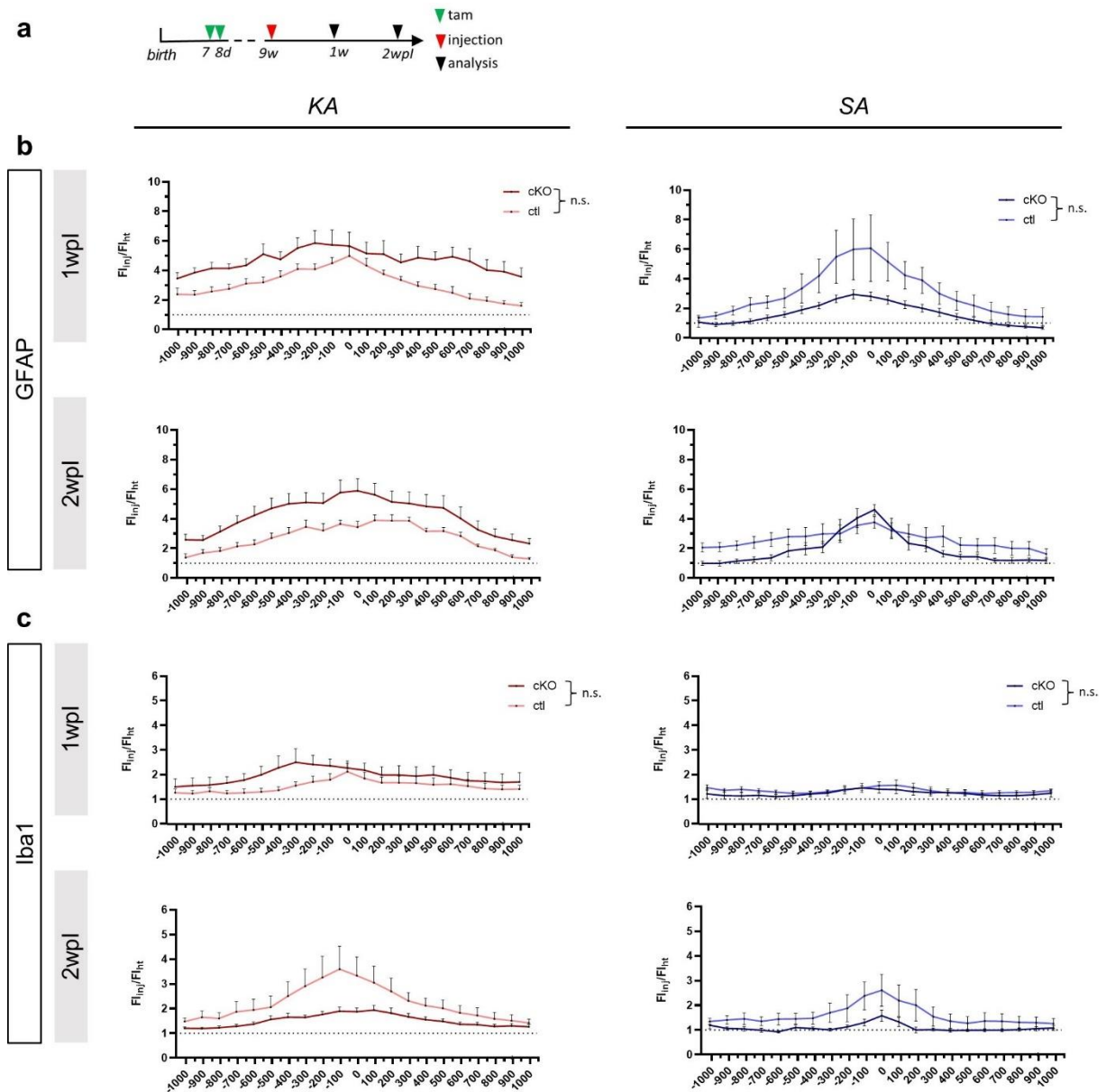


Figure 17. Oligodendroglial GABA_BR signalling does not affect astrocyte and microglia activation at the site of epileptic lesion. a, Experimental schedule. **b and c**, Quantification of GFAP (**b**) and Iba1 (**c**) FI increase at the injection site as a product of hypothalamic FI 1wpl and 2wpl. Statistical analysis: 2way ANOVA.

To assess how far kainate impact extended from the injection site in GABA_BR cKO mice and ctrl mice, we analysed an area extending 1000 μm to each side from the injection (Fig. 16b1-

c1). GFAP FI intensity between ctl and cKO mice were comparable at both 1w and 2wpl of saline and kainate (Fig. 17b). Likewise, Iba1 FI was equally increased in GABA_BR cKO and ctl mice for both epileptic and non-epileptic group (Fig. 17c). Therefore, our data shows that GABA_BR signalling of OPCs is not required for gliosis at the early chronic phase of epileptogenesis.

5. Discussion

OPCs are extensively integrated in neuronal networks, as they communicate with neurons via synaptic transmission (Orduz et al., 2015; Mount et al., 2019). Moreover, by pairing with interneurons, OPCs form a close functional and anatomical companion and even mirroring electric activity of their paired interneuron (Mangin et al., 2008). OPCs are hypothesized to be critical regulators of E/I balance (Bai et al., 2021) bringing attention towards their potential role in the process of epileptogenesis. In a previous study, we showed that OPCs are in fact regulating E/I balance, as they influence cortical PV⁺ interneuron density and function via a GABA_BR-TWEAK pathway (Fang et al., 2022). Here, we demonstrate that OPCs transiently increase their proliferation at the onset of the chronic phase of epilepsy in GABA_BR cKO mice resulting in both increased density of OPCs as well as oligodendrocytes at the epileptic lesion. As the density of oligodendrocytes remains to be elevated at the following week, we speculate that oligodendrocyte formation might be sustained further into the chronic phase of epileptogenesis in GABA_BR cKO mice. Thus, the myelin damage observed to persist even during the chronic phase of epileptogenesis (Sierra et al., 2011; Drenthen et al., 2020) might be prevented or at least lessened by inhibition of OPC-GABA_BRs. Furthermore, we show that interneuronal susceptibility to excitotoxicity in GABA_BR cKO mice is reduced, as the contralateral cortex of ctl mice was slowly depleted of interneurons while interneuronal density was preserved in GABA_BR cKO mice. Therefore, reduction of GABA_BR activation of OPCs could potentially attenuate severity of epilepsy by curtailing loss of inhibitory neurotransmission. Our results though showed no impact of GABA_BR signalling of OPCs on OPC-interneuron pairing as well as activation of astrocytes and microglia during epileptogenesis.

5.1 OPC-GABA_B receptor transiently promotes cortical OPC proliferation and density

OPC proliferation is mediated by growth factors and neurotransmitters (Yang et al., 2013). However, the effect of GABA on OPC proliferation is a matter of debate. In vitro study showed increased proliferation and migration of OPCs upon GABA_B receptor activation using OPC cell line (Luyt et al., 2007). However, this phenotype was not observed in organotypic cerebral cortex slices, neither by blocking nor by activating GABA_B receptors (Hamilton et al., 2017). In addition, previous study from our working group has demonstrated that neither the OPC density nor the proliferation was altered in the cKO mPFC and somatosensory cortex (Fang et al., 2022). In line with that, in cortex, CA1 region or DG, OPC density remained unchanged in the healthy cKO mice. Therefore, it is feasible to speculate that OPC proliferation in CA1 and DG is also not affected by the deletion of GABA_BR. Under epileptic conditions, however, the scenario was different. Reduction of GABA_B receptor expression in OPCs translated to

increase of OPC density and proliferation in cortex and hippocampus at one week post kainate injection. Such increase was attributed to the enhanced cell proliferation. However, already at 2 weeks post injection, OPC density and density of proliferating cells was similar in ctl and cKO cortex. Therefore, it is possible that GABA_BR mediated modulation of OPC proliferation varies upon the progression of the epilepsy. However, this hypothesis needs further studies to demonstrate.

Increasing expression of postsynaptic GABA_B receptors in neurons in turn enhances the expression of AMPA-type glutamate receptors (AMPA receptors), which has been suggested as mechanism for maintaining E/I balance (Terunuma et al., 2014). The link between GABA_B receptor signalling and AMPAR expression was not specifically demonstrated for OPCs. Still, it is well conceivable that OPCs possess this quality, as they express both functional AMPARs and GABA_BRs (Bergles et al., 2000; Luyt et al., 2007). Moreover, they receive synaptic input from excitatory as well as inhibitory neurons and hence are well positioned to sense changes in E/I balance (Bergles et al., 2000; Ziskin et al., 2007; Orduz et al., 2015). We suggest, that in OPC-GABA_BR cKO mice, the expression of AMPARs on the cell surface of OPCs is reduced as well. Several studies show, that activation of AMPARs decreases OPC proliferation in vitro (Gallo et al., 1996; Yang et al., 2013; Fannon et al., 2015). Hence, decreased AMPAR mediated signalling of OPCs constitutes a mechanism by which OPC proliferation could be increased, as we observed in the cortex and CA1 region of epileptic cKO mice. Still, we wondered why OPCs proliferated increasingly specifically under epileptic conditions in GABA_BR cKO mice. Intriguingly, a recent study conducted in a model of demyelinating brain injury demonstrates, that overexpression of the AMPAR subunit GluA2 promotes post-injury OPC proliferation and restoration of the oligodendrocyte population (Khawaja et al., 2021). Integration of the GluA2 subunit in AMPARs reduces calcium permeability (Pellegrini-Giampietro et al., 1997), thus calcium currents of OPCs could contribute to regulating OPC proliferation and oligodendrocyte regeneration in response to CNS injury. We suggest that following epileptogenic insult, OPC proliferation is regulated by AMPAR mediated calcium influx as well. Therefore, decreasing AMPAR expression of OPCs by cKO of GABA_BRs could promote OPC proliferation especially at the epileptic lesion. Future studies should address the effect of GABA_B receptor signalling on OPCs AMPA receptor expression and calcium permeability. Of note, different to previous observations in various epileptic paradigms (Luo et al., 2015; Wu et al., 2019; Bell et al., 2020) we did not observe any increase of OPC density despite the obvious increase of PDGFR α and GFP fluorescence intensity at the site of kainate injection compared to saline injection in ctl mice. Previous work has demonstrated, that kainate injection suppresses Olig2 expression in a subset of OPCs (Fang et al., 2023). In this study we identified OPCs as PDGFR α and Olig2 positive cells, due to the difficulty of recognizing OPCs with sole PDGFR α expression at the ipsilateral side. Therefore, the actual number of

OPCs in the brain of kainate injected mice is likely slightly higher. This effect could conceal an increase of OPCs in kainate injected ctl mice compared to saline injected mice.

5.2 OPC-GABA_B receptor for oligodendrocyte generation in the epileptic cortex

OPC-GABA_BR signalling has been suggested to promote differentiation of OPCs into myelinating oligodendrocytes, as observed in purified rat OPC cultures (Serrano-Regal et al., 2019). Our previous study also demonstrated a marked decrease of oligodendrocyte density in the mPFC of GABA_BR cKO mice. Moreover, we observed that interneuronal myelination was impaired in OPC-GABA_BR cKO mPFC which is well accountable to reduced oligodendrocyte density. However, in the current study, healthy control mice displayed no difference in oligodendrocyte density between ctl and cKO in neither of the inspected regions, including somatosensory cortex, CA1 and dentate gyrus. This might be due to the heterogeneity of the cells and the functions of the GABA_BRs in these cells. Meanwhile, one must bear in mind that the sample size for healthy control in this set of experiments was rather small (ctl: n=2; cKO: n=3), while in our previous set of experiments a bigger sample size was available (ctl: n=7; cKO: n=8). Under epileptic conditions, however, the oligodendrocyte population appears to be affected differentially by GABA_BR activity of OPCs, as oligodendrocyte density in GABA_BR cKO mice was increased by 54% compared to epileptic control mice one week after induced SE. Hence, cortical OPCs newly generated by increased proliferation do not solely increase the pool of OPCs, but in part progress into oligodendrocytes. Moreover, while the density of cortical OPCs returns to basal levels at 2wpKA, oligodendrocyte density remained stable at 2wpKA compared to 1wpKA. One possible explanation is, that in OPC-GABA_BR cKO mice oligodendrocytes are less susceptible towards excitotoxicity and their survival is increased. Another possibility is, that oligodendrocytes die in response to excitotoxic input but continuous regeneration from the increased pool of OPCs counterbalances oligodendrocyte loss.

Several studies report myelin abnormalities in patients and animal models of epilepsy (Schoene-Bake et al., 2009; Scanlon et al., 2013; Ye et al., 2013). Moreover, myelin damages induced by initial excitotoxic insults persist in parts during the chronic phase of epileptogenesis, pointing towards insufficient myelin repair mechanism (Sierra et al., 2011; Drenthen et al., 2020). Our current study suggested an increase of OPC proliferation and subsequently increased generation of oligodendrocytes in the cKO mouse cortex, which could be an adaptive mechanism beneficial in suppressing epilepsy severity. Conversely, OPC-GABA_BR activation could prevent the increased generation of mature oligodendrocytes under epileptic conditions, thusly contributing to incapacitating myelin repair mechanisms. Thereby, OPC-GABA_BRs could be an interesting therapeutic target for drugs aiming to attenuate structural myelin damages occurring under epileptic conditions and prevent aggravation of neuronal hyperexcitability. However, from previous experiments conducted in OPC-GABA_BR cKO mice, we know that

under healthy conditions the myelination of interneurons in mPFC is reduced. Myelination is a process guided by neuronal activity (Fields, 2015; Almeida and Lyons, 2017). Excessive neuronal activity as seen under epileptic conditions is likely to affect neuron-oligodendroglia communication (Donkels et al., 2020), and therefore could perturbate the regulation of the myelinating process. In this study, we only analysed oligodendroglia densities and did not include mRNA or protein expression of proteins such as myelin basic protein (MBP). Neither did we perform structural analysis of myelin sheaths. Therefore, at this point we can only speculate that reduction of OPC-GABA_B signalling positively affects myelination under epileptic conditions, as the density of oligodendrocytes are increased in the cKO brain. Whether GABA_BR cKO mice display differential susceptibility to initial myelin damage or improved myelin repair properties, further analysis of myelin content and oligodendroglial proteasome is required.

Besides protective effects of reduced GABA_B receptor signalling on OPCs, the possibility of pro-epileptogenic effects also requires careful consideration. GABA_B receptors on OPCs are negatively coupled to the adenylyl cyclase, resulting in a decrease of intracellular cyclic adenosine monophosphate (cAMP) concentration upon activation (Luyt et al., 2007). Subsequently reduced activity of protein kinase A and reduced phosphorylation of cAMP response element-binding protein (CREB) could result in suppressed transcription of brain derived neurotrophic factor (BDNF) (Tao et al., 1998; Khundakar and Zetterström, 2011; Bai et al., 2021). Therefore, it is tempting to speculate that in OPC-GABA_B cKO mice the expression of BDNF is increased. Following seizure activity, the expression of BDNF is increased (Nawa et al., 1995) and several studies draw a link between BDNF and neuronal hyperexcitability (Scharfman, 1997; Binder et al., 2001). For instance, mice overexpressing BDNF experience more severe seizures following kainate administration (Croll et al., 1999) while reduced expression of BDNF renders mice less susceptible to develop seizures in a kindling model (Kokaia et al., 1995). BDNF contributes to synaptic plasticity (Leal et al., 2014). It has been proposed that increased expression of neurotrophic factors constitutes a mechanism, by which lasting network rearrangements occurring over the process of epileptogenesis are mediated (Gall, 1993). Therefore, higher severity of disease and increased susceptibility to network changes induced by seizure activity are within the realm of possibility for OPC-GABA_BR cKO mice as well.

5.3 Interneurons demonstrate increased resistance to excitotoxicity in OPC-GABA_B cKO mice

Interneuron loss and dysfunction is named as a crucial driving force in epileptogenesis, as they serve as critical regulators of E/I balance. Especially PV⁺ interneurons are effective in regulating network excitability by targeting the peri-somatic domain of excitatory neurons and

generating stable inhibitory signals at a high firing frequency. Several studies have described the loss of PV⁺ interneurons in the epileptic brain, however the extent of interneuron loss varies ranging from complete loss to a slight reduction depending on brain regions examined, animal model utilized or patient features, such as extent of hippocampal sclerosis (Sloviter et al., 1991; Boulleret et al., 2000; Wittner et al., 2001; Wyeth et al., 2010; Marx et al., 2013). In mice receiving intracortical kainate injection, we observed that one week after SE induction, PV⁺ interneurons were almost completely ablated from the ipsilateral cortex and CA1 region, while being preserved in the anatomically more distant DG. This effect occurred in both control and cKO mice. One needs to consider though, that we counted PV⁺ cells directly at the cortical injection site and the subjacent CA1 region where neurons were directly exposed to high doses of kainate, which exerts very strong excitotoxic effects. Hence, only extremely drastic changes in the susceptibility to excitotoxic input between control and cKO would have manifested in those regions. However, in the contralateral cortex PV⁺ interneurons are affected only indirectly by kainate through progressive network shifts towards hyperexcitability and entailing spontaneous reoccurring seizures, which are propagated from the initial epileptic onset region to the contralateral hemisphere. Here, we observed that in control mice the cortex was gradually depleted of PV⁺ interneurons from 1 day to 2 weeks post injection of kainate, while the PV⁺ interneuron density in OPC-GABA_BR cKO mice remained stable. Consequently, we concluded that in the cortex of OPC-GABA_BR cKO mice, PV⁺ interneurons are less vulnerable to excitotoxic influences during the progression of epileptogenesis.

We induced GABA_BR cKO in OPCs at the end of the first postnatal week, early in CNS development. OPC-GABA_BR signalling is crucial for regulating interneuronal density and activity in mPFC during development. OPC-GABA_BR cKO mice displayed increased interneuronal density, but the interneurons were functionally hypoactive and E/I ratio was increased. This condition was already established in postnatal week 9, before we induced epileptogenesis. Here, our data demonstrated that these interneurons were differentially affected during epileptogenesis in the cKO brain. It is likely that hypoactive interneurons are less integrated to the network than the ctrl cells, thereby being less susceptible to excitotoxicity. However, how their resilience to excitotoxic input is increased is at this point still subject to speculation and requires further investigation. Of course, we cannot exclude the idea that OPC-GABA_BR signalling directly affects interneuronal survival under epileptic conditions, since we already demonstrated its potential to regulate interneuron survival during development. However, we cannot functionally connect OPC-GABA_BR signalling to excitotoxicity at this point, and therefore find it more feasible that altered interneuronal survival in the epileptic cortex is attributable to intrinsic interneuronal properties altered during development in cKO mice. Future studies in epileptic OPC-GABA_BR cKO mice should aim to explore the interneuronal reaction towards excitotoxicity in the ipsilateral hemisphere more closely.

5.4 Soma-somatic communication between OPCs and PV⁺ interneurons doesn't mediate increased OPC proliferation and resistance to excitotoxicity

OPCs communicate with interneurons in a soma-somatic manner, forming OPC-interneuron pairs (Mangin et al., 2008). As much as 40% of OPCs in the adult neocortex are in close anatomical relationship with interneurons, amounting to about 25% of neocortical interneurons partaking in these OPC-neuron-pairs (Boulanger and Messier, 2017). Administration of the GABA_BR agonist baclofen increased the density of OPC-interneuron pairs (Boulanger and Messier, 2017). The exact biological significance of OPC-interneuron pair is yet illusive. Interestingly, OPCs are similarly integrated into local networks as their paired interneuron, meaning they receive synaptic input from the same excitatory neurons and mirror the electrical activity of their paired interneuron (Mangin et al., 2008). Therefore, OPCs are ideally positioned to sense changes in neuronal activity and network excitability. What's more, they are capable of responding to increased neuronal activity by proliferating and differentiating into oligodendrocytes (Li et al., 2010; Gibson et al., 2014; Mitew et al., 2018). OPCs themselves might be capable of monitoring network activity and participate in promoting neuronal synchrony, a function otherwise well known for interneurons (Sohal et al., 2009; Bai et al., 2021). Thus, we wondered whether somato-somatic communication between OPCs and interneurons could mediate increased proliferation of OPCs in epileptic cKO mice and exert protective effects on interneurons. However, in the ipsilateral cortex and CA1 region, where we observed increased OPC proliferation, interneurons and consequently OPC-interneuron pairs were completely lost in both control and cKO. Additionally, increased PV⁺ interneuron survival in the contralateral cortex of epileptic cKO mice did not coincide with altered OPC-interneuron pair density in this region. Ergo we concluded, that the effects observed in epileptic OPC-GABA_BR cKO mice on the OPC and interneuronal population are not mediated by somato-somatic communication between interneurons and OPCs.

5.5 GABA_B receptor mediated signalling on OPCs does not affect the activation of astrocytes and microglia in the epileptic cortex

Astrocytes and microglia activation under epileptic conditions, also referred to as gliosis, is characterized by upregulation of GFAP and Iba1 expression, respectively. Gliosis is one of the most common histopathological hallmarks encountered in animal models and patients with chronic focal epilepsy, however whether astrocyte and microglia activation is consequence or cause of hyperexcitability still remains elusive (Sofroniew, 2014; Patel et al., 2019). We previously established, that E/I balance is increased in OPC-GABA_BR cKO mice, a condition already established previous to the induction of epileptogenesis (Fang et al., 2022). Hence, we wondered whether astrocyte and microglia activation at the epileptic lesion could be affected by the altered conditions. Here we analysed fluorescence intensity of GFAP and Iba1

as an indirect marker for protein expression. By normalizing fluorescence intensity measured in the gliotic cortex to fluorescence intensity from the non-gliotic hypothalamus, we deduced the relative increase in GFAP and Iba1 protein expression in the affected cortex and hence the extent of astrocyte and microglia activation. This analysis did not reveal an impact of reduced GABA_BR mediated signalling of OPCs on the manifestation of gliosis at the beginning of the chronic phase epileptogenesis and 1 week later.

5.6 Outlook

In this study, we describe a histological phenotype observed in OPC-GABA_BR cKO mice during the early stages of epileptogenesis ranging from the acute aftermath of SE at 1dpl to the early chronic phase at 2wpl. However, epileptogenesis is a chronic process which is sustained well after the first two weeks following SE. Hence, we recommend that future studies conducted on the matter of OPC-GABA_BR signalling in epileptogenesis should investigate later time points as well, for instance 4 weeks and 8 weeks post SE. Possible questions for those studies include, whether the peak of OPC proliferation and density at 1 week post SE is an isolated occurrence or OPCs proliferate again later during epileptogenesis. Moreover, it should be illuminating to assess, whether oligodendrocyte density remains to be increased also during the late chronic phase as could be seen in the early chronic phase. In addition, mechanistic studies should be conducted to deliver an explanation for the histological phenotype we observed. We suggested that OPC proliferation could be increased due to reduced expression of AMPARs on OPCs. It would be most interesting to establish if AMPAR expression of OPCs in GABA_BR cKO mice is in fact diminished. This would confirm the link between GABA_BR activity and AMPAR expression observed in neurons for OPCs as well.

Moreover, we wondered whether myelin damage occurring during epileptogenesis could be prevented in OPC-GABA_BR cKO mice, as oligodendrocyte population was preserved at 2 weeks post SE. To tackle this question, analysis of MBP expression in oligodendrocytes and structural analysis of myelin sheaths on the axons of inhibitory and excitatory neurons should be conducted. We furthermore posed the question, whether the increase in OPC and oligodendrocyte density constitute a mechanism beneficial in attenuating epilepsy severity. To assess the course of disease, we propose to evaluate seizure frequency, duration and severity by implantation of cortical surface electrodes and EEG recording.

Additionally, the interneuronal dynamics during the late chronic phase of epileptogenesis (e.g. 4 weeks and 8 weeks post SE) should be investigated. Is the interneuronal population in the contralateral cortex of GABA_BR cKO mice preserved also during the chronic phase? Is the dentate gyrus affected at later time points in the intracortical injection model or is this region

spared also during the late chronic phase as we demonstrated for the acute and early chronic phase? We established, that interneuronal vulnerability is in fact reduced in GABA_BR cKO mice which becomes apparent in the contralateral cortex. However, in the ipsilateral cortex we only evaluated interneuronal density in close proximity to the injection site. Here, kainate impact was most pronounced, likely exceeding tolerance of excitotoxicity even more resistant mice revealing no difference between cKO and control. Therefore, we suggest that future investigations should also examine within which distance from the injection site the ipsilateral cortex and CA1 region are devoid of interneurons. Thereby, more nuanced changes in susceptibility to excitotoxicity could be revealed in the ipsilateral hemisphere as well.

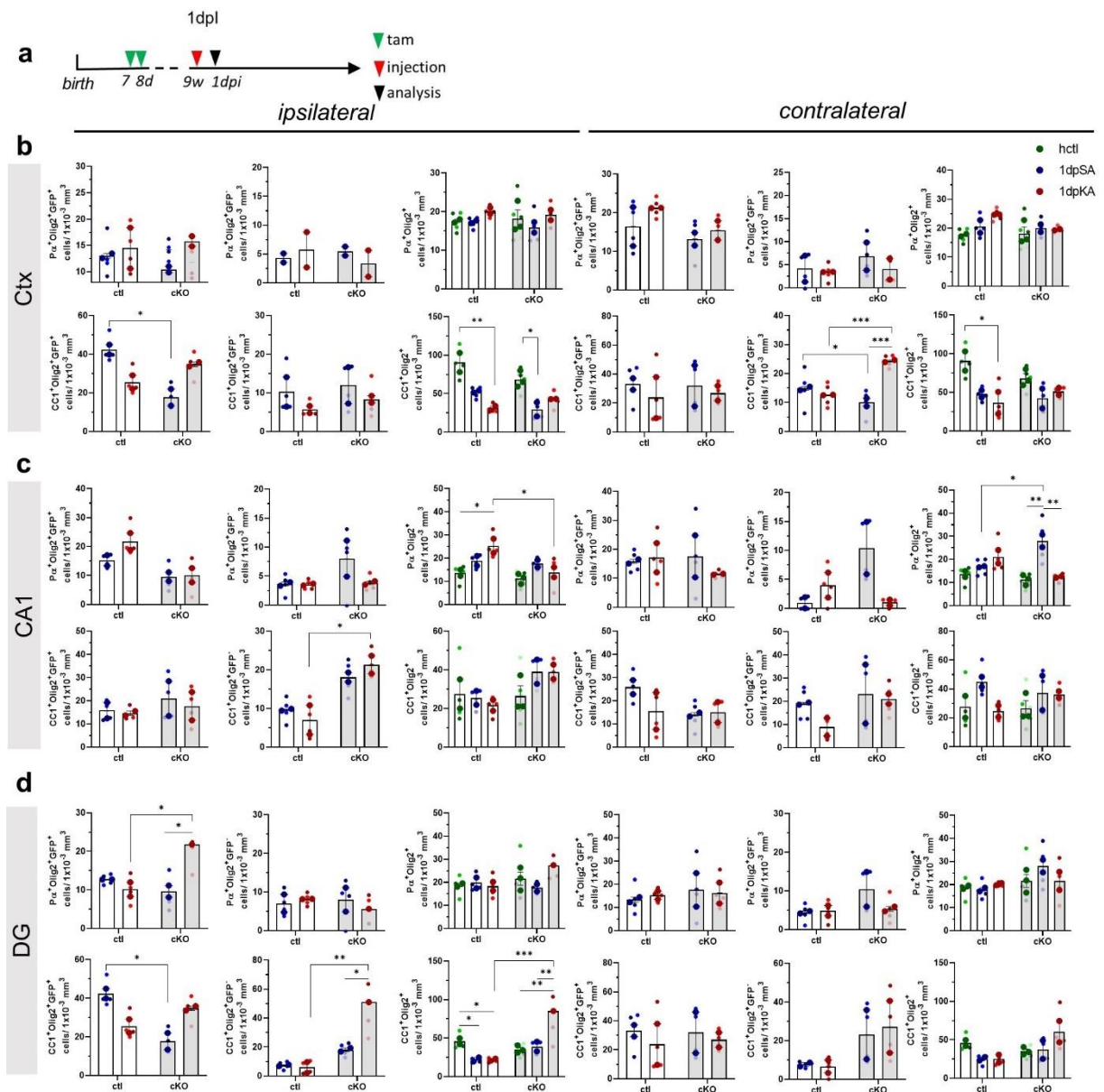
Moreover, it should be investigated more closely if the different subtypes of PV⁺ interneurons are impacted differentially in epileptic OPC-GABA_BR cKO mice and how altered interneuronal survival reflects on phenotypical parameters, such as seizure severity and frequency. Different interneuronal subtypes are affected differently in what seems to be a highly specific pattern of cell loss and altered synaptic transmission (Buckmaster and Jongen-Rêlo, 1999; Hellier et al., 1999) and their role in epileptogenesis might be just as diverse (reviewed by Liu et al., 2014). Examining PV⁺ bouton density on an individual granule cell level in the dentate gyrus of epileptic patients revealed, that basket cells and chandelier cells were reacted differently. Namely, while bouton density from chandelier cells was reduced, the density of basket cell boutons increased (Alhourani et al., 2020). Chandelier cells only represent a small portion of PV⁺ interneurons. Nonetheless, their loss could result in a severe deficiency of functional inhibition, as they target the axon initial segment wielding great inhibitory power (Wang et al., 2016). Increased synaptic coverage from basket cells might constitute an adaptive response, however might also promote abnormal neuronal synchrony, as the same inhibitory neuron might contact a greater number of excitatory neurons (Alhourani et al., 2020). This supports the notion, that rather than a mere loss of GABAergic signalling, the establishment of dysfunctional inhibitory connections contributes to the dysregulation of network excitability observed during epileptogenesis (Thind et al., 2010). In fact, several studies report increased, progressively synchronous interneuronal firing just before onset of seizures (Gnatkovsky et al., 2008; Grasse et al., 2013; Uva et al., 2015) and optogenetic activation interneurons is sufficient to initiate seizure-like events in hippocampal slices *in vitro* (Yekhlief et al., 2015; Chang et al., 2018). These findings underscore the ictogenic potential of aberrant interneuronal activity and raise the question, how altered interneuronal survival in epileptic OPC-GABA_BR cKO mice reflects on disease severity.

Another question that needs further consideration is whether PV⁺ interneurons themselves are in fact lost, or just lose their expression of PV protein as has been debated in previous studies (Wittner et al., 2005; Liu et al., 2014). To remove ambiguity surrounding this issue, we suggest

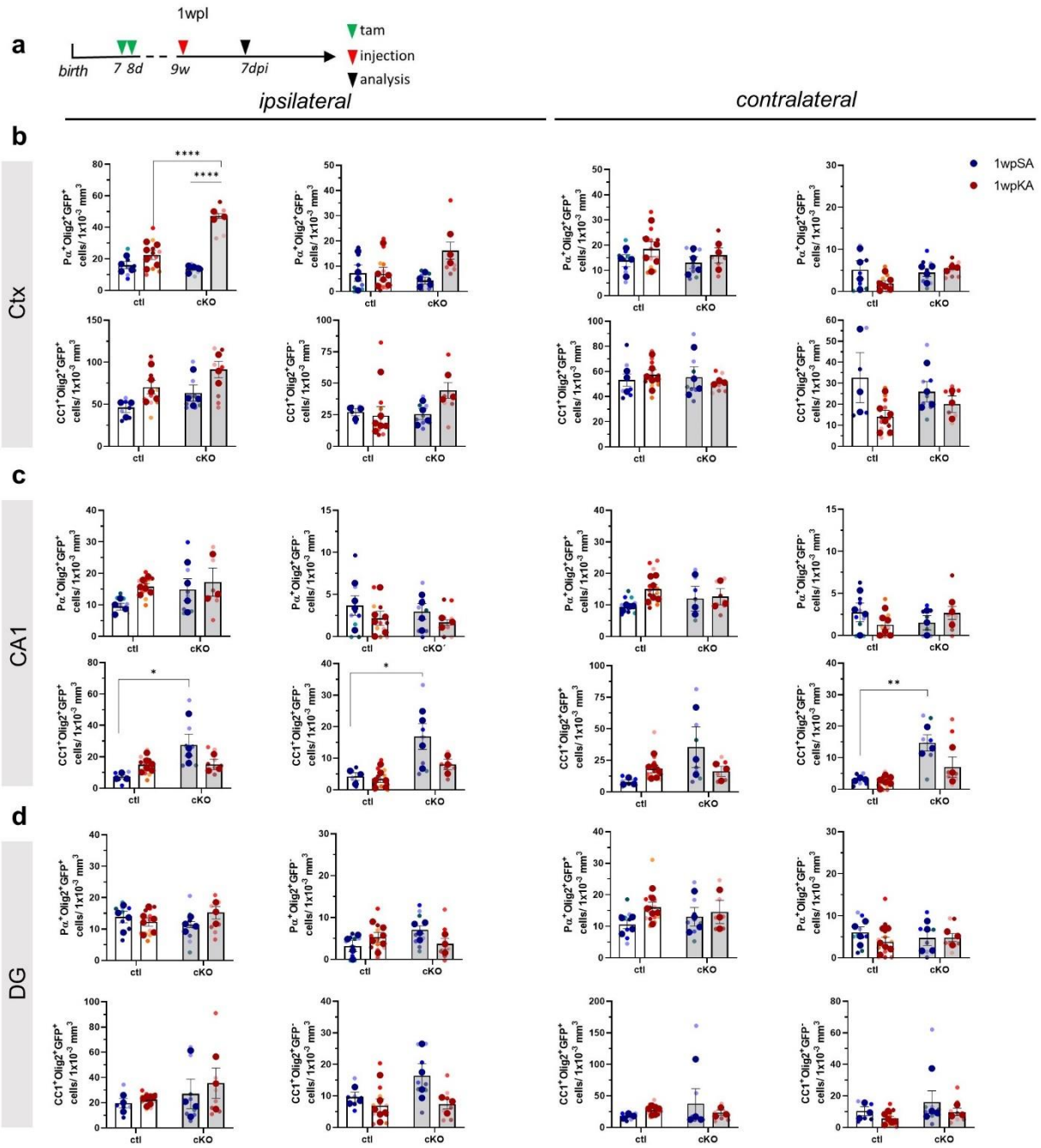
to induce reporter recombination specifically in PV-expressing cells prior to injection of kainate. This would allow us to detect surviving interneurons in the epileptic brain, even if PV-content would be lost. What's more, electrophysiological assays should be conducted to address whether the E/I ratio is altered in epileptic OPC-GABA_BR cKO mice. We established in previous experiments that E/I ratio is increased in healthy GABA_BR cKO mice. However, as interneuronal survival following SE is increased in cKO mice, it is also feasible that E/I ratio is decreased under epileptic conditions.

Moreover, by measuring fluorescence intensity we can only indirectly quantify the GFAP and Iba1 protein content of astrocytes and microglia. Nonetheless, this method bears the advantage of visualizing activation in relation to the distance to the injection side. Thereby, the spatial dimension of the effect of OPC-specific GABA_BR on gliosis is considered. A higher level of certainty in regards to the actual protein content could be gained by employing Western blots. However, while allowing a more precise measurement of protein content, spatial differentiation would be lost.

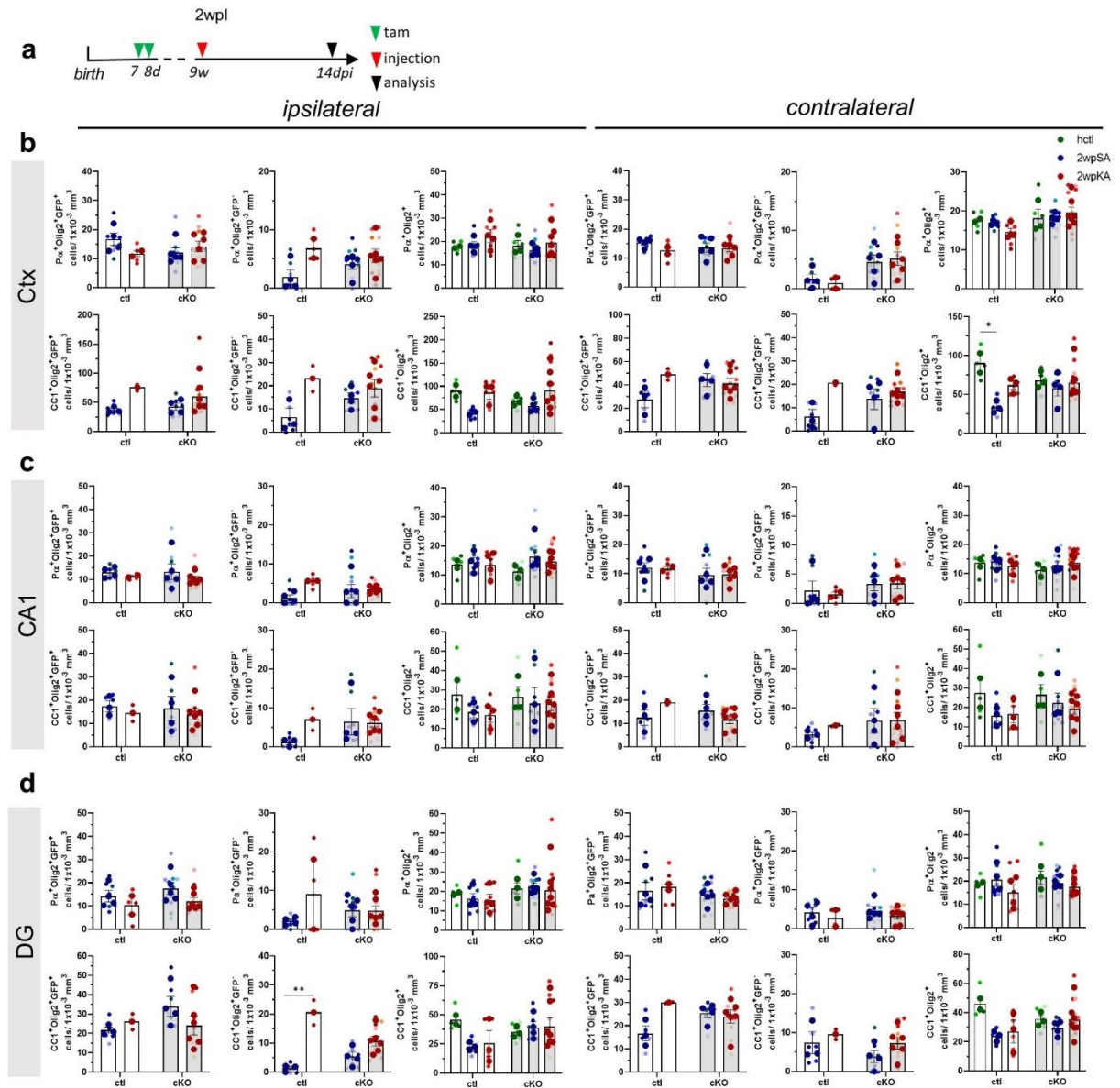
6. Supplementary Figures



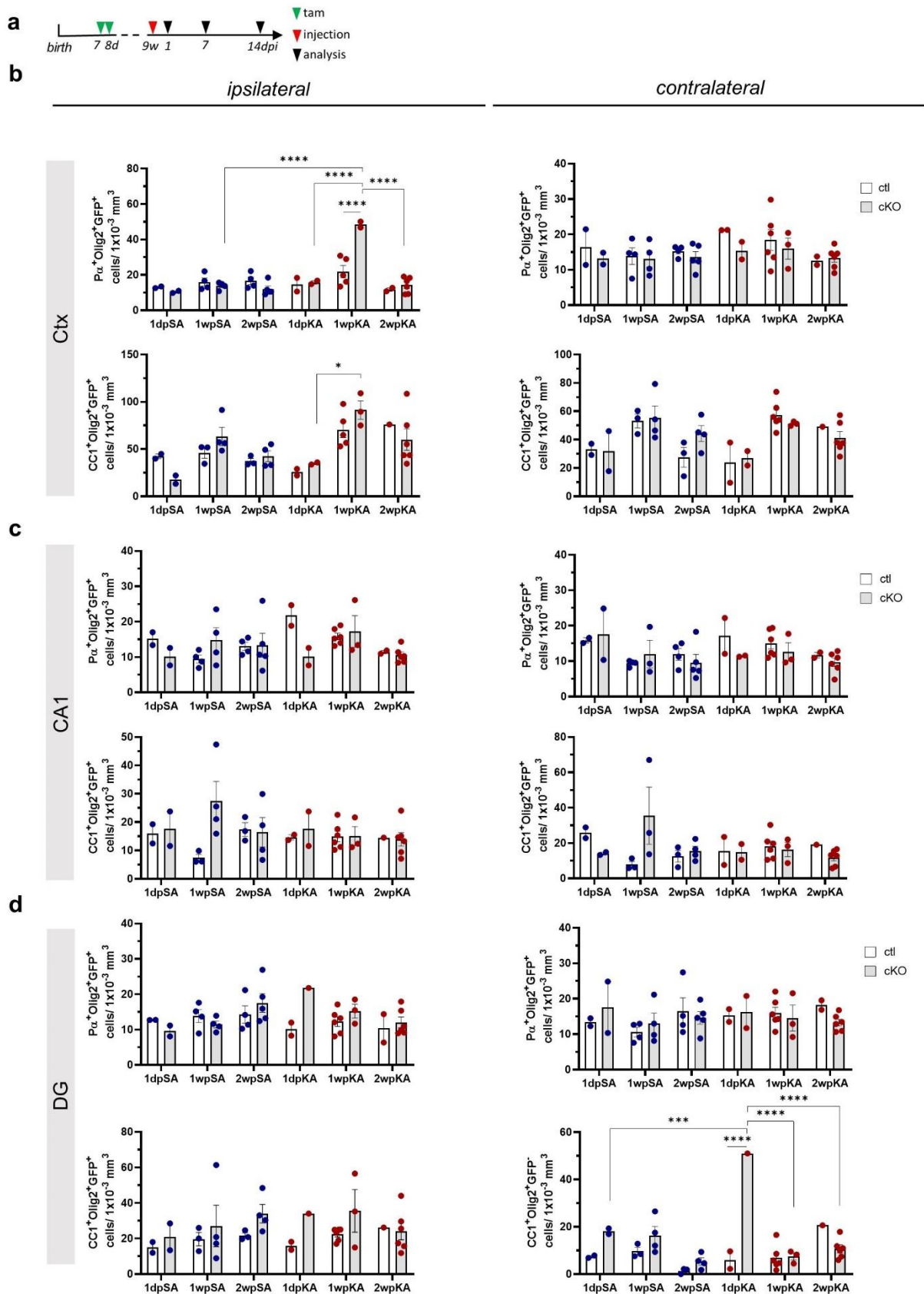
Supplementary Figure 1. OPC and OL density 1dpi. a, Experimental schedule. **b-d**. Quantification of recombined, non-recombined and total OPC and OL density in the Ctx, CA1 and DG of healthy control, saline and kainate injected ctl and cKO mice (2way ANOVA). Big dots signify individual biological sample, small dots of the same colour signify biological sample from the same mouse.



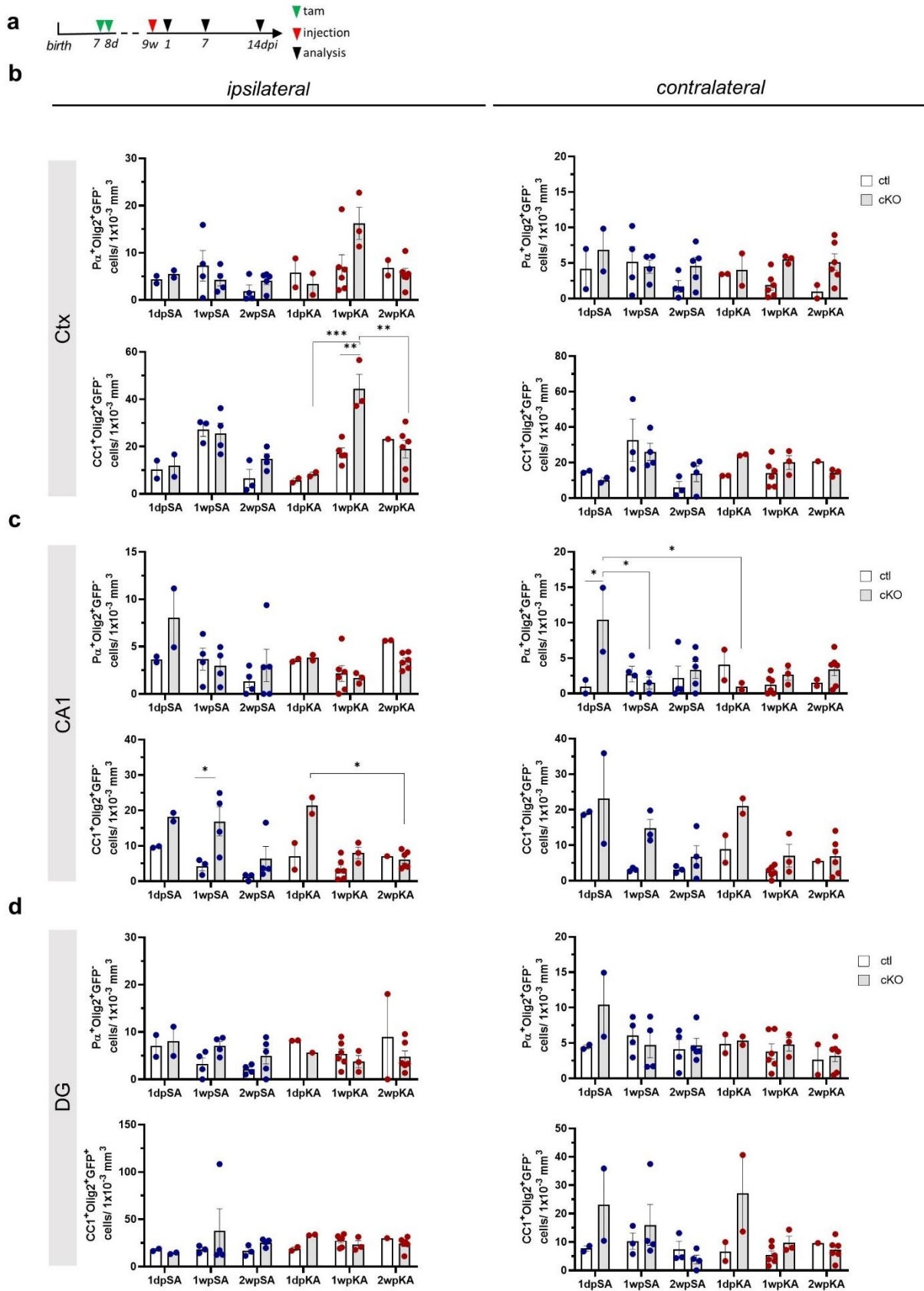
Supplementary Figure 2. OPC and OL density 1wpl. **a**, Experimental schedule. **b-d**. Quantification of recombined and non-recombined OPC and OL density in the Ctx, CA1 and DG of saline and kainate injected ctl and cKO mice (2way ANOVA). Big dots signify individual biological sample, small dots of the same colour signify biological sample from the same mouse.



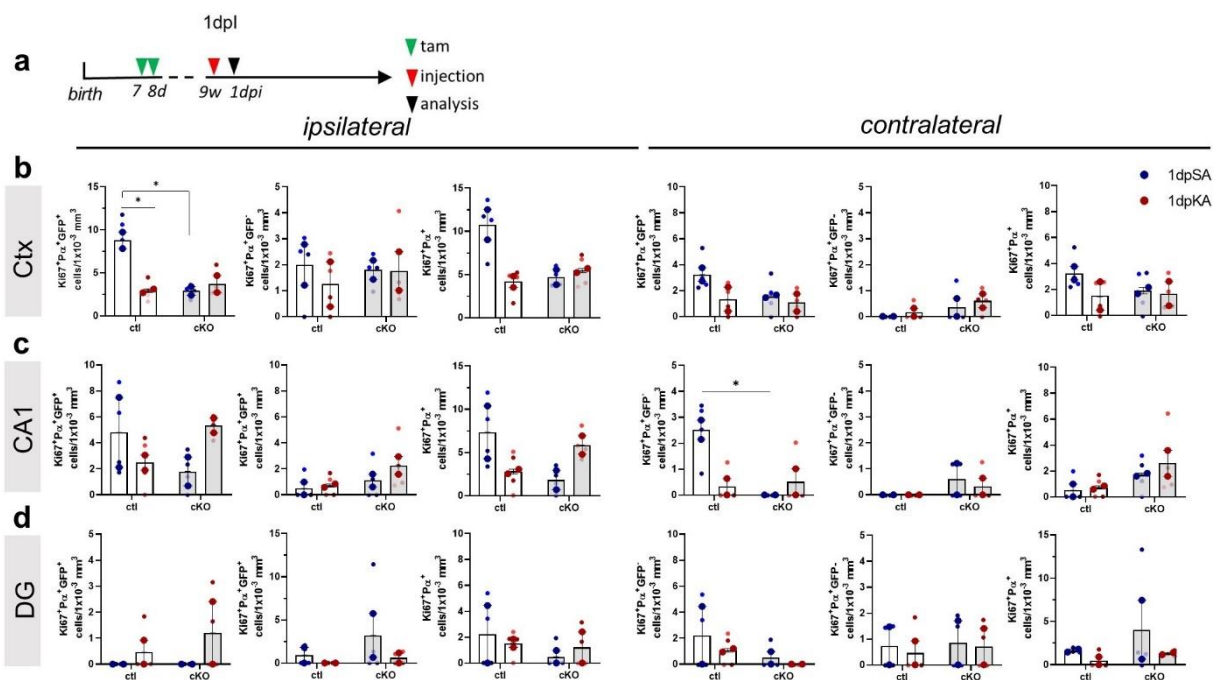
Supplementary Figure 3. OPC and OL density 2wpl. a, Experimental schedule. **b-d**. Quantification of recombined, non-recombined and total OPC and OL density in the Ctx, CA1 and DG of healthy control, saline and kainate injected ctl and cKO mice (2way ANOVA). Big dots signify individual biological sample, small dots of the same colour signify biological sample from the same mouse.



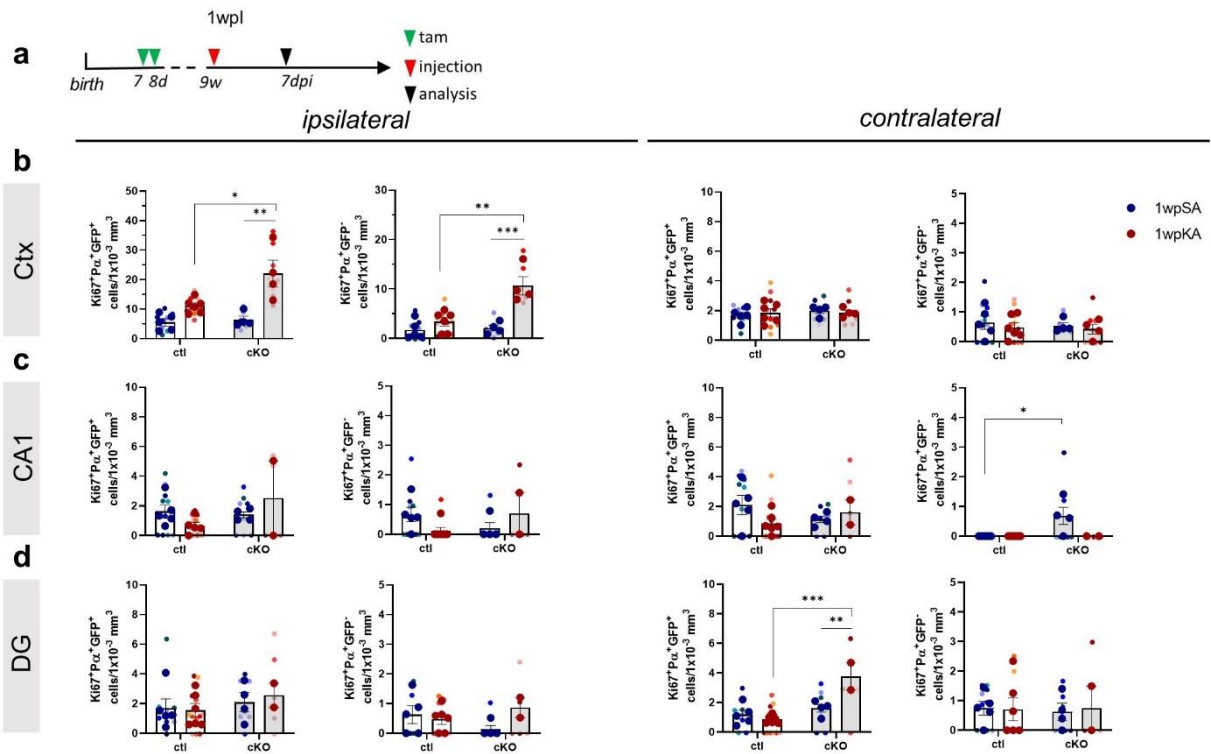
Supplementary Figure 4. Density of recombined OPCs and OLs 1 day, 1 week and 2 weeks post injection. **a**, Experimental schedule for the groups of 1dpl, 1wpl and 2wpl. **b-d**, Quantification of OPC and OL density in ctl and cKO mice at different time points: 1 day, 1 week and 2 weeks post injection of SA or KA (2way ANOVA). Each dot indicates independent biological sample.



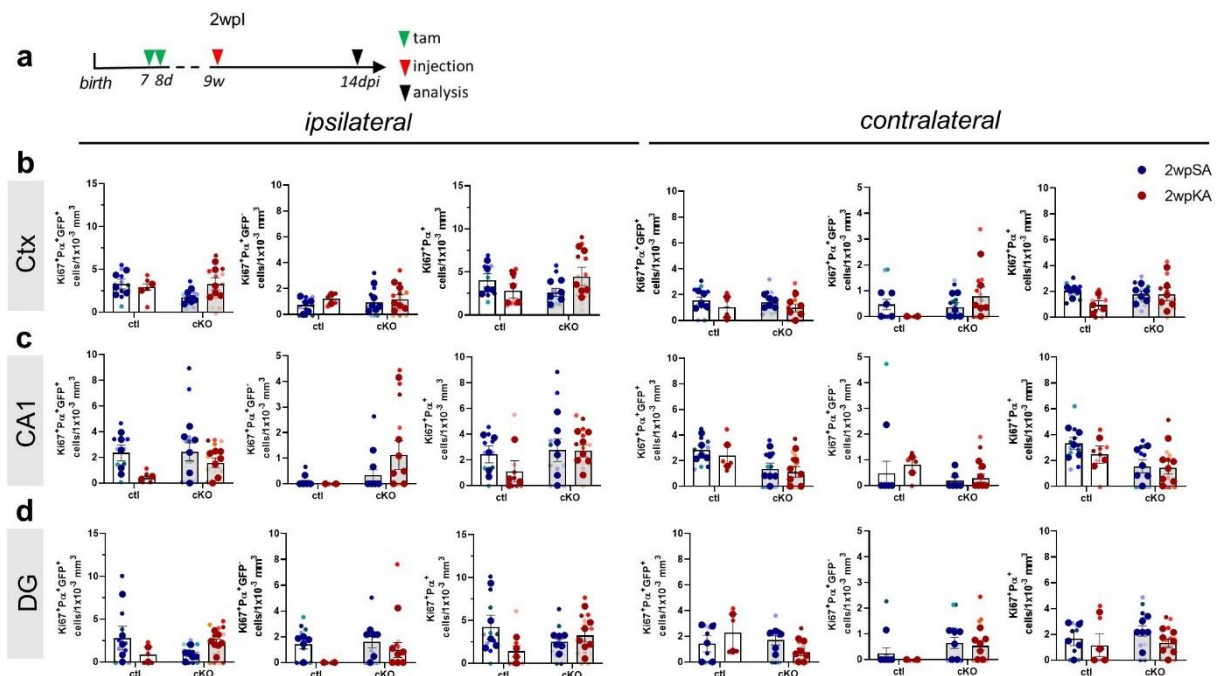
Supplementary Figure 5. Density of non-recombined OPCs and OLs 1 day, 1 week and 2 weeks post injection. **a**, Experimental schedule for the groups of 1dpl, 1wpl and 2wpl. **b-d**, Quantification of OPC and OL density in ctl and cKO mice at different time points: 1 day, 1 week and 2 weeks post injection of SA or KA (2way ANOVA). Each dot indicates independent biological sample.



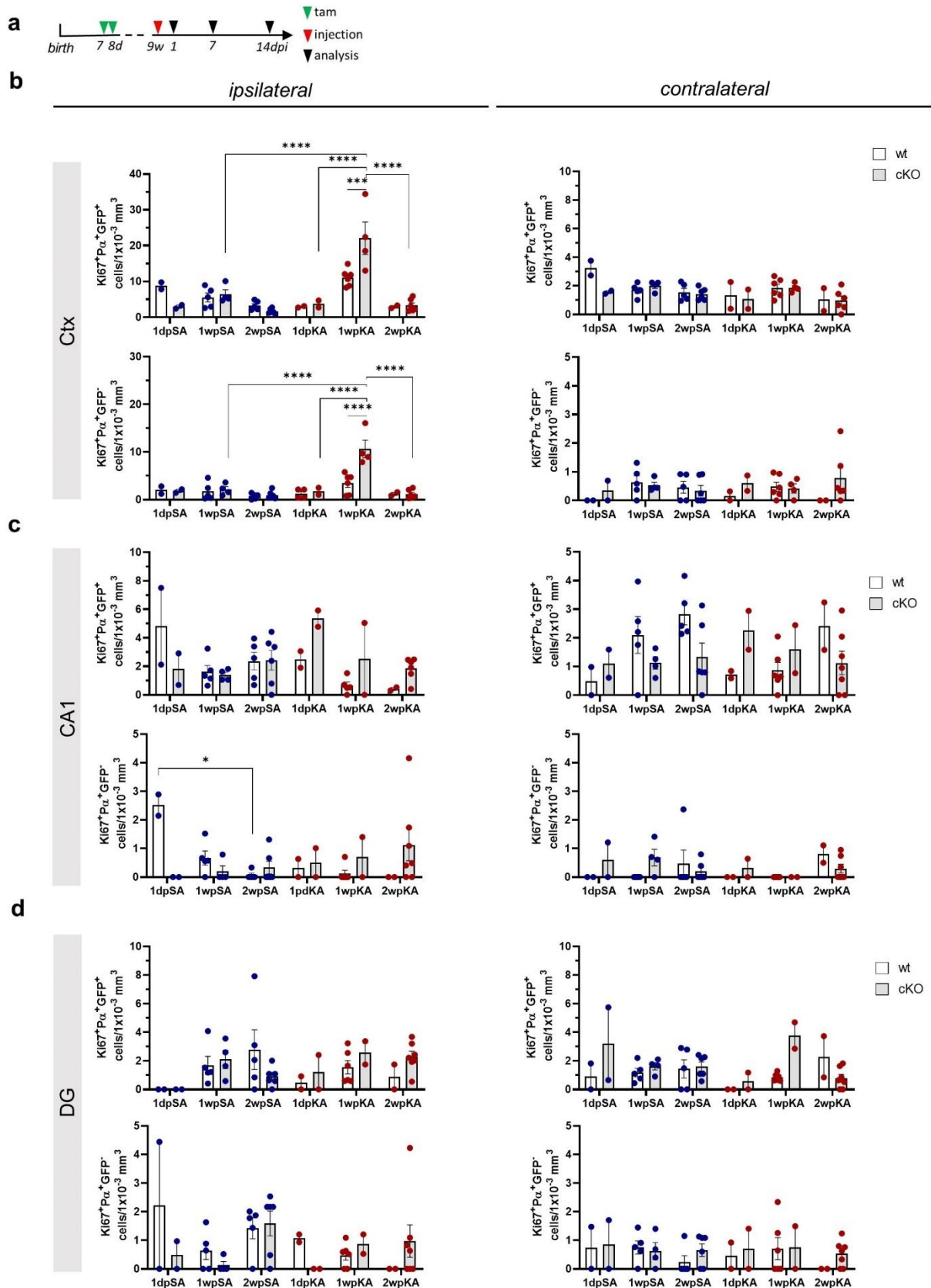
Supplementary Figure 6. Density of proliferating OPCs 1dpi. a, Experimental schedule. **b-d**, Quantification of proliferating recombined, non-recombined and total OPC density in the Ctx, CA1 and DG of saline and kainate injected ctl and cKO mice (2way ANOVA). Big dots signify individual biological sample, small dots of the same colour signify biological sample from the same mouse.



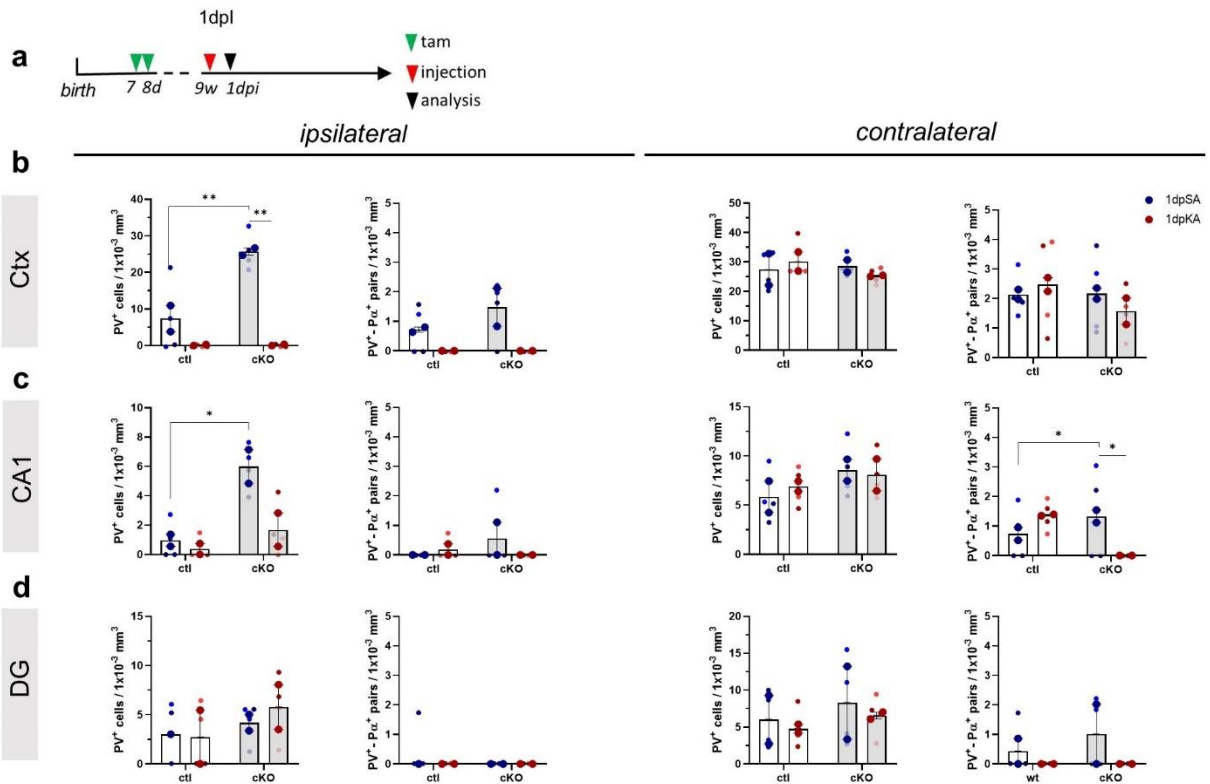
Supplementary Figure 7. Density of proliferating OPCs 1wpl. **a**, Experimental schedule. **b-d**, Quantification of proliferating recombined and non-combined OPC density in the Ctx, CA1 and DG of saline and kainate injected ctl and cKO mice (2way ANOVA). Big dots signify individual biological sample, small dots of the same colour signify biological sample from the same mouse.



Supplementary Figure 8. Density of proliferating OPCs 2wpl. **a**, Experimental schedule. **b-d**, Quantification of proliferating recombined, non-recombined and total OPC density in the Ctx, CA1 and DG of saline and kainate injected ctl and cKO mice (2way ANOVA). Big dots signify individual biological sample, small dots of the same colour signify biological sample from the same mouse.



Supplementary Figure 9. Density of proliferating recombined and non-recombined OPCs 1 day, 1 week and 2 weeks post injection. **a**, Experimental schedule for the groups of 1dpl, 1wpl and 2wpl. **b-d**, Quantification of proliferating OPC density in ctl and cKO mice at different time points: 1 day, 1 week and 2 weeks post injection of SA or KA (2way ANOVA). Each dot indicates independent biological sample.



Supplementary Figure 10. Density of interneurons and interneuron-OPC pairs 1dpl. a, Experimental schedule. **b-d,** Quantification PV⁺ interneuron and PV⁺Pα⁺ pair density in the Ctx, CA1 and DG of saline and kainate injected cti and cKO mice (2way ANOVA). Big dots signify individual biological sample, small dots of the same colour signify biological sample from the same mouse.

7. References

- Alhourani A, Fish KN, Wozny TA, Sudhakar V, Hamilton RL, Richardson RM (2020) GABA bouton subpopulations in the human dentate gyrus are differentially altered in mesial temporal lobe epilepsy. *J Neurophysiol* 123:392-406.
- Almeida RG, Lyons DA (2017) On Myelinated Axon Plasticity and Neuronal Circuit Formation and Function. *J Neurosci* 37:10023-10034.
- Asadi-Pooya AA, Stewart GR, Abrams DJ, Sharan A (2017) Prevalence and Incidence of Drug-Resistant Mesial Temporal Lobe Epilepsy in the United States. *World Neurosurg* 99:662-666.
- Attwell D, Buchan AM, Charpak S, Lauritzen M, Macvicar BA, Newman EA (2010) Glial and neuronal control of brain blood flow. *Nature* 468:232-243.
- Avoli M, de Curtis M, Gnatkovsky V, Gotman J, Köhling R, Lévesque M, Manseau F, Shiri Z, Williams S (2016) Specific imbalance of excitatory/inhibitory signaling establishes seizure onset pattern in temporal lobe epilepsy. *J Neurophysiol* 115:3229-3237.
- Bai X, Kirchhoff F, Scheller A (2021) Oligodendroglial GABAergic Signaling: More Than Inhibition! *Neurosci Bull* 37:1039-1050.
- Balia M, Benamer N, Angulo MC (2017) A specific GABAergic synapse onto oligodendrocyte precursors does not regulate cortical oligodendrogenesis. *Glia* 65:1821-1832.
- Becker AJ (2018) Review: Animal models of acquired epilepsy: insights into mechanisms of human epileptogenesis. *Neuropathol Appl Neurobiol* 44:112-129.
- Bedner P, Dupper A, Hüttmann K, Müller J, Herde MK, Dublin P, Deshpande T, Schramm J, Häussler U, Haas CA, Henneberger C, Theis M, Steinhäuser C (2015) Astrocyte uncoupling as a cause of human temporal lobe epilepsy. *Brain* 138:1208-1222.
- Bell LA, Wallis GJ, Wilcox KS (2020) Reactivity and increased proliferation of NG2 cells following central nervous system infection with Theiler's murine encephalomyelitis virus. *J Neuroinflammation* 17:369.
- Benamer N, Vidal M, Angulo MC (2020) The cerebral cortex is a substrate of multiple interactions between GABAergic interneurons and oligodendrocyte lineage cells. *Neurosci Lett* 715:134615.
- Benson MJ, Manzanero S, Borges K (2015) Complex alterations in microglial M1/M2 markers during the development of epilepsy in two mouse models. *Epilepsia* 56:895-905.
- Bergles DE, Roberts JD, Somogyi P, Jahr CE (2000) Glutamatergic synapses on oligodendrocyte precursor cells in the hippocampus. *Nature* 405:187-191.
- Bezaire MJ, Soltesz I (2013) Quantitative assessment of CA1 local circuits: knowledge base for interneuron-pyramidal cell connectivity. *Hippocampus* 23:751-785.
- Binder DK, Croll SD, Gall CM, Scharfman HE (2001) BDNF and epilepsy: too much of a good thing? *Trends Neurosci* 24:47-53.
- Bloom FE, Iversen LL (1971) Localizing 3H-GABA in nerve terminals of rat cerebral cortex by electron microscopic autoradiography. *Nature* 229:628-630.
- Blümcke I, Pauli E, Clusmann H, Schramm J, Becker A, Elger C, Merschhemke M, Meencke HJ, Lehmann T, von Deimling A, Scheiwe C, Zentner J, Volk B, Romstöck J, Stefan H, Hildebrandt M (2007) A new clinico-pathological classification system for mesial temporal sclerosis. *Acta Neuropathol* 113:235-244.
- Boddum K, Jensen TP, Magloire V, Kristiansen U, Rusakov DA, Pavlov I, Walker MC (2016) Astrocytic GABA transporter activity modulates excitatory neurotransmission. *Nat Commun* 7:13572.
- Bouilleret V, Ridoux V, Depaulis A, Marescaux C, Nehlig A, Le Gal La Salle G (1999) Recurrent seizures and hippocampal sclerosis following intrahippocampal kainate injection in adult mice: electroencephalography, histopathology and synaptic reorganization similar to mesial temporal lobe epilepsy. *Neuroscience* 89:717-729.
- Boulanger JJ, Messier C (2017) Doublecortin in Oligodendrocyte Precursor Cells in the Adult Mouse Brain. *Front Neurosci* 11:143.
- Buckmaster PS, Jongen-Rêlo AL (1999) Highly specific neuron loss preserves lateral inhibitory circuits in the dentate gyrus of kainate-induced epileptic rats. *J Neurosci*

19:9519-9529.

- Bucurenciu I, Bischofberger J, Jonas P (2010) A small number of open Ca²⁺ channels trigger transmitter release at a central GABAergic synapse. *Nat Neurosci* 13:19-21.
- Chang M, Dian JA, Dufour S, Wang L, Moradi Chameh H, Ramani M, Zhang L, Carlen PL, Womelsdorf T, Valiante TA (2018) Brief activation of GABAergic interneurons initiates the transition to ictal events through post-inhibitory rebound excitation. *Neurobiol Dis* 109:102-116.
- Colonna M, Butovsky O (2017) Microglia Function in the Central Nervous System During Health and Neurodegeneration. *Annu Rev Immunol* 35:441-468.
- Cossart R, Dinocourt C, Hirsch JC, Merchan-Perez A, De Felipe J, Ben-Ari Y, Esclapez M, Bernard C (2001) Dendritic but not somatic GABAergic inhibition is decreased in experimental epilepsy. *Nat Neurosci* 4:52-62.
- Davalos D, Grutzendler J, Yang G, Kim JV, Zuo Y, Jung S, Littman DR, Dustin ML, Gan WB (2005) ATP mediates rapid microglial response to local brain injury in vivo. *Nat Neurosci* 8:752-758.
- Dawson MR, Polito A, Levine JM, Reynolds R (2003) NG2-expressing glial progenitor cells: an abundant and widespread population of cycling cells in the adult rat CNS. *Mol Cell Neurosci* 24:476-488.
- de Lanerolle NC, Kim JH, Robbins RJ, Spencer DD (1989) Hippocampal interneuron loss and plasticity in human temporal lobe epilepsy. *Brain Res* 495:387-395.
- DeFelipe J et al. (2013) New insights into the classification and nomenclature of cortical GABAergic interneurons. *Nat Rev Neurosci* 14:202-216.
- Dibaj P, Nadrigny F, Steffens H, Scheller A, Hirrlinger J, Schomburg ED, Neusch C, Kirchhoff F (2010) NO mediates microglial response to acute spinal cord injury under ATP control in vivo. *Glia* 58:1133-1144.
- Dinocourt C, Petanjek Z, Freund TF, Ben-Ari Y, Esclapez M (2003) Loss of interneurons innervating pyramidal cell dendrites and axon initial segments in the CA1 region of the hippocampus following pilocarpine-induced seizures. *J Comp Neurol* 459:407-425.
- Donkels C, Peters M, Fariña Núñez MT, Nakagawa JM, Kirsch M, Vlachos A, Scheiwe C, Schulze-Bonhage A, Prinz M, Beck J, Haas CA (2020) Oligodendrocyte lineage and myelination are compromised in the gray matter of focal cortical dysplasia type IIa. *Epilepsia* 61:171-184.
- Drenthen GS, Backes WH, Aldenkamp AP, Vermeulen RJ, Klinkenberg S, Jansen JFA (2020) On the merits of non-invasive myelin imaging in epilepsy, a literature review. *J Neurosci Methods* 338:108687.
- Epsztein J, Milh M, Bihi RI, Jorquera I, Ben-Ari Y, Represa A, Crépel V (2006) Ongoing epileptiform activity in the post-ischemic hippocampus is associated with a permanent shift of the excitatory-inhibitory synaptic balance in CA3 pyramidal neurons. *J Neurosci* 26:7082-7092.
- Eugenín-von Bernhardt J, Dimou L (2016) NG2-glia, More Than Progenitor Cells. *Adv Exp Med Biol* 949:27-45.
- Fang LP, Zhao N, Caudal LC, Chang HF, Zhao R, Lin CH, Hainz N, Meier C, Bettler B, Huang W, Scheller A, Kirchhoff F, Bai X (2022) Impaired bidirectional communication between interneurons and oligodendrocyte precursor cells affects social cognitive behavior. *Nat Commun* 13:1394.
- Fang LP, Liu Q, Meyer E, Welle A, Huang W, Scheller A, Kirchhoff F, Bai X (2023) A subset of OPCs do not express Olig2 during development which can be increased in the adult by brain injuries and complex motor learning. *Glia* 71:415-430.
- Fannon J, Tarmier W, Fulton D (2015) Neuronal activity and AMPA-type glutamate receptor activation regulates the morphological development of oligodendrocyte precursor cells. *Glia* 63:1021-1035.
- Fiest KM, Sauro KM, Wiebe S, Patten SB, Kwon CS, Dykeman J, Pringsheim T, Lorenzetti DL, Jetté N (2017) Prevalence and incidence of epilepsy: A systematic review and meta-analysis of international studies. *Neurology* 88:296-303.

- Fisher RS, van Emde Boas W, Blume W, Elger C, Genton P, Lee P, Engel J (2005) Epileptic seizures and epilepsy: definitions proposed by the International League Against Epilepsy (ILAE) and the International Bureau for Epilepsy (IBE). *Epilepsia* 46:470-472.
- Freund TF, Buzsáki G (1996) Interneurons of the hippocampus. *Hippocampus* 6:347-470.
- Fritschy JM (2008) Epilepsy, E/I Balance and GABA(A) Receptor Plasticity. *Front Mol Neurosci* 1:5.
- Ge WP, Yang XJ, Zhang Z, Wang HK, Shen W, Deng QD, Duan S (2006) Long-term potentiation of neuron-glia synapses mediated by Ca²⁺-permeable AMPA receptors. *Science* 312:1533-1537.
- Gibson EM, Purger D, Mount CW, Goldstein AK, Lin GL, Wood LS, Inema I, Miller SE, Bieri G, Zuchero JB, Barres BA, Woo PJ, Vogel H, Monje M (2014) Neuronal activity promotes oligodendrogenesis and adaptive myelination in the mammalian brain. *Science* 344:1252304.
- Gnatkovsky V, Librizzi L, Trombin F, de Curtis M (2008) Fast activity at seizure onset is mediated by inhibitory circuits in the entorhinal cortex in vitro. *Ann Neurol* 64:674-686.
- Grasse DW, Karunakaran S, Moxon KA (2013) Neuronal synchrony and the transition to spontaneous seizures. *Exp Neurol* 248:72-84.
- Gröticke I, Hoffmann K, Löscher W (2008) Behavioral alterations in a mouse model of temporal lobe epilepsy induced by intrahippocampal injection of kainate. *Exp Neurol* 213:71-83.
- Guo Q, Scheller A, Huang W (2021) Progenies of NG2 glia: what do we learn from transgenic mouse models? *Neural Regen Res* 16:43-48.
- Hamilton NB, Clarke LE, Arancibia-Carcamo IL, Kougioumtzidou E, Matthey M, Káradóttir R, Whiteley L, Bergersen LH, Richardson WD, Attwell D (2017) Endogenous GABA controls oligodendrocyte lineage cell number, myelination, and CNS internode length. *Glia* 65:309-321.
- Heo K, Cho YJ, Cho KJ, Kim HW, Kim HJ, Shin HY, Lee BI, Kim GW (2006) Minocycline inhibits caspase-dependent and -independent cell death pathways and is neuroprotective against hippocampal damage after treatment with kainic acid in mice. *Neurosci Lett* 398:195-200.
- Hill RA, Patel KD, Goncalves CM, Grutzendler J, Nishiyama A (2014) Modulation of oligodendrocyte generation during a critical temporal window after NG2 cell division. *Nat Neurosci* 17:1518-1527.
- Hiragi T, Ikegaya Y, Koyama R (2018) Microglia after Seizures and in Epilepsy. *Cells* 7.
- Horner PJ, Thalhammer M, Gage FH (2002) Defining the NG2-expressing cell of the adult CNS. *J Neurocytol* 31:469-480.
- Hu H, Jonas P (2014) A supercritical density of Na(+) channels ensures fast signaling in GABAergic interneuron axons. *Nat Neurosci* 17:686-693.
- Hu H, Gan J, Jonas P (2014) Interneurons. Fast-spiking, parvalbumin⁺ GABAergic interneurons: from cellular design to microcircuit function. *Science* 345:1255263.
- Huang W, Guo Q, Bai X, Scheller A, Kirchhoff F (2019) Early embryonic NG2 glia are exclusively gliogenic and do not generate neurons in the brain. *Glia* 67:1094-1103.
- Huang W, Zhao N, Bai X, Karram K, Trotter J, Goebbels S, Scheller A, Kirchhoff F (2014) Novel NG2-CreERT2 knock-in mice demonstrate heterogeneous differentiation potential of NG2 glia during development. *Glia* 62:896-913.
- Hughes EG, Kang SH, Fukaya M, Bergles DE (2013) Oligodendrocyte progenitors balance growth with self-repulsion to achieve homeostasis in the adult brain. *Nat Neurosci* 16:668-676.
- Imai Y, Iбата I, Ito D, Ohsawa K, Kohsaka S (1996) A novel gene *iba1* in the major histocompatibility complex class III region encoding an EF hand protein expressed in a monocytic lineage. *Biochem Biophys Res Commun* 224:855-862.
- Jefferys J, Steinhäuser C, Bedner P (2016) Chemically-induced TLE models: Topical application. *J Neurosci Methods* 260:53-61.
- Kang SH, Fukaya M, Yang JK, Rothstein JD, Bergles DE (2010) NG2+ CNS glial progenitors

- remain committed to the oligodendrocyte lineage in postnatal life and following neurodegeneration. *Neuron* 68:668-681.
- Katsumaru H, Kosaka T, Heizmann CW, Hama K (1988) Immunocytochemical study of GABAergic neurons containing the calcium-binding protein parvalbumin in the rat hippocampus. *Exp Brain Res* 72:347-362.
- Keränen T, Riekkinen P (1988) Severe epilepsy: diagnostic and epidemiological aspects. *Acta Neurol Scand Suppl* 117:7-14.
- Kettenmann H, Kirchhoff F, Verkhratsky A (2013) Microglia: new roles for the synaptic stripper. *Neuron* 77:10-18.
- Khawaja RR, Agarwal A, Fukaya M, Jeong HK, Gross S, Gonzalez-Fernandez E, Soboloff J, Bergles DE, Kang SH (2021a) GluA2 overexpression in oligodendrocyte progenitors promotes postinjury oligodendrocyte regeneration. *Cell Rep* 35:109147.
- Khawaja RR, Agarwal A, Fukaya M, Jeong HK, Gross S, Gonzalez-Fernandez E, Soboloff J, Bergles DE, Kang SH (2021b) GluA2 overexpression in oligodendrocyte progenitors promotes postinjury oligodendrocyte regeneration. *Cell Rep* 35:109147.
- Khundakar AA, Zetterström TS (2011) Effects of GABAB ligands alone and in combination with paroxetine on hippocampal BDNF gene expression. *Eur J Pharmacol* 671:33-38.
- Klausberger T, Somogyi P (2008) Neuronal diversity and temporal dynamics: the unity of hippocampal circuit operations. *Science* 321:53-57.
- Knight AR, Bowerly NG (1996) The pharmacology of adenylyl cyclase modulation by GABAB receptors in rat brain slices. *Neuropharmacology* 35:703-712.
- Kokaia M, Ernfors P, Kokaia Z, Elmér E, Jaenisch R, Lindvall O (1995) Suppressed epileptogenesis in BDNF mutant mice. *Exp Neurol* 133:215-224.
- Kumar SS, Buckmaster PS (2006) Hyperexcitability, interneurons, and loss of GABAergic synapses in entorhinal cortex in a model of temporal lobe epilepsy. *J Neurosci* 26:4613-4623.
- Kwan P, Brodie MJ (2000) Early identification of refractory epilepsy. *N Engl J Med* 342:314-319.
- Köhler S, Winkler U, Hirrlinger J (2021) Heterogeneity of Astrocytes in Grey and White Matter. *Neurochem Res* 46:3-14.
- Leal G, Comprido D, Duarte CB (2014) BDNF-induced local protein synthesis and synaptic plasticity. *Neuropharmacology* 76 Pt C:639-656.
- Lee SE, Lee Y, Lee GH (2019) The regulation of glutamic acid decarboxylases in GABA neurotransmission in the brain. *Arch Pharm Res* 42:1031-1039.
- Leite JP, Garcia-Cairasco N, Cavalheiro EA (2002) New insights from the use of pilocarpine and kainate models. *Epilepsy Res* 50:93-103.
- Levine JM, Reynolds R, Fawcett JW (2001) The oligodendrocyte precursor cell in health and disease. *Trends Neurosci* 24:39-47.
- Li Q, Brus-Ramer M, Martin JH, McDonald JW (2010) Electrical stimulation of the medullary pyramid promotes proliferation and differentiation of oligodendrocyte progenitor cells in the corticospinal tract of the adult rat. *Neurosci Lett* 479:128-133.
- Liu J, Reeves C, Michalak Z, Coppola A, Diehl B, Sisodiya SM, Thom M (2014a) Evidence for mTOR pathway activation in a spectrum of epilepsy-associated pathologies. *Acta Neuropathol Commun* 2:71.
- Liu YQ, Yu F, Liu WH, He XH, Peng BW (2014b) Dysfunction of hippocampal interneurons in epilepsy. *Neurosci Bull* 30:985-998.
- Luo Y, Hu Q, Zhang Q, Hong S, Tang X, Cheng L, Jiang L (2015) Alterations in hippocampal myelin and oligodendrocyte precursor cells during epileptogenesis. *Brain Res* 1627:154-164.
- Luyt K, Slade TP, Dorward JJ, Durant CF, Wu Y, Shigemoto R, Mundell SJ, Váradi A, Molnár E (2007) Developing oligodendrocytes express functional GABA(B) receptors that stimulate cell proliferation and migration. *J Neurochem* 100:822-840.
- Lévesque M, Avoli M (2013) The kainic acid model of temporal lobe epilepsy. *Neurosci Biobehav Rev* 37:2887-2899.
- MacVicar BA, Newman EA (2015) Astrocyte regulation of blood flow in the brain. *Cold Spring*

- Harb Perspect Biol 7.
- Mahmoud S, Gharagozloo M, Simard C, Gris D (2019) Astrocytes Maintain Glutamate Homeostasis in the CNS by Controlling the Balance between Glutamate Uptake and Release. *Cells* 8.
- Mangin JM, Kunze A, Chittajallu R, Gallo V (2008) Satellite NG2 progenitor cells share common glutamatergic inputs with associated interneurons in the mouse dentate gyrus. *J Neurosci* 28:7610-7623.
- Marx M, Haas CA, Häussler U (2013) Differential vulnerability of interneurons in the epileptic hippocampus. *Front Cell Neurosci* 7:167.
- Mitew S, Gobius I, Fenlon LR, McDougall SJ, Hawkes D, Xing YL, Bujalka H, Gundlach AL, Richards LJ, Kilpatrick TJ, Merson TD, Emery B (2018) Pharmacogenetic stimulation of neuronal activity increases myelination in an axon-specific manner. *Nat Commun* 9:306.
- Mount CW, Yalçın B, Cunliffe-Koehler K, Sundaresh S, Monje M (2019) Monosynaptic tracing maps brain-wide afferent oligodendrocyte precursor cell connectivity. *Elife* 8.
- Mula M (2011) GABAergic drugs in the treatment of epilepsy: modern or outmoded? *Future Med Chem* 3:177-182.
- Müller J, Timmermann A, Henning L, Müller H, Steinhäuser C, Bedner P (2020) Astrocytic GABA Accumulation in Experimental Temporal Lobe Epilepsy. *Front Neurol* 11:614923.
- Nawa H, Carnahan J, Gall C (1995) BDNF protein measured by a novel enzyme immunoassay in normal brain and after seizure: partial disagreement with mRNA levels. *Eur J Neurosci* 7:1527-1535.
- Nimmerjahn A, Kirchhoff F, Helmchen F (2005) Resting microglial cells are highly dynamic surveillants of brain parenchyma in vivo. *Science* 308:1314-1318.
- Nishiyama A, Lin XH, Giese N, Heldin CH, Stallcup WB (1996) Co-localization of NG2 proteoglycan and PDGF alpha-receptor on O2A progenitor cells in the developing rat brain. *J Neurosci Res* 43:299-314.
- Orduz D, Benamer N, Ortolani D, Coppola E, Vigier L, Pierani A, Angulo MC (2019) Developmental cell death regulates lineage-related interneuron-oligodendroglia functional clusters and oligodendrocyte homeostasis. *Nat Commun* 10:4249.
- Orduz D, Maldonado PP, Balia M, Vélez-Fort M, de Sars V, Yanagawa Y, Emiliani V, Angulo MC (2015) Interneurons and oligodendrocyte progenitors form a structured synaptic network in the developing neocortex. *Elife* 4.
- Pascual MR (2007) Temporal lobe epilepsy: clinical semiology and neurophysiological studies. *Semin Ultrasound CT MR* 28:416-423.
- Patel DC, Tewari BP, Chaunsali L, Sontheimer H (2019) Neuron-glia interactions in the pathophysiology of epilepsy. *Nat Rev Neurosci* 20:282-297.
- Paukert M, Agarwal A, Cha J, Doze VA, Kang JU, Bergles DE (2014) Norepinephrine controls astroglial responsiveness to local circuit activity. *Neuron* 82:1263-1270.
- Pelkey KA, Chittajallu R, Craig MT, Tricoire L, Wester JC, McBain CJ (2017) Hippocampal GABAergic Inhibitory Interneurons. *Physiol Rev* 97:1619-1747.
- Pellegrini-Giampietro DE, Gorter JA, Bennett MV, Zukin RS (1997) The GluR2 (GluR-B) hypothesis: Ca(2+)-permeable AMPA receptors in neurological disorders. *Trends Neurosci* 20:464-470.
- Petroff OA (2002) GABA and glutamate in the human brain. *Neuroscientist* 8:562-573.
- Psachoulia K, Jamen F, Young KM, Richardson WD (2009) Cell cycle dynamics of NG2 cells in the postnatal and ageing brain. *Neuron Glia Biol* 5:57-67.
- Quarato PP, Di Gennaro G, Mascia A, Grammaldo LG, Meldolesi GN, Picardi A, Giampà T, Falco C, Sebastiano F, Onorati P, Manfredi M, Cantore G, Esposito V (2005) Temporal lobe epilepsy surgery: different surgical strategies after a non-invasive diagnostic protocol. *J Neurol Neurosurg Psychiatry* 76:815-824.
- Riban V, Boullieret V, Pham-Lê BT, Fritschy JM, Marescaux C, Depaulis A (2002) Evolution of hippocampal epileptic activity during the development of hippocampal sclerosis in a mouse model of temporal lobe epilepsy. *Neuroscience* 112:101-111.

- Roberts E, Frankel S (1950) gamma-Aminobutyric acid in brain: its formation from glutamic acid. *J Biol Chem* 187:55-63.
- Roberts E, Frankel S (1951) Glutamic acid decarboxylase in brain. *J Biol Chem* 188:789-795.
- Rogawski MA, Löscher W (2004) The neurobiology of antiepileptic drugs. *Nat Rev Neurosci* 5:553-564.
- Rouach N, Koulakoff A, Abudara V, Willecke K, Giaume C (2008) Astroglial metabolic networks sustain hippocampal synaptic transmission. *Science* 322:1551-1555.
- Rudy B, Fishell G, Lee S, Hjerling-Leffler J (2011) Three groups of interneurons account for nearly 100% of neocortical GABAergic neurons. *Dev Neurobiol* 71:45-61.
- Scanlon C, Mueller SG, Cheong I, Hartig M, Weiner MW, Laxer KD (2013) Grey and white matter abnormalities in temporal lobe epilepsy with and without mesial temporal sclerosis. *J Neurol* 260:2320-2329.
- Scharfman HE (1997) Hyperexcitability in combined entorhinal/hippocampal slices of adult rat after exposure to brain-derived neurotrophic factor. *J Neurophysiol* 78:1082-1095.
- Scheller A, Bai X, Kirchhoff F (2017) The Role of the Oligodendrocyte Lineage in Acute Brain Trauma. *Neurochem Res* 42:2479-2489.
- Schoene-Bake JC, Faber J, Trautner P, Kaaden S, Tittgemeyer M, Elger CE, Weber B (2009) Widespread affections of large fiber tracts in postoperative temporal lobe epilepsy. *Neuroimage* 46:569-576.
- Seifert G, Hüttmann K, Binder DK, Hartmann C, Wyczynski A, Neusch C, Steinhäuser C (2009) Analysis of astroglial K⁺ channel expression in the developing hippocampus reveals a predominant role of the Kir4.1 subunit. *J Neurosci* 29:7474-7488.
- Serrano-Regal MP, Luengas-Escuza I, Bayón-Cordero L, Ibarra-Aizpurua N, Alberdi E, Pérez-Samartín A, Matute C, Sánchez-Gómez MV (2019) Oligodendrocyte Differentiation and Myelination Is Potentiated via GABA. *Neuroscience*.
- Sharma AK, Rani E, Waheed A, Rajput SK (2015) Pharmacoresistant Epilepsy: A Current Update on Non-Conventional Pharmacological and Non-Pharmacological Interventions. *J Epilepsy Res* 5:1-8.
- Sierra A, Laitinen T, Lehtimäki K, Rieppo L, Pitkänen A, Gröhn O (2011) Diffusion tensor MRI with tract-based spatial statistics and histology reveals undiscovered lesioned areas in kainate model of epilepsy in rat. *Brain Struct Funct* 216:123-135.
- Sieu LA, Eugène E, Bonnot A, Cohen I (2017) Disrupted Co-activation of Interneurons and Hippocampal Network after Focal Kainate Lesion. *Front Neural Circuits* 11:87.
- Sillanpää M, Jalava M, Kaleva O, Shinnar S (1998) Long-term prognosis of seizures with onset in childhood. *N Engl J Med* 338:1715-1722.
- Silver J, Miller JH (2004) Regeneration beyond the glial scar. *Nat Rev Neurosci* 5:146-156.
- Sloviter RS (1994) The functional organization of the hippocampal dentate gyrus and its relevance to the pathogenesis of temporal lobe epilepsy. *Ann Neurol* 35:640-654.
- Sloviter RS, Sollas AL, Barbaro NM, Laxer KD (1991) Calcium-binding protein (calbindin-D28K) and parvalbumin immunocytochemistry in the normal and epileptic human hippocampus. *J Comp Neurol* 308:381-396.
- Sofroniew MV (2014) Astrogliosis. *Cold Spring Harb Perspect Biol* 7:a020420.
- Sohal VS, Zhang F, Yizhar O, Deisseroth K (2009) Parvalbumin neurons and gamma rhythms enhance cortical circuit performance. *Nature* 459:698-702.
- Suzuki F, Junier MP, Guilhem D, Sørensen JC, Onteniente B (1995) Morphogenetic effect of kainate on adult hippocampal neurons associated with a prolonged expression of brain-derived neurotrophic factor. *Neuroscience* 64:665-674.
- Takahashi K, Rochford CD, Neumann H (2005) Clearance of apoptotic neurons without inflammation by microglial triggering receptor expressed on myeloid cells-2. *J Exp Med* 201:647-657.
- Tao X, Finkbeiner S, Arnold DB, Shaywitz AJ, Greenberg ME (1998) Ca²⁺ influx regulates BDNF transcription by a CREB family transcription factor-dependent mechanism. *Neuron* 20:709-726.
- Terunuma M, Revilla-Sanchez R, Quadros IM, Deng Q, Deeb TZ, Lumb M, Sicinski P, Haydon PG, Pangalos MN, Moss SJ (2014) Postsynaptic GABAB receptor activity

- regulates excitatory neuronal architecture and spatial memory. *J Neurosci* 34:804-816.
- Thind KK, Yamawaki R, Phanwar I, Zhang G, Wen X, Buckmaster PS (2010) Initial loss but later excess of GABAergic synapses with dentate granule cells in a rat model of temporal lobe epilepsy. *J Comp Neurol* 518:647-667.
- Trevelyan AJ, Sussillo D, Yuste R (2007) Feedforward inhibition contributes to the control of epileptiform propagation speed. *J Neurosci* 27:3383-3387.
- Trevelyan AJ, Sussillo D, Watson BO, Yuste R (2006) Modular propagation of epileptiform activity: evidence for an inhibitory veto in neocortex. *J Neurosci* 26:12447-12455.
- Uva L, Breschi GL, Gnatkovsky V, Taverna S, de Curtis M (2015) Synchronous inhibitory potentials precede seizure-like events in acute models of focal limbic seizures. *J Neurosci* 35:3048-3055.
- van Vliet EA, Otte WM, Wadman WJ, Aronica E, Kooij G, de Vries HE, Dijkhuizen RM, Gorter JA (2016) Blood-brain barrier leakage after status epilepticus in rapamycin-treated rats I: Magnetic resonance imaging. *Epilepsia* 57:59-69.
- Vezzani A, French J, Bartfai T, Baram TZ (2011) The role of inflammation in epilepsy. *Nat Rev Neurol* 7:31-40.
- Vélez-Fort M, Maldonado PP, Butt AM, Audinat E, Angulo MC (2010) Postnatal switch from synaptic to extrasynaptic transmission between interneurons and NG2 cells. *J Neurosci* 30:6921-6929.
- Wang BS, Bernardez Sarria MS, An X, He M, Alam NM, Prusky GT, Crair MC, Huang ZJ (2021) Retinal and Callosal Activity-Dependent Chandelier Cell Elimination Shapes Binocularity in Primary Visual Cortex. *Neuron* 109:502-515.e507.
- Wang N, Mi X, Gao B, Gu J, Wang W, Zhang Y, Wang X (2015) Minocycline inhibits brain inflammation and attenuates spontaneous recurrent seizures following pilocarpine-induced status epilepticus. *Neuroscience* 287:144-156.
- Wang Y, Zhang P, Wyskiel DR (2016) Chandelier Cells in Functional and Dysfunctional Neural Circuits. *Front Neural Circuits* 10:33.
- Wittner L, Eross L, Czirják S, Halász P, Freund TF, Maglóczy Z (2005) Surviving CA1 pyramidal cells receive intact perisomatic inhibitory input in the human epileptic hippocampus. *Brain* 128:138-152.
- Wittner L, Maglóczy Z, Borhegyi Z, Halász P, Tóth S, Eross L, Szabó Z, Freund TF (2001) Preservation of perisomatic inhibitory input of granule cells in the epileptic human dentate gyrus. *Neuroscience* 108:587-600.
- Wu XL, Zhou JS, Wang LH, Liu JX, Hu HB, Zhang XT, Li YJ, Tang FR (2019) Proliferation of NG2 cells in the epileptic hippocampus. *Epilepsy Res* 152:67-72.
- Wyeth MS, Zhang N, Mody I, Houser CR (2010) Selective reduction of cholecystokinin-positive basket cell innervation in a model of temporal lobe epilepsy. *J Neurosci* 30:8993-9006.
- Ye Y, Xiong J, Hu J, Kong M, Cheng L, Chen H, Li T, Jiang L (2013) Altered hippocampal myelinated fiber integrity in a lithium-pilocarpine model of temporal lobe epilepsy: a histopathological and stereological investigation. *Brain Res* 1522:76-87.
- Yekhlef L, Breschi GL, Lagostena L, Russo G, Taverna S (2015) Selective activation of parvalbumin- or somatostatin-expressing interneurons triggers epileptic seizurelike activity in mouse medial entorhinal cortex. *J Neurophysiol* 113:1616-1630.
- Zaitsev AV, Povysheva NV, Lewis DA, Krimer LS (2007) P/Q-type, but not N-type, calcium channels mediate GABA release from fast-spiking interneurons to pyramidal cells in rat prefrontal cortex. *J Neurophysiol* 97:3567-3573.
- Zentner J, Hufnagel A, Wolf HK, Ostertun B, Behrens E, Campos MG, Solymosi L, Elger CE, Wiestler OD, Schramm J (1995) Surgical treatment of temporal lobe epilepsy: clinical, radiological, and histopathological findings in 178 patients. *J Neurol Neurosurg Psychiatry* 58:666-673.
- Ziskin JL, Nishiyama A, Rubio M, Fukaya M, Bergles DE (2007) Vesicular release of glutamate from unmyelinated axons in white matter. *Nat Neurosci* 10:321-330.

8. Acknowledgements

Foremost, I would like to thank Prof. Dr. Frank Kirchhoff for giving me the opportunity to work in his group. I have always profited from and enjoyed the constructive and friendly atmosphere he has created. For enabling me to contribute to this exciting project, I am most grateful.

My special thanks also goes to my mentor Dr. Xianshu Bai, who helped me so much with her extensive knowledge but also taught me all the practical skills I needed to perform my experiments and showed me the ropes on practically anything I needed to know in the world of research. I also want to express my gratitude, for performing surgery and perfusion for me, since I was not able to attend the animal welfare course due to Covid-19. Without your persistent and patient guidance, constructive criticism and practical help, this thesis would not have been possible. Thank you for bringing me onboard!

Furthermore, I want to thank Lipao Fang who has helped me in so many ways during my time in the lab. Especially for performing perfusions for me, I am thankful but I also really appreciated that I could always count on you to answer my many questions and help me find my way around the lab. It was a joy working together with you on this project.

I also want to express my gratitude to Dr. Anja Scheller for her amazing work on the AxioScan! Thank you for all the time you invested in scanning my slices.

To all the former and present members of the Kirchhoff lab, I want say thank you for the amazing time I could spend with you. I really appreciated, that you were always so supportive in answering my questions and welcomed me so openly in your group. Thank you for all the help you so generously extended to me. Also, the funny conversations at lunch and workbench banter we shared, really sweetened my time at the lab. I wish you all the best of luck for your future endeavors and hopefully we will cross paths again.

Last but not least, I am thanking my family and close friends for always supporting me.

9. Curriculum vitae

For reasons of data protection, the curriculum vitae will not be published in the electronic version of this thesis.

Kolloquiumsvermerk

Tag der Promotion:

27.11.2023

Dekan:

Prof. Dr. med. Michael D. Menger

Berichterstatter:

Prof. Dr. Frank Kirchhoff

Prof. Dr. Tobias Hartmann